# CULTURED PEARL CLASSIFICATION EQUIPMENT DEVELOPMENT

*A. P. Hawkins*

FISHERIES
RESEARCH &
DEVELOPMENT
CORPORATION

PEARL PRODUCERS
ASSOCIATION (INC)

**Project *93/194***

applied sorting

Tel: +61 3 850 7622 Fax: +61 3 852 0027

Applied Sorting Technologies Pty Ltd

5 Kim Close, Bulleen
Victoria, 3105, Australia

A.C.N. 056 145 914

# Cultured Pearl Classification Equipment Development

## Report on Initial Feasibility Study

### Prepared for The Pearl Producers' Association Of WA

15th May, 1995

Principal Investigator: A. P. Hawkins
Applied Sorting Technologies Pty Limited

Directors: A.P.Hawkins, D.Santwyk-Anderson, A.Boyle, R.W.Tamblyn

# Cultured Pearl Classification Equipment Development

**Report on Initial Feasibility Study**

**Prepared for the Pearl Producers' Association of WA.**
**by**
**Applied Sorting Technologies Pty Ltd**

**15th May, 1995**


**Researchers:**

| | | |
|---|---|---|
| Peter Hawkins (Principal Investigator) | AST | Coordinator/Optics/Classification |
| David Santwyk-Anderson | AST | Mechanical Design |
| Prof. Keith Nugent | Dept of Physics, University of Melbourne | Spherical Harmonics Theory |
| Anthony Burgess | CEDS | Windows Programming/Electronic Design |
| Arthur Richards | Sensel P/L | Pascal Programming |


## 1. Introduction

This report covers work carried out at Applied Sorting Technologies Pty Ltd (AST) on behalf of the Pearl Producers Association of WA for Fisheries Research and Development Corporation into the feasibility of automatic grading techniques for pearls. The project was initially defined in terms of the requirement for a consistent pearl quality classifying instrument, capable of accurately and repeatedly inspecting pearls placed in the instrument, returning (via screen and hard copy) a report on the pearl quality indicators -

*colour*
*shape*
*size*
*lustre*
*surface blemishes.*

However, it became quickly clear that the industry expected an on line classifier working at production rates capable of carrying out automatic placement of pearls in their different "quality" parcels. The emphasis then shifted toward carrying out a preliminary screening classification perhaps not to the accuracy of a trained grader, but able to do a useful and fast pre-sort, saving grader time to concentrate on the more skilled end of the grading process.

Although all of the above variables were examined, the results of the study, combined with industry feedback, suggest that the most useful form of machine would be one that classifies according to shape, colour and size, leaving the more difficult lustre and blemish measurements (initially at least) to the grader. A conceptual machine has been outlined which would be able to carry out this abbreviated task continuously at a rate approaching a pearl each few seconds.

The project concentrated on designing and building a flexible measurement station, together with the necessary image processing hardware and software for acquiring pearl characteristics, and development of decision-making paradigms for assessing accuracy in the above parameters compared to human grader examples. The pregraded samples provided by Broome Pearls formed the basis for developing rules of classification, and were used to evaluate especially the shape routines developed during the study.

This report consists of a drawing together of a number of interim reports provided during the course of the project, together with results of concluding tests carried out following the report to the PPA Annual General Meeting in October, 1994 on shape classification and colour.

The emphasis during the work was on the evolution of practical measurement techniques with potential to be transferred to useful equipment. Hence there was not a major emphasis on backgrounding any other research in the field. Experience in the development of a range of diamond classification machines for Argyle Diamond Mines was used in determining the approaches to practical machine planning.

## 2. Summary

The scope of the project proved in practice to be more extensive than initially planned. As result, only the *shape* parameter has been "automated" to degree initially intended for all measurements. This has in fact demonstrated the intended way in which the system would be controlled and operated. It has exhibited good results on the initial carefully chosen groups of pearls, but further investigation is necessary as demonstrated by somewhat poorer results on much larger samples made available toward the end of the work.

Some problems with software have delayed this side of project - eg it was intended to have had by the end of the work an equivalent routine for size, but the script (macro) version of Global Lab Image for returning major axis length routine has an as yet unfound bug and so this has been deferred until a following phase.

Non-shape parameter procedures have been trialled manually on a limited number of pearls supplied by Broome Pearls. The general opinion is that *shape* and *size* can meet requirements (once the industry and in particular graders become more familiar with the objective nature of the process). *Flaws* can be automatically identified but the procedure is time consuming due to the need to scan the whole pearl surface in detail. It would be difficult to do more than count and size such defects. *Lustre* appears to be usefully characterised by reflections of structured illumination sources, although with the samples available there hasn't been the chance to fully quantify this. *Colour* at present would seem to be confined to the more obvious changes - yellow from white/blue/grey has been confirmed on limited samples but the spherical mirror nature of the pearl means this task is difficult. A different approach using a fibre optic- coupled spectrophotometer close to the pearl surface has been usefully demonstrated at least in an initial form, and could be readily transferred to an integrated rig. It may allow blues and blue/greys to be separated as well as yellows.

Mechanical handling with stepper-motor controlled vacuum probes for presentation of the pearl in different views has been found to have some minor limitations when dealing with grossly irregular pearls. Some more work is needed here based on not releasing the vacuum grip when carrying out the shape procedure. However we would need to remove the influence of the holding probe from the image (eg digital image subtraction or accurate Region of Interest masking).

Mechanical speed would probably need to be increased for a useful sorting machine, primarily through a reduction in the number of pearl movements during a cycle, and through the use of larger stepper motors.

### 2.1 Future Investigations

Following reporting to potential users at the AGM of the PPA in October, 1994, feedback suggested that there was interest in a classifying system based on the work carried out during this project, based on grouping pearls by shape, size and colour, whilst carrying out accurate counting of batches being so classified.

A number of aspects of the classification systems for such a shape/colour/size equipment would need further work to extend and improve on the work to date. These would ideally be the subject of a Phase 2 study, and would include -

- mechanical singulation / orientation / presentation station with mechanical feed arrangement to encourage pearls to align along their long axis for presentation to the horizontal pickup probe
- system to capture images without releasing the horizontal vacuum holder ( to save process time)
- confirmation of the ability to use a much lower number of shape views (say 4 cf current 16)
- investigation of some more advanced classification routines on the shape spherical harmonic data
- extension of the classification routine to colour data from fibre optic probe system
- realisation of fast spectrometer for fibre optic probe system.

Such a Phase 2 aim would be toward early realisation of a relocatable piece of equipment that might not be able to operate at full production speed requirements, but would give graders a chance to look in detail at the types of decisions the machine is capable of giving. It would encourage them to evaluate the basis of their own decision making, (in particular in the possible definition of subgroups within a particular shape class that the computer could more easily recognise, and eventually recombine) and thus provide excellent feedback for the detailed design of a full production equipment.

An estimated production cost in very low numbers after removal of further research costs and production engineering costs would be around $75,000 per unit. The throughput rate would be around a target of 1 pearl per second. Development cost estimates for such a Phase 2 relocatable prototype, without final form of output separation system is expected to be in the range of $100,000 to $150,000.

A drawing showing the essential parts of a possible final equipment is sketched below as fig.1. It indicates discharge of each pearl into an appropriate physical output category via transfer to a carousel with a large number of possible divisions.

Possible prototype
classifying system

20/2/95

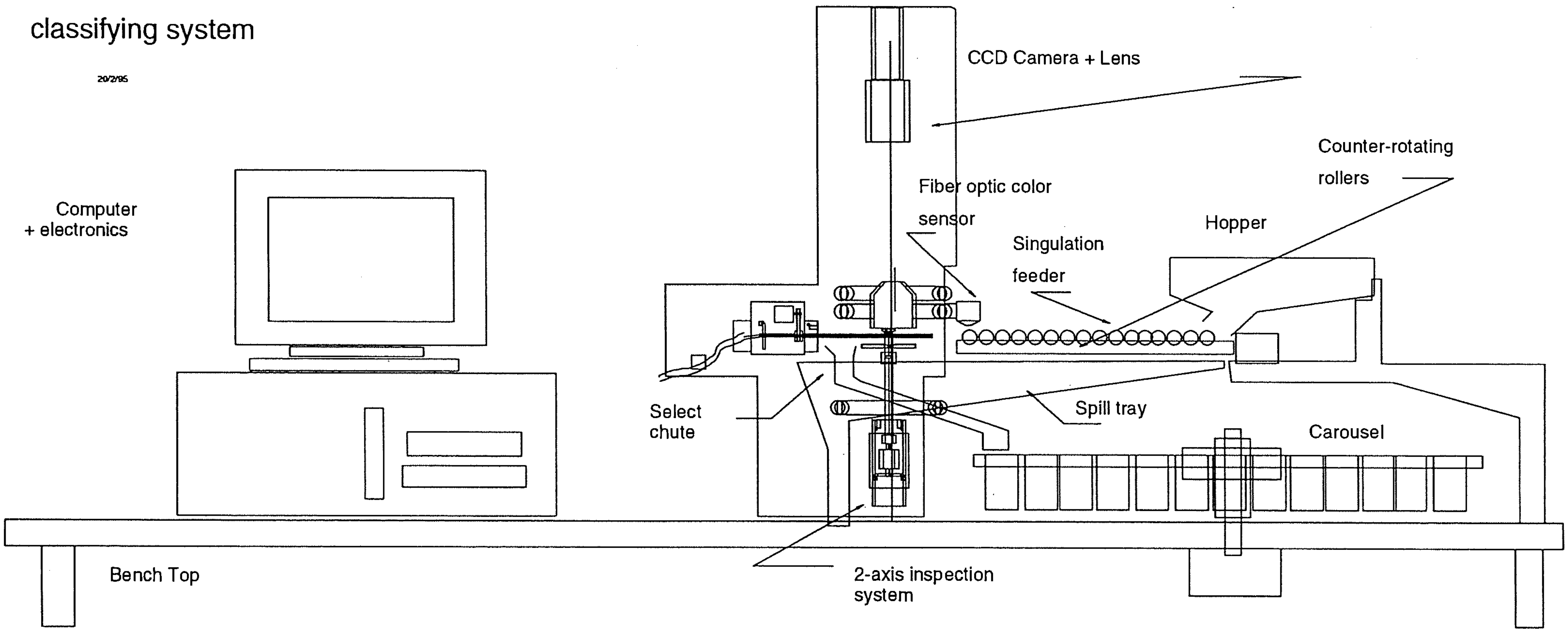


Fig. 1

## 3. Measurement Station

A large part of the initial phase of this project largely involved designing and building a flexible pearl inspection station. This unit is shown in figs. 3 & 4 and the drawing shown in fig. 2, and a video of its operation was shown at the PPA Annual General Meeting.

The system was constructed to allow, under computer control, the translation and rotation of pearls placed individually in the sample holder. Reasonable pearl stability on all except the extreme shaped baroques was achieved through the use of solenoid-controlled vacuum, for which special rotating vacuum bearings were designed.

By means of stepper motors driven by a Windows program [PEARL], it was possible to present any part of the pearl surface to the colour CCD video camera, and hence to the image acquisition printed circuit board and proprietary image measurement program Global Lab Image (GLI). A sequence of commands can be given to the PEARL program to accomplish a series of movements. The same program is able to coordinate and command the GLI image acquisition and processing steps.

The equipment has been developed with three different forms of lighting in order to enhance the optical characteristics of the pearl under inspection. These were:

- Backlit - using small circular fluorescent tubes placed below the base table. The view of the pearl from the camera is such that it appears in silhouette against a diffusely illuminated perspex background. This arrangement is used for shape and size measurements.

- Frontlit - using diffuse light from a translucent walled optical chamber enclosing the pearl. This chamber is illuminated by a pair of circular fluorescent lamps. It was used for the initial colour measurements.

- Frontlit - using structured lighting, for lustre and flaw measurements, where the pearl surface is considered more or less as a spherical mirror. The camera then looks at deviations from this ideal.

The whole mechanical-optical arrangement together with software control was designed with a final machine application in mind. Included in this is the ability to use the results of the GLI measurements to guide the path of following measurements. For example, it may be necessary to align the long axis of a drop-shaped pearl so that the axis is parallel to the horizontal probe axis. This can be done by steps involving GLI measuring the pearl's major axis with respect to the horizontal probe axis, commanding then the rotation around the vertical axis by the measured amount to achieve the desired alignment.

An alternate rig was used for the second series of colour measurements (see section 8. below). This arrangement consisted of an optical fibre bundle, white light source and scanning monochromator.

Pearl Classification Project

2-axis inspection rig

ph, nov 93

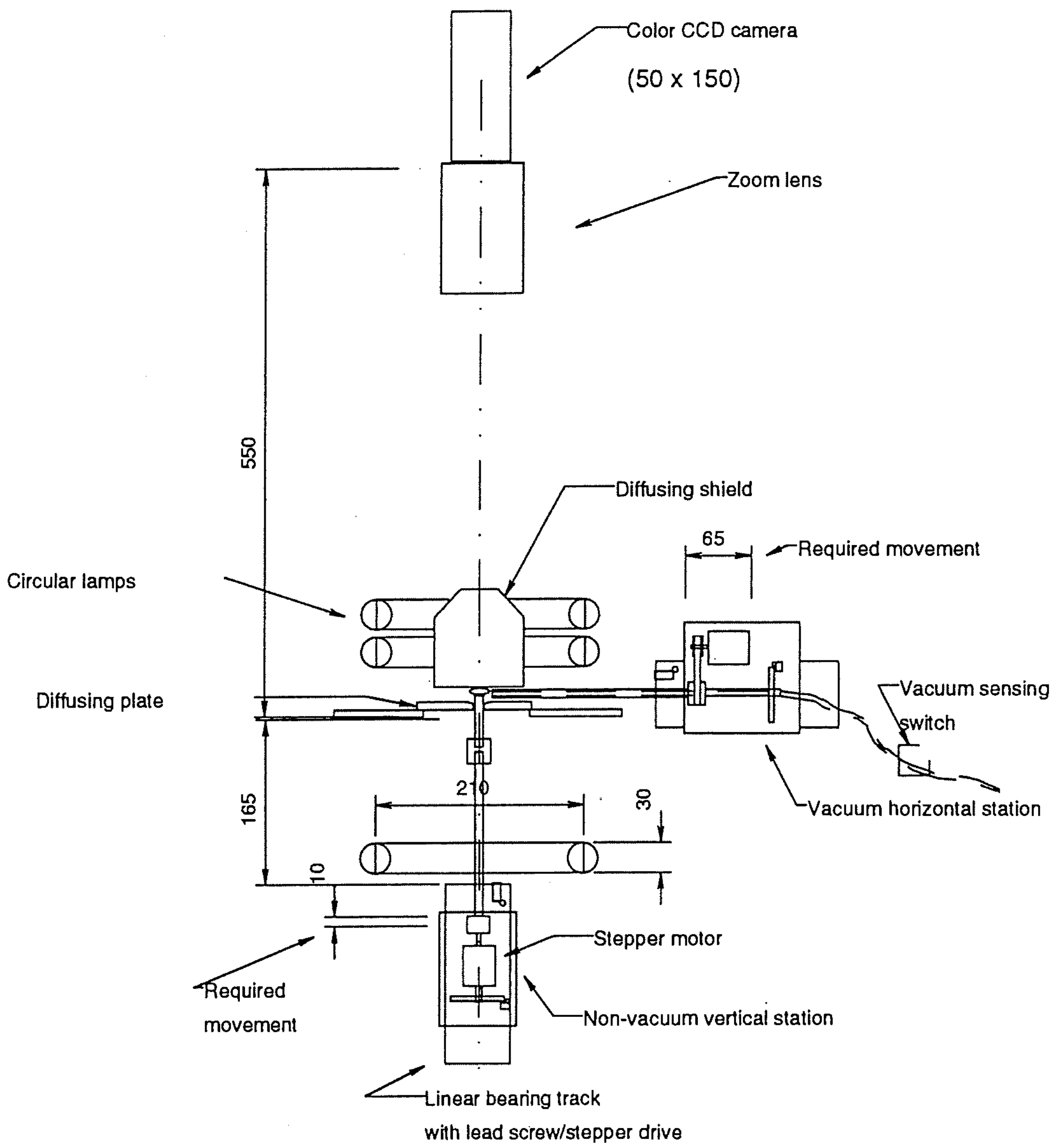


Fig. 2

View of Measurement Station

featuring horizontal translation/rotation stage, and showing top illumination diffuse chamber with CCD camera above

Fig. 3

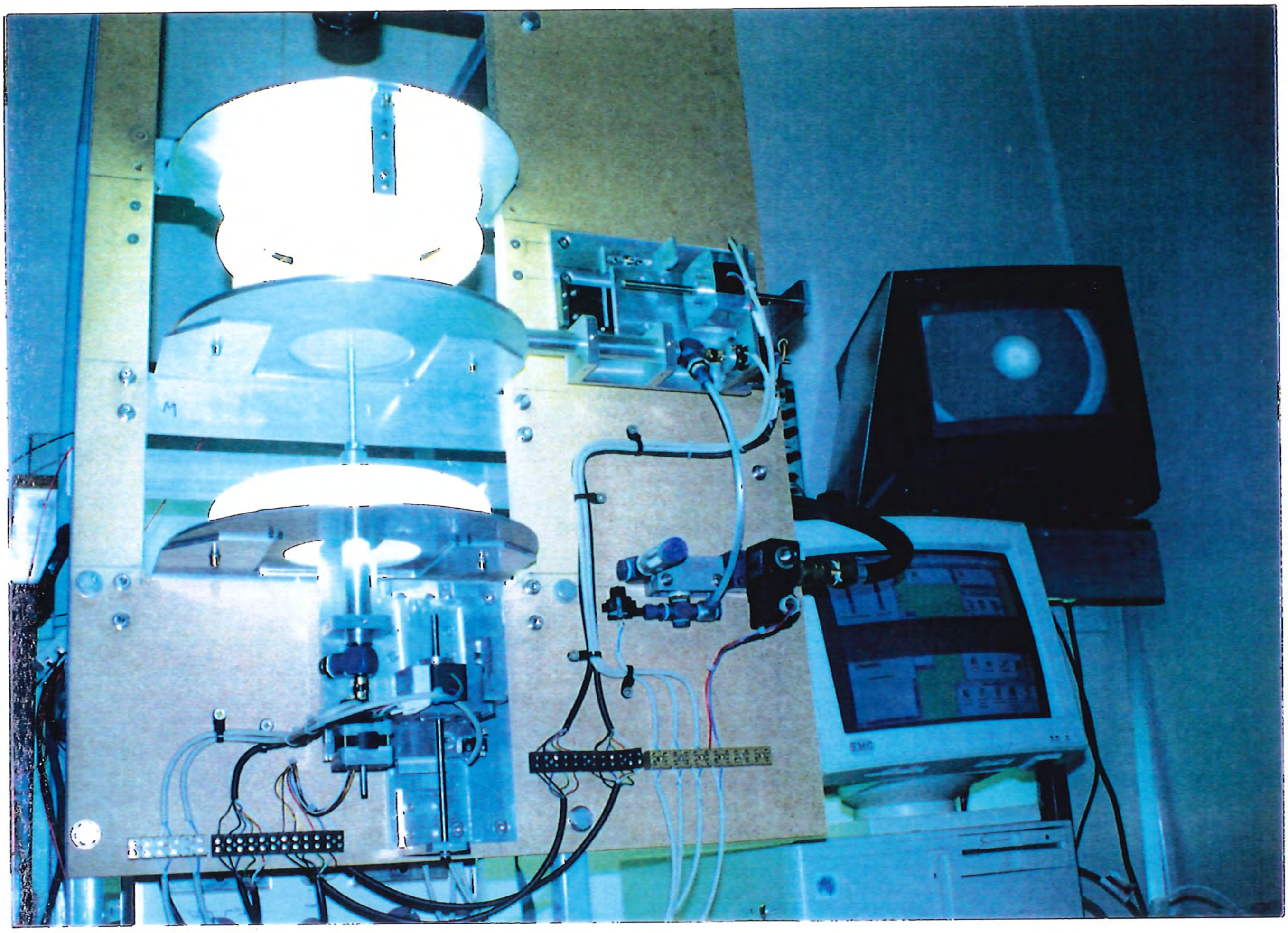

View of Measurement Station

featuring vertical translation/rotation stage, and colour monitor showing top illuminated image of pearl

Fig. 4

### 3.1 Inspection Machine Considerations

The details of the hardware sub-systems used in the Phase 1 setup are set out below:

| | |
|---|---|
| Computer: | 486 - DX66 PC with 8 Mb RAM |
| Data Translation | DT55 (black/white) "Quick capture" frame capture board |
| Data Translation | DT2851 (HSI colour) frame capture board |
| Pulnix TMC 76 | CCD camera with c-mount Zoom lens |

Low power stepper motors (4), with drive boards and PC control via special Windows-based operating program

| | |
|---|---|
| Light sources | NEC Miniature 20W circular fluorescent lamps for front and rear illumination |

20 watt strip fluorescent lamps for structured illumination

Vacuum chuck for presenting pearls horizontally
Rotating vacuum bearings for sample rotation
Lead screw/linear bearings for translation

Cycle time for typical procedure;
eg *shape* 16 views, approx 2 seconds per view after first pick up.
This is dominated by slow stepper motor. A more powerful stepper motor could be used to improve motor speed by between 2 and 4 times. A fast image processing computer could be chosen to run very rapid calculations. A reasonable target may be to carry out a shape measurement in under 2 seconds.

Note the possibility that several parameter measurements could be derived from the same mechanical procedure.

The longest procedure is that of flaw detection, which needs about 360 views to cover a whole surface. Small angular steps are needed so the mechanical arrangement could be continuous, with a frame rate (50Hz) image processing system. Rapid "blob" analysers are now available which may allow over 1000 views per second, which could be used if the pearl is rapidly rotating.

It has been found difficult to keep track of location of flaws due largely to mechanical imprecise transfer of the pearl from one axis to the other. This is especially so for strongly non-spherical shapes. There is a general problem with these shapes in the present set up. Some modifications have been discussed which may assist this problem in the next phase.

## 4. Size

The approach to pearl size measurement adopted here has been based on extraction via computer imaging routines, of the major diameter of the shadow of the backlit pearl taken in a number of orientations. Ideally an infinite number of orientations would be used, and the smallest major diameter so found would be used as the best approximation to a "sieve size". In fact, in most measurements reported here, an automatic procedure was followed whereby four views were taken during a series of four x and y axis rotations.

The method in general will tend to overestimate the pearl size when only a few projections are used, as the smallest major diameter may not be found. However the pearls have relatively slowly changing outlines, enabling reasonable assessment to be made from such few projections.

Calibration of the system is carried out by introducing precision ball bearings into the measurement station, of approximately the same size as the pearls under test. The Global Lab Image system allows the teaching of the transformation measurements between the image and the real world.

A number of tests were then carried out on pearl samples. The results are summarised in tables of figs 5 & 6.. The first used the initial (AS) series of pearls (se table in fig. 7), all labelled Size 10/11 mm, with 24 pearls covering all 6 Broome Pearl shape categories. As could be anticipated, the most irregular shapes (baroque) gave the largest difference between micrometer measured size and image derived size, but all except 2 of the 24 were well within 0.5mm of the micrometer size, with most of the non-baroque being closer than 0.2mm. (refer to fig. 5) With no proper pearl screens at our disposal, a micrometer was used to estimate the minimum circular opening through which a particular pearl would pass.

A further test was carried out with 10 samples of each of the 5 shape groups in the Broome Pearls second series (no baroques), and minimum, average and maximum image sizes presented in the table in fig. 6B, with the samples tested all labelled as 10/11 mm size. Again the image derived size data matched closely the labelled size.

A final test was carried out using 15 low quality pearls taken from previously supplied feed test samples. These covered the size range from 9 to 14 mm. As the table in fig. 6A shows, the computer image derived sizes correlated to micrometer sizes to a correlation factor of 0.99942 - very good indeed - and fig. 6C shows the size comparison across the size range.

We are confident that this measurement can be tied down well in a practical system. The operational speed is limited by the number of views needed and the time taken to transfer samples between vertical and horizontal vacuum probes, probably taking ~ 1 second per view in a realistic system. This would be a combined measurement with that of shape, with some of the shape projections being used to compute size. However, unlike the proposed shape regime, the size procedure would be slowed slightly by the need to rotate around two axes.

The current rig did have some difficulty in manipulating the extreme baroque shapes - it is believed that by slight redesign of the probe design and pickup/image capture sequence, these mechanical difficulties can be overcome.

| | | Micrometer size | | Computer size | | Difference | |
|---|---|---|---|---|---|---|---|
| Pearl | | mm | | mm | | mm | |
| (First BP Samples) | | | | | | | |
| | | | | | | | |
| | Round | | | | | | |
| AS1 | | 10.95 | | 10.84 | | 0.11 | |
| AS2 | | 10.85 | | 10.77 | | 0.08 | |
| AS3 | | 10.71 | | 10.61 | | 0.10 | |
| AS4 | | 10.90 | | 10.80 | | 0.10 | |
| AS5 | | 10.79 | | 10.70 | | 0.09 | |
| AS6 | | 10.16 | | 10.08 | | 0.08 | |
| | Drop | | | | | | |
| AS7 | | 10.50 | | 10.47 | | 0.03 | |
| AS8 | | 10.32 | | 10.31 | | 0.01 | |
| AS9 | | 10.41 | | 10.45 | | 0.04 | |
| | Button | | | | | | |
| AS10 | | 10.29 | | 10.10 | | 0.19 | |
| AS11 | | 10.15 | | 10.01 | | 0.14 | |
| AS12 | | 9.95 | | 9.92 | | 0.03 | |
| | Semi- | | | | | | |
| AS13 | baroque | 10.96 | | 10.85 | | 0.11 | |
| AS14 | | 10.90 | | 10.86 | | 0.04 | |
| AS15 | | 10.59 | | 10.42 | | 0.17 | |
| AS16A | | 11.05 | | 10.73 | | 0.32 | |
| AS16B | | 10.78 | | 10.91 | | 0.13 | |
| | Baroque | | | | | | |
| AS17A | | 10.60 | | 10.92 | | 0.32 | |
| AS17B | | 10.90 | | 11.60 | | 0.70 | |
| AS17C | | 11.80 | | 11.15 | | 0.65 | |
| AS17D | | 11.00 | | 11.56 | | 0.56 | |
| | Circle | | | | | | |
| AS18 | | 10.40 | | 10.19 | | 0.21 | |
| AS19 | | 10.79 | | 10.47 | | 0.32 | |
| AS20 | | 11.00 | | 11.02 | | 0.02 | |
| | | | | | | | |
| | | | | | | | |
| | | | | | | | |
| | Basis - 4 mutualy orthogonal views - smallest of 4 major axis values | | | | | | |

Fig. 5

| Size Measurements - Smallest Major Axis basis - 15 low quality pearls | |
|---|---|
| (a) Micrometer | Image Pro |
| 9.17 | 9.17 |
| 9.35 | 9.29 |
| 10.41 | 10.40 |
| 11.45 | 11.39 |
| 11.61 | 11.56 |
| 11.91 | 11.81 |
| 12.15 | 12.08 |
| 12.33 | 12.30 |
| 12.49 | 12.51 |
| 12.53 | 12.47 |
| 12.59 | 12.48 |
| 12.97 | 12.88 |
| 13.23 | 13.24 |
| 13.77 | 13.83 |
| 14.10 | 14.06 |

(c)

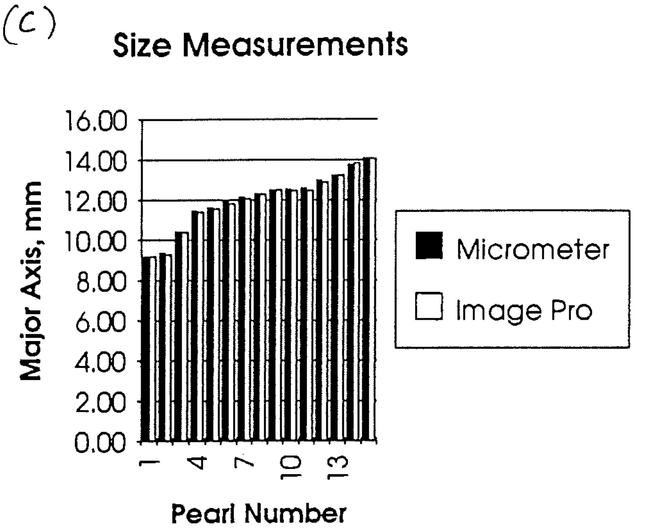


| Correlation | | |
|---|---|---|
| | *Column 1* | *Column 2* |
| Column 1 | 1 | |
| Column 2 | 0.99942 | 1 |

(b) Size Measurements on 10 New Samples per shape group - all labelled 10/11mm

| Shape | Minimum | Average | Maximum |
|---|---|---|---|
| Round | 10.21 | 10.57 | 10.85 |
| Drop | 9.95 | 10.49 | 10.80 |
| Button | 10.64 | 10.87 | 11.10 |
| Semi-baroque | 10.04 | 10.42 | 10.76 |
| Circle | 10.21 | 10.50 | 10.87 |



Fig. 6

PIONEERS IN PEARLING

A Member of the M.G. Kailis Group of Companies

Incorporated in Western Australia

**Broome Pearls Pty Ltd** A.C.N. 008 831 669
Blackman Street, P.O. Box 178,
Broome, Western Australia 6725
Telephone (091) 92 1295
Fax (091) 92 2597

**Head Office:**
12 Stirling Highway,
P.O. Box 353, Nedlands, W.A. 6009
Telephone (09) 389 1277
Telex AA93300 Fax (09) 386 1141

7 September 1993

Applied Sorting Technologies
5 Kim Close
BULLEEN VIC 3105

## CONSIGNMENT

| LOT NO | SIZE | PIECES | DESCRIPTION | MOMME | TOTAL AUD |
|---|---|---|---|---|---|
| AS 1 | 10-11 | 1 | Round grade 1 | 0.53 | 100.00 |
| 2 | 10-11 | 1 | Round grade 2 | 0.49 | 100.00 |
| 3 | 10-11 | 1 | Round grade 3 | 0.49 | 100.00 |
| 4 | 10-11 | 1 | Round grade 4 | 0.50 | 100.00 |
| 5 | 10-11 | 1 | Round blue/grey | 0.48 | 100.00 |
| 6 | 10-11 | 1 | Round yellow | 0.38 | 100.00 |
| 7 | 10-11 | 1 | Drop grade 1 | 0.52 | 100.00 |
| 8 | 10-11 | 1 | Drop grade 2 | 0.46 | 100.00 |
| 9 | 10-11 | 1 | Drop grade 3 | 0.49 | 100.00 |
| 10 | 10-11 | 1 | Button | 0.40 | 100.00 |
| 11 | 10-11 | 1 | Button blue/grey | 0.34 | 100.00 |
| 12 | 10-11 | 1 | Button yellow | 0.34 | 100.00 |
| 13 | 10-11 | 1 | Semi baroque grade 1 | 0.53 | 100.00 |
| 14 | 10-11 | 1 | Semi baroque grade 2 | 0.56 | 100.00 |
| 15 | 10-11 | 1 | Semi baroque grade 3 | 0.56 | 100.00 |
| 16 | 10-11 | 2 | Semi baroque blue/grey | 0.98 | 200.00 |
| 17 | 10-11 | 4 | Baroque white/grey | 2.26 | 400.00 |
| 18 | 10-11 | 1 | Circle | 0.48 | 100.00 |
| 19 | 10-11 | 1 | Circle blue | 0.53 | 100.00 |
| 20 | 10-11 | 1 | Circle yellow | 0.65 | 100.00 |
| | | 24 | | 11.97 | 2,400.00 |

GOODS ARE DELIVERED ON CONSIGNMENT SUBJECT ONLY TO CONDITION THAT THE GOODS ARE AT THE RISK OF THE CONSIGNEE UNTIL RETURNED IN ORIGINAL STATE AND GOOD CONDITION AND THAT THE CONSIGNEE IS LIABLE FOR ANY LOSSES OR DAMAGE HOWEVER INCURRED.

GOODS NOT RETURNED AFTER ................................ WILL BE INVOICED

DATE: ..............................................................

SIGNATURE: ........DR Norman........

c:\wpwin\dm\appsort\kfp1

Fig. 7

## 5. Shape Classification

A large part of the project effort went into the investigation of pearl shape classification by machine training.

Following discussions with Prof Nugent of Melbourne University regarding appropriate 3-dimensional descriptors for shape representation, it was decided to use a back projection technique (see appendix 1 for details). Here in a fashion similar to X-ray CAT scanning procedures, a series of back-lit "shadows" of each pearl would be stored in the computer video frame store, and for each, a set of boundary coordinates would be automatically extracted.

A software procedure for extracting spherical harmonic series from the set of such boundaries was written and tested on mathematically generated model shapes. The two sets of coefficients generated by this procedure characterised (a) the rotation of a radius vector around 360 of the perimeter, with (b) rotation of the pearl to present 16 profiles or shadows. Appendix 2 has further details.

It was found that for most pearls, there was substantial symmetry around a major ellipsoidal axis, (ie the perimeter set of data were the same for the 16 views as long as rotation around the long axis of symmetry was chosen). As a major amount of time is used in rotating and capturing images of each view, savings such as this are potentially very important. Obviously, suitable mechanical means would have to be found in an automatic machine to ensure correct orientation.

### 5.1 Processing Details

Initially the coefficients of the spherical harmonic series were loaded into an Excel spread sheet for a series of training sets of pearls (see fig 7 for description). This spread sheet took numbers (coefficients) from each individual pearl in each predefined shape group, and calculated average values for each of the coefficients (1-8) , suitably normalised to the zeroeth coefficient. Test pearl data could then be introduced, one at a time, and a least distance algorithm used in order to quantify divergence away from the average as a single number (sum of magnitude of differences).

For an "unknown" test pearl, this procedure would be carried out comparing its spherical harmonic coefficients with the average of each of the training shape groups, adding each time the magnitude of the differences between the test harmonic and the training average harmonic. By adding these differences, the closest fit would be the training shape class with smallest difference in this set of numbers.

Other ways of training and evaluating are available, most being mathematically more sophisticated than this least distance procedure, eg artificial neural networks. It may be useful in a future phase of the development process to investigate these other classification algorithms, still using the data generated via the spherical harmonic series as the numerical description data for each pearl.

Figs 8 - 10 show in graphical form the relationship of coefficients up to the eighth harmonic for one of each of the six different shape types supplied in this sample from Broome Pearls. The table in fig. 11 is the result of the self application procedure (ie training set identical to test set, being pearls listed in fig 7).

This showed that the pre-categorised pearls were quite consistent and well clustered, with only the semi baroque group having a couple of misclassified examples, in that only 2 of the 5 examples in that group were closer to the semi baroque average than the averages of other categories (1 drop, 1 round and 1 button). Because of the small number of pearls (maximum of 6 in any one shape category), it wasn't practical to set the usual one half of each group aside as the test set with the remaining half the training set.

Subsequently, a much larger test set of classified pearls from Broome Pearls (~ 50 per shape group) was obtained including all except the baroque category (as this category was found to be highly distinctive, and hence readily identifiable). The initial (AS series) shape data was then used as the training set for evaluating the method, and the second series was used as the evaluation set. In order to carry out the classification process in reasonable time for the larger number of pearls, a further C program was written to replace the least distance spread sheet classifier.

The following then was the final procedure for this shape sorting exercise:

- the PEARL Windows program is the main program, controlling presentation of the pearl to the imaging camera via translation and rotation commands with vacuum hold down.

- embedded in PEARL is a Global Lab Image script routine which, under PEARL control, captures each image view and finds perimeter pixel coordinates. PEARL then computes the centroid value for each shadow image, and writes centroid and perimeter coordinate data for each of the 16 views to a data file.

- a DOS program, PDATA, currently running separate to PEARL but with the capability to be incorporated into the main program, carries out the following steps -

    1. it computes for each of the 16 views, the length of "radius" from centroid to perimeter for each of the 16 equal angular increments from 0 to 360.

    2. it then normalises these 16 lengths for each of the 16 shadow projections from the given PEARL filename to the largest radius (which is defined as = 1).

    3. it then applies the spherical harmonic series-generating program, FIT_2, to the resulting data, generating files with series of 8 coefficients;

- A further program, PCLASS, uses PDATA information to both train (learn) and classify pearls to and from 5 groups, viz round,, drop, button, semi-baroque, and circle. A typical output screen display from this program is shown in fig. 12.

AS7 - DROP GRADE 1

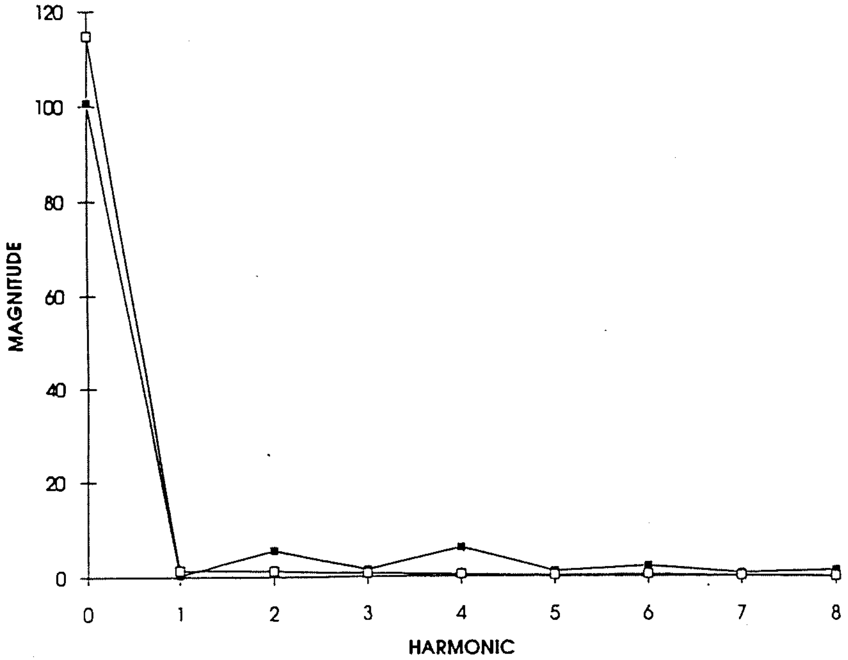


AS1 - ROUND GRADE 1

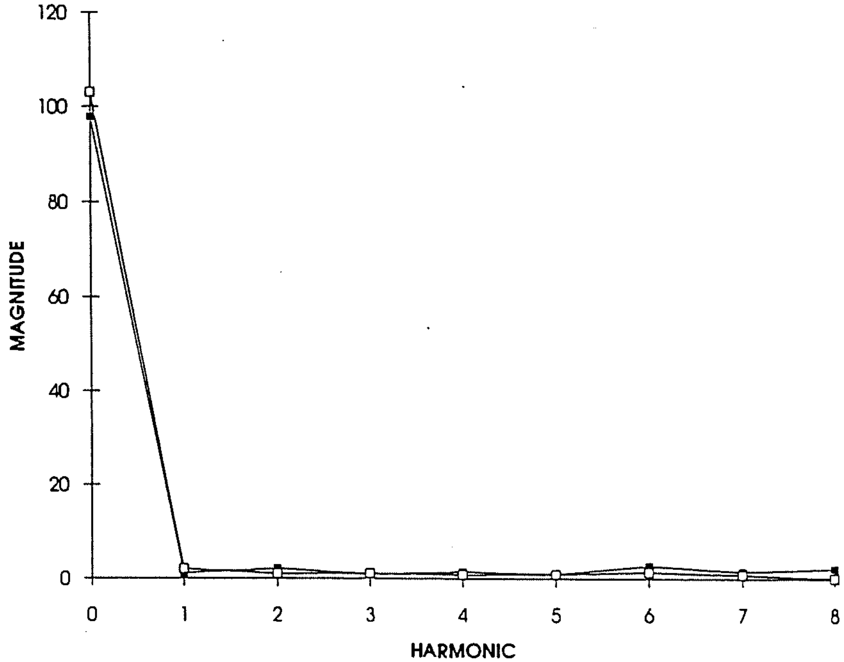


Fig. 8

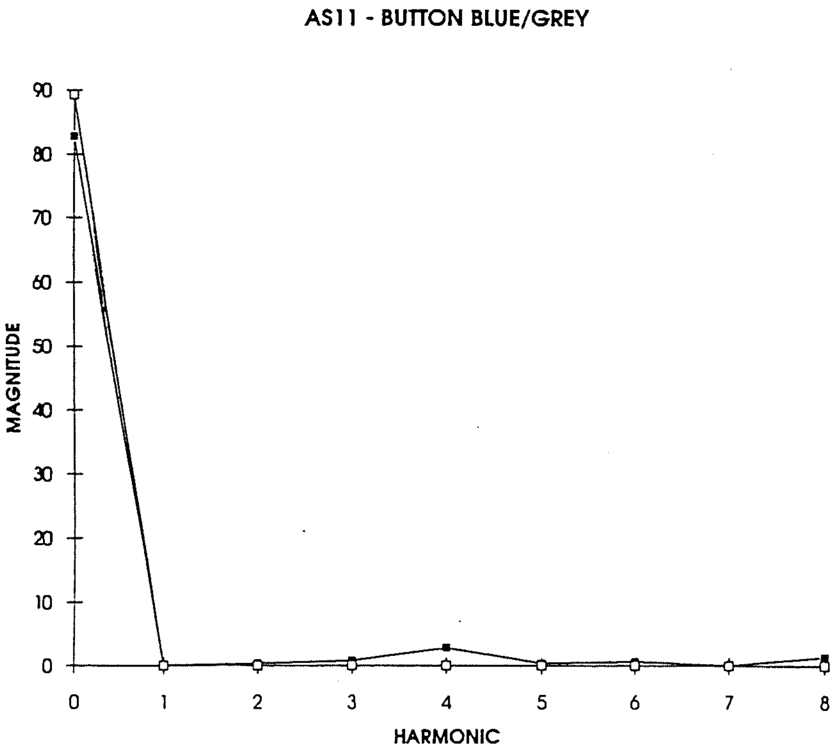
AS11 - BUTTON BLUE/GREY
MAGNITUDE
90
80
70
60
50
40
30
20
10
0
0
1
2
3
4
5
6
7
8
HARMONIC

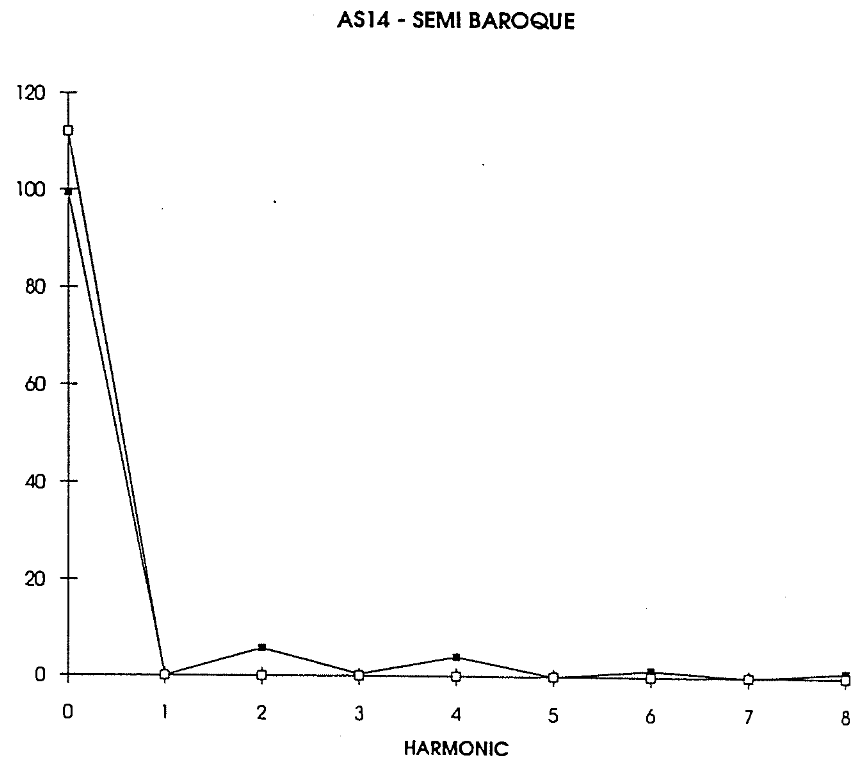
AS14 - SEMI BAROQUE
120
100
80
60
40
20
0
0
1
2
3
4
5
6
7
8
HARMONIC

Fig. 9

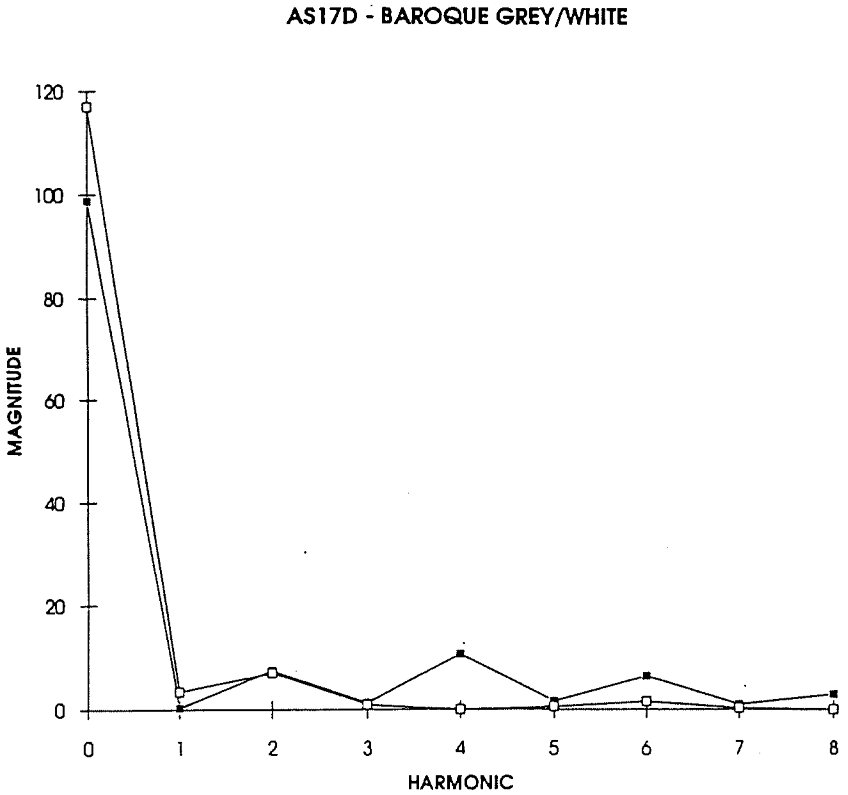
AS17D - BAROQUE GREY/WHITE
120
100
80
60
40
20
0
MAGNITUDE
0
1
2
3
4
5
6
7
8
HARMONIC





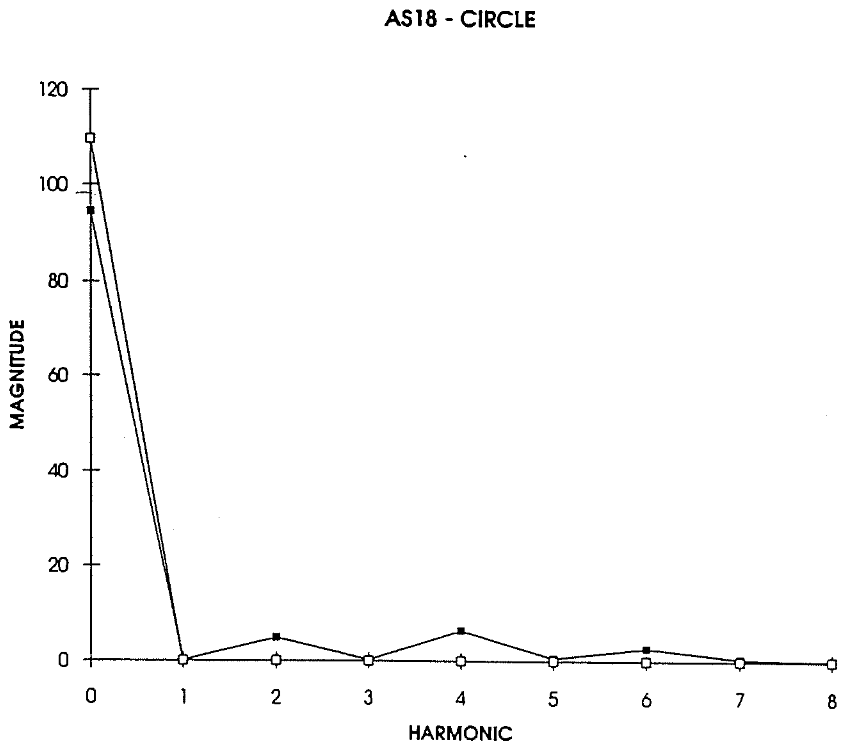
AS18 - CIRCLE
120
100
80
60
40
20
0
MAGNITUDE
0
1
2
3
4
5
6
7
8
HARMONIC



Fig. 10

| Shape Tests - Least distance classifier with harmonics normalised to H0 | | | | | | | | |
|---|---|---|---|---|---|---|---|---|
| Pearl | | Round | Drop | Button | Semi baroque | Baroque | Circle | Decision |
| AS1 | Round | 4.58 | 9.77 | 7.70 | 8.18 | 20.80 | 14.69 | Round |
| AS2 | | 1.06 | 9.27 | 4.53 | 4.92 | 25.01 | 14.15 | Round |
| AS3 | | 1.01 | 9.21 | 4.42 | 4.75 | 25.19 | 14.24 | Round |
| AS4 | | 1.02 | 9.21 | 4.42 | 4.75 | 25.19 | 14.24 | Round |
| AS5 | | 1.08 | 9.01 | 4.38 | 4.38 | 25.25 | 13.98 | Round |
| AS6 | | 0.91 | 8.61 | 4.28 | 4.43 | 24.82 | 13.38 | Round |
| | | | | | | | | |
| AS7 | Drop | 9.02 | 2.81 | 9.35 | 6.87 | 18.34 | 5.89 | Drop |
| AS8 | | 7.07 | 2.59 | 7.02 | 5.32 | 19.38 | 8.81 | Drop |
| AS9 | | 11.39 | 3.45 | 12.46 | 10.77 | 13.92 | 6.13 | Drop |
| | | | | | | | | |
| AS10 | Button | 4.76 | 9.75 | 1.08 | 5.21 | 26.97 | 14.41 | Button |
| AS11 | | 6.62 | 8.39 | 2.47 | 4.84 | 24.75 | 14.35 | Button |
| AS12 | | 3.63 | 10.13 | 2.18 | 6.35 | 27.00 | 15.72 | Button |
| | | | | | | | | |
| AS13 | Semi- | 5.91 | 10.05 | 2.69 | 3.90 | 27.17 | 14.47 | Button |
| AS14 | baroque | 3.38 | 8.82 | 5.38 | 3.11 | 25.13 | 13.70 | Semibaro |
| AS15 | | 9.65 | 5.51 | 9.55 | 5.40 | 20.37 | 10.44 | Semibaro |
| AS16A | | 9.45 | 5.27 | 8.40 | 5.91 | 19.85 | 7.99 | Drop |
| AS16B | | 4.19 | 12.37 | 5.35 | 4.94 | 27.07 | 17.13 | Round |
| | | | | | | | | |
| AS17A | Baroque | 23.83 | 16.86 | 25.89 | 23.57 | 7.65 | 12.62 | Baroque |
| AS17B | | 26.55 | 20.43 | 26.90 | 23.60 | 9.62 | 18.63 | Baroque |
| AS17C | | 26.58 | 18.40 | 27.70 | 26.00 | 8.65 | 15.66 | Baroque |
| | | | | | | | | |
| AS18 | Circle | 16.03 | 9.16 | 16.74 | 14.57 | 9.76 | 4.22 | Circle |
| AS19 | | 14.67 | 7.72 | 16.08 | 13.46 | 14.84 | 3.44 | Circle |
| AS20 | | 12.44 | 5.22 | 13.52 | 10.84 | 16.52 | 3.77 | Circle |



Fig. 11

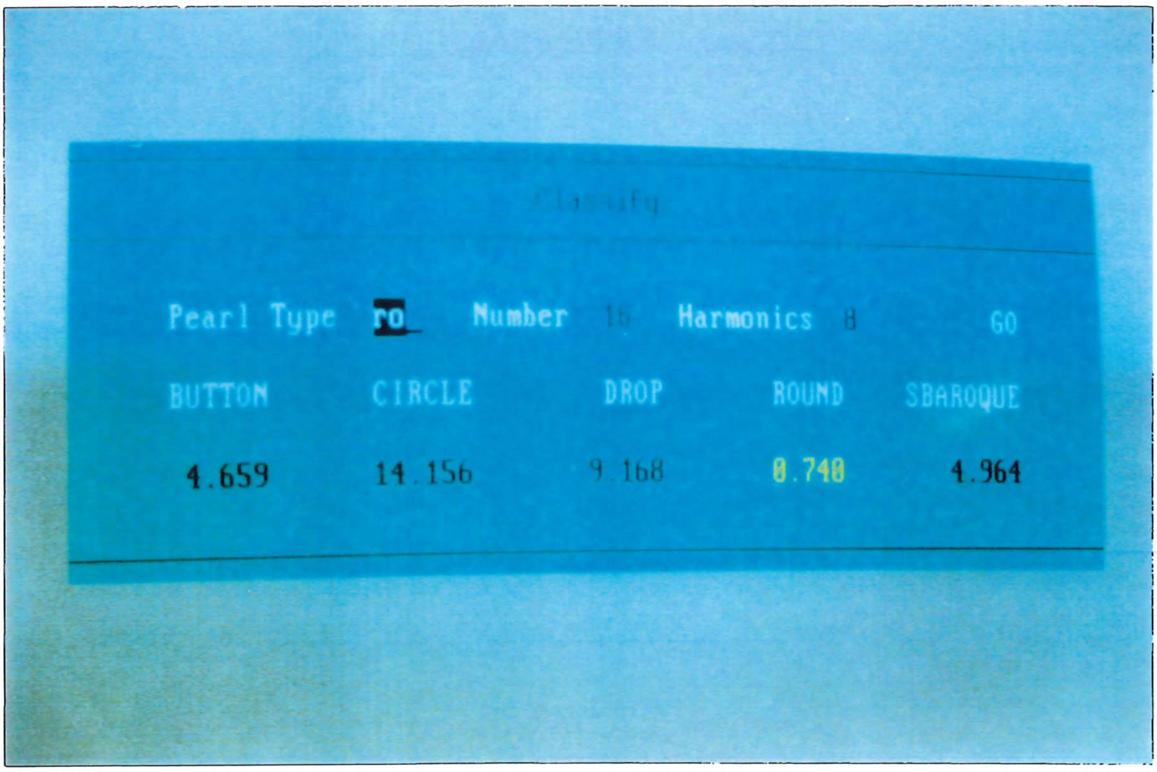


**Output Data Display from PData Classification Program**

**(showing machine selection of *round* (with minimum difference of 0.740) for sample labelled *ro16*, ie no. 16 example from *round* group)**

Fig. 12

## 5.2 Results of Larger Trial

Using the AS series 20 pearls in 5 shape groups as the training set, the 14th September consignment from Broome Pearls were measured as the test and evaluation set and the resulting data processed via the above routines. With unmodified training, the evaluation of the test sets resulted in the following classification results; (see appendix 3).

- *Round* Group BP 88 - 31 pearls, all placed correctly into the *Round* category;

- *Drop* group - BP 183 - 49 pearls
  22 correctly into *Drop* category
  23 into Semi-baroque category
  3 into Circle category
  1 into Button category

- *Button* Group - BP 241 - 29 pearls
  12 into *Button* category
  16 into Round category
  1 into Drop category

- *Semi-baroque* Group - BP 303 - 50 pearls
  9 into *Semi-baroque* category
  27 into Round category
  8 into Drop category
  5 into Circle category
  1 into Button category

- *Circle* Group - BP 32 - 49 pearls
  18 into *Circle* category
  17 into Drop category
  8 into Round category
  3 into Semi-baroque category
  3 into button category

The table below illustrates the differences in classification by choosing different pearls to make up the training sets. It illustrates the degree of care needed in choice of pearls when making up a training set. For example, the only difference between sets 2 and 6 was that for 6, one extra button and one extra semi baroque were added to the AS series training set. As can be seen, circles and semi baroque identification improved slightly, but button recognition was reduced to only one of 30.

| Training basis | Initial AS series with AS test set | AS series with 2nd test set | 1st 1/2 of 2nd set | 1st 1/2 of 2nd set with extra SB examples | AS series with added BU & SB | Middle 1/2 of 2nd series |
|---|---|---|---|---|---|---|
| | 1 | 2 | 3 | 4 | 5 | 6 |
| Round | 6/6 | 31/31 | 9/31 | 23/31 | 15/31 | 31/31 |
| Drop | 3/3 | 22/50 | 28/50 | 22/30 | 21/50 | 18/50 |
| Button | 3/3 | 11/30 | 13/30 | 20/30 | 22/30 | 1/30 |
| Semi-baroque | 2/5 | 9/50 | 12/50 | 20/50 | 12/50 | 11/50 |
| Circle | 3/3 | 17/50 | 15/50 | 15/50 | 15/50 | 19/50 |
| Baroque | 4/4 | | | | | |

Importantly, it is noticeable that objective rules can only go a certain way toward automatic classification, with results heavily dependent on choice of training examples. The first small set (#1 above) were reasonably uniformly constituted and self-consistent, as shown by the table in fig. 11. as well as the above table. Appendix 4 shows shadow images of all AS series pearls.

Looking however at the second series, (#2 in above table), detailed results are given in tables in Appendix 3. In the Drop series, we can refer to example images in appendix 5, labelled DR##. The images in the Drop series are wrongly numbered, and we should subtract 10 to get correspondence with the table in appendix 3. Of the example images shown, only DR44 was classified as a drop when taught by the AS7-9 examples in the first series. Most of the others "leaked" to the semi-baroque category (AS13-16 training set).DR45 and DR55 images show extra lobes not encountered in the initial training set but suggested in the semi-baroque image AS14.

Button examples in appendix 3 show BU11 has been selected properly as a button, but BU12 however narrowly is selected as semi-baroque over button, whilst BU21 is quite spherical and is selected clearly as round over button.

Semi-baroque images which were selected as being semi-baroque were SB 13, 21, 24, 32, and 43, these being similar to training samples AS13-16. Most of the other images shown in the appendix 5 were drops, with a few of circles, button and round.

Circles with images in appendix 5 showed significant leakage across categories, especially to drops.

### 5.3 Discussion

There are a number of ways of improving this performance. One is to set tolerance limits for acceptable closeness of fit, so that a new category of "don't know" would cover pearl shapes which didn't fit well to any of the trained groups. In this way it would be preferable to have a defined difficult category which would need to be hand-sorted rather than having such examples leak across to other groups.

The second way would be to make a more thorough attempt to cover the different shape "sub-groups" within each overall shape group. This would allow a larger number of categories, eg DR1,2,3,4,5 etc, each having its own set of training examples. The overall classification system, could be readily adapted to then aggregate the subgroups as required.

A third possibility would be to set up overlap categories which may occur when the experienced grader might not see a large difference between two shape groups which an individual pearl may be able to be put. A suitable algorithm could be invoked to place the pearl into the most valuable of the two groups.

As well, there is the chance that a more sophisticated classification procedure, such as a suitably structured artificial neural network might improve the decision process.

## 6. Flaw Measurement

According to Lyman (Guide to Gems and Precious Stones, Simon and Schuster, 1986), flaws in cultured pearls are minor irregularities which are either small, almost conical, protuberances or more likely barely noticeable cavities in the surface which resemble lunar craters.

Because of the smooth spherical nature of pearls, we have found that a suitable way to find such surface flaws (cavities) has been to present the pearl in two x 360° rotations with axes of rotation 90° apart to the CCD camera to ensure viewing of the entire surface. The image captured for each step is that of a strip of light similar to a linear fluorescent tube. This produces a bright "image" of the light source on the surface of the pearl. As the pearl is rotated, the light area moves over the surface, and pits are seen as small "craters" with highly contrasting edges compared with the rest of the unblemished surface.

The GLI program can be configured to find such transitions by thresholding and feature area discrimination. The procedure for a whole pearl is reasonably lengthy, as we can't jump too many degrees in one step if we are to avoid missing small pits.

Typically the pit would remain detected by this routine over approx 5 - 10°, however some may require inspection at every 2°. In this case then, 360 images need to be examined for each pearl to cover the while surface.

In the current setup, 1 pixel is equivalent to 0.06mm. We need at least 5 pixels for GLI to pick up the flaw as a separate entity.

Our initial estimate of the processing time required for finding "craters" in around 360 frames for one pearl was with a processor running at frame rate of 50 per second. Since then, in discussions with the CSIRO Division of Manufacturing Technology, we have found available "blob" analyser card systems designed by this group and subsequently manufactured and sold by Vision Systems, which are able to find blobs an a rate of more than 200 per second. Using this sort of image analyser, it would be possible to consider spinning the pearl at a high rate of say 180 steps per second, for complete rotation around one axis, then a 90 rotation around the orthogonal axis, followed by another high rotation scan of 180 steps in another second. The complete cycle would then take around 3 - 5 seconds. Whether flaw coordinates would be able to be stored at that rate would require detailed evaluation. However such a quick scan could possibly be used to screen and separate on flaw/no flaw basis.

The other problem with the above scheme in practice is keeping track of the location of detected flaws which has proved a mechanical difficulty with the current handling system especially due to instability when larger irregular shapes are involved.

The images of a couple of flaws on pearl number AS4 (round) are shown in fig 13, and the table in fig. 14 shows the progression around one of the $360^{0}$ scans, indicating the positions at which the Global Lab Image program found flaws, with the area of these flaws at each viewing angle. In some cases such as 3,4 7,8 11,12 and 20,21 two flaws appear simultaneously (hence the notation Flaw A and Flaw B).

The sensitivity of the technique is seen from this to be very high because of the optical magnification and the severe light and dark crater formations shown up by the structured lighting.

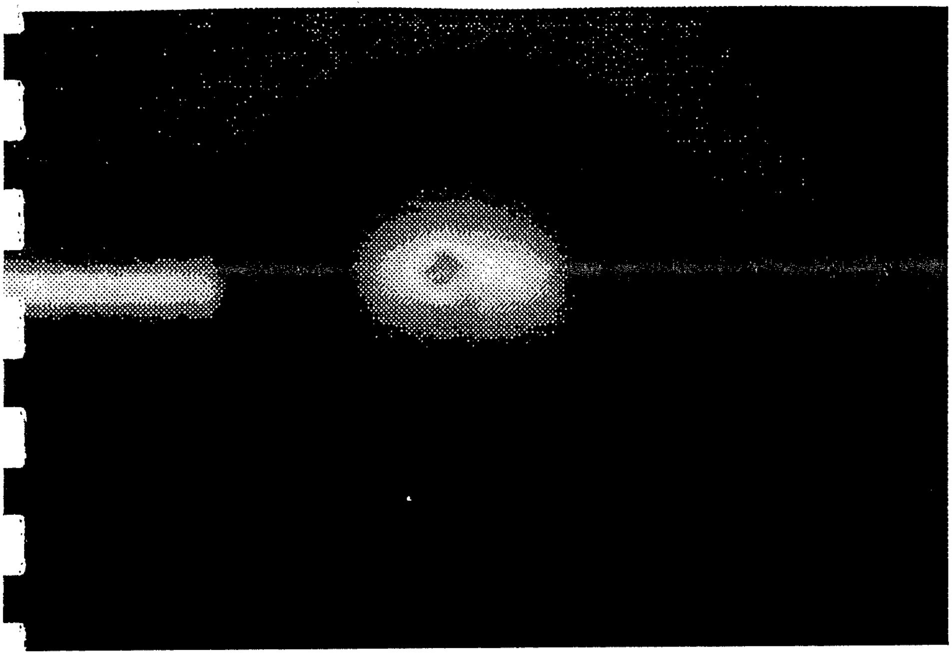

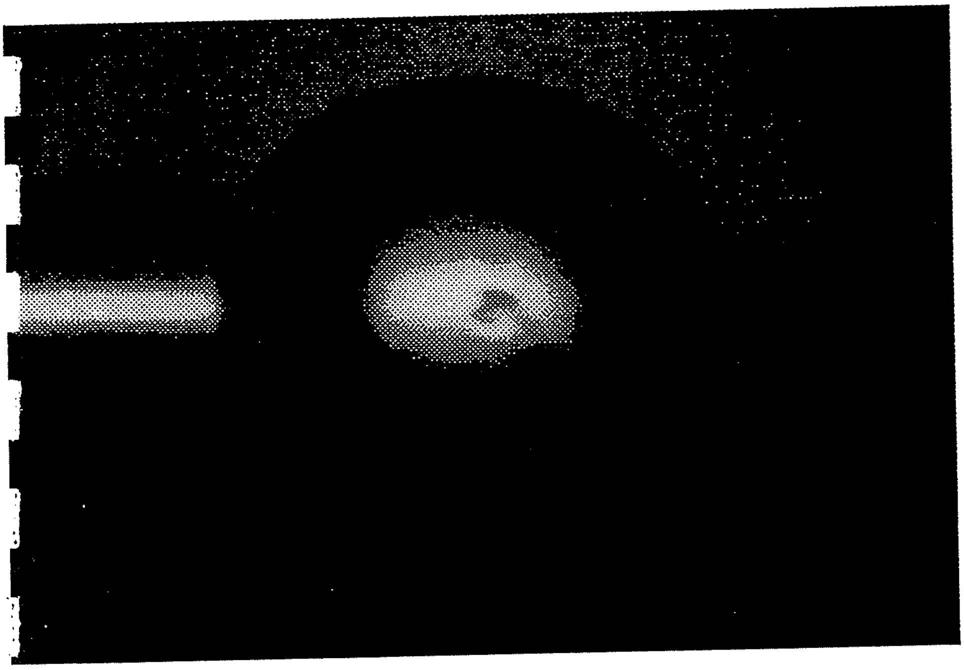

Flaw Image Examples.

Fig. 13

| | | | | | | | |
|---|---|---|---|---|---|---|---|
| Flaw Measurements | | | | | | | |
| | | | | | | NB 1 pixel + 0.06mm | |
| Sample AS4 | | Round Grade 4 | | | | | |
| | | | | Area of | | 2 degree steps | |
| Flaw # | | Rotational | | detected flaw | | | |
| | | angle | | (pixels) | | | |
| | | | | Flaw A | Flaw B | | |
| 1 | | 20 | | 13 | | | |
| | | 22 | | 11 | | | |
| | | 24 | | 12 | | | |
| | | 26 | | 10 | | | |
| | | | | | | | |
| 2 | | 38 | | 46 | | | |
| | | 40 | | 25 | | | |
| | | | | | | | |
| 3 | | 42 | | 8 | | | |
| 3 | | 44 | | 53 | | | |
| 3,4 | | 46 | | 90 | 6 | | |
| 3 | | 48 | | 44 | 38 | | |
| 3,4 | | 50 | | 49 | 7 | | |
| 3 | | 52 | | 63 | | | |
| 3 | | 54 | | 60 | | | |
| 3 | | 56 | | 20 | | | |
| 3 | | 58 | | 5 | | | |
| | | | | | | | |
| 5 | | 76 | | 6 | | | |
| | | 84 | | 9 | | | |
| | | | | | | | |
| 6 | | 106 | | 11 | | | |
| 7,8 | | just grazed edge - v. small both missed | | | | | |
| 9 | | 168 | | 25 | | | |
| 10 | | 170 | | 18 | | | |
| 11,12 | | 186 | | 19 | 18 | | |
| 12 | | 188 | | 8 | | | |
| 13 | | 196 | | 39 | | | |
| 14 | | 220 | | 8 | | | |
| 15 | | 240 | | 11 | | | |
| | | | | | | | |
| 16 | | 260 | | 9 | | | |
| 16 | | 270 | | 29 | | | |
| | | | | | | | |
| 17 | | 306 | | 11 | | | |
| 18 | | 308 | | 20 | | | |
| 19 | | 310 | | 29 | | | |
| 20 | | 312 | | 10 | | | |
| 20,21 | | 316 | | 11 | 29 | | |



Fig. 14

## 7. Lustre

The property of lustre is related to measurable physical properties such as refractive index, flatness (macroscopic and microscopic) and hardness (ability to take a polish). In a gem and pearl context, lustre is a difficult parameter to quantify, but at the same time it is obviously very commercially important.

In the gemstone context, there are a number of descriptive terms that are used to indicate the type of lustre, viz

| | | |
|---|---|---|
| metallic | - | (metals) |
| adamantine | - | (diamond, etc) |
| vitreous | - | (glasslike) |
| resinous | - | (amber) |
| waxy | - | (eg turquoise, opal, jadeite) |
| greasy | - | (nephrite) |
| pearly | - | (pearl and moonstone) |
| silky | - | (satin-like) |

The term *silky* is applied to gemstones with many needle like inclusions on the surface. So lustre is related to both surface and sub surface structure.

*Sheen* is a related term indicating the idea of light reflected from beneath the surface of a stone. Such terms as opalescence and silky or pearly reflection as shown by common opal are a result of the effect of the light reflecting from thin layers in the internal structure of the stone. In the final analysis, it is really the chemical composition and atomic structure of the gem which actually determines lustre. (references: Read, Gemmological Instruments, Newnes-Butterworth, 1978, and Liddicoat, Handbook of Gem Identification, Gemmological Institute of America, 1981).

Lustre instruments of reasonably primitive nature are sometimes used for diamond identification, measuring specular reflection from polished diamond facets. These are of little use for pearl due to the different nature of the lustre related to both surface and near sub surface properties, the opacity and the spherical shape. In addition, although there are large differences in lustre between high quality pearls and dull susa dama pearl, the real difficulty lies in the subtle gradations of quality as seen by the expert grader.

Having participated in the grading process of a couple of Broome operations, and attempted to extract by example a quantitative procedure, it appeared to the writer logical to use the property of image formation in a strong illumination field by reflection. This was done by holding a pearl in a position where, even with distortion due to the spherical mirror effect, one can view distant objects by reflection in the pearl surface. This procedure was then checked by endeavouring to produce demonstration of visual grading acceptable to the expert graders participating in the tests.

Two practical methods were then tried to produce an automatic lustre reading using the above principle. Both had the common link of the measurement of image quality (sharpness) using the imaging tools at hand in the Global Lab Image software. These approaches were applied to only a limited number of pearls to illustrate the type of results that may be achieved. Lack of time and insufficient range of samples selected for lustre variations made a systematic evaluation difficult, however eventual applicability will depend on industry feedback.

### 7.1 Contrast Histograms

Initially we captured the reflected image of a light/dark grid pattern, which, if ideally specularly reflected from a metallic surface would have brightness values of essentially only two levels, high (being the brightness of the source of light) and low (dark). The GLI program was then used to produce a brightness histogram of the image. The ideal reflector would have two tightly clustered lobes, one for white (light source) and the other dark, with virtually no intermediate grey values. With a dull surface these lobes would be blurred towards a continuos distribution of grey values.

Typical such histograms are shown for high and low lustre pearls in fig 15.

### 7.2 Contrast Measurement Method

It was initially intended to use the above histograms to form quantifiable lustre numbers for each pearl via neural network or fuzzy logic procedures. The fuzzy logic analysing system available to us proved unduly complex and unsuitable, and a simpler procedure was formulated, following the optical set-up used with the above flaw measurement rig.

Essentially this again used the spherical mirror concept, but with a light/dark/light target reflected off the pearl surface. Example images are shown in fig 16. The GLI program was then used to extract a peak-to-valley ratio from a line brightness profile across these regions of the captured image.

Examples of such brightness line profiles of a stainless steel ball bearing (ideal metallic reflector), two good quality round pearls and a completely dull pearl from a bag labelled "Roebuck Bay Recoverables" are shown in fig 16.

In order to extract a single lustre index, a simple arithmetic rule was applied to line profile readings as shown in fig 17 and table in fig 18. The table shows the lustre index being very high for the ball bearing, intermediate for the two high quality round pearls (with very little difference between the grade 1 AS1 and grade 4 AS4 examples) to very low for the dull pearl. The numerical results were extracted by averaging the lustre index taken over 6 regions of the surface of each example.

The routine so far has been only partially automated, although it is not anticipated that a fully automatic routine would be difficult to set up. All samples sent over specifically for this project were of high lustre, so the routine hasn't been systematically explored in the mid-quality lustre region.

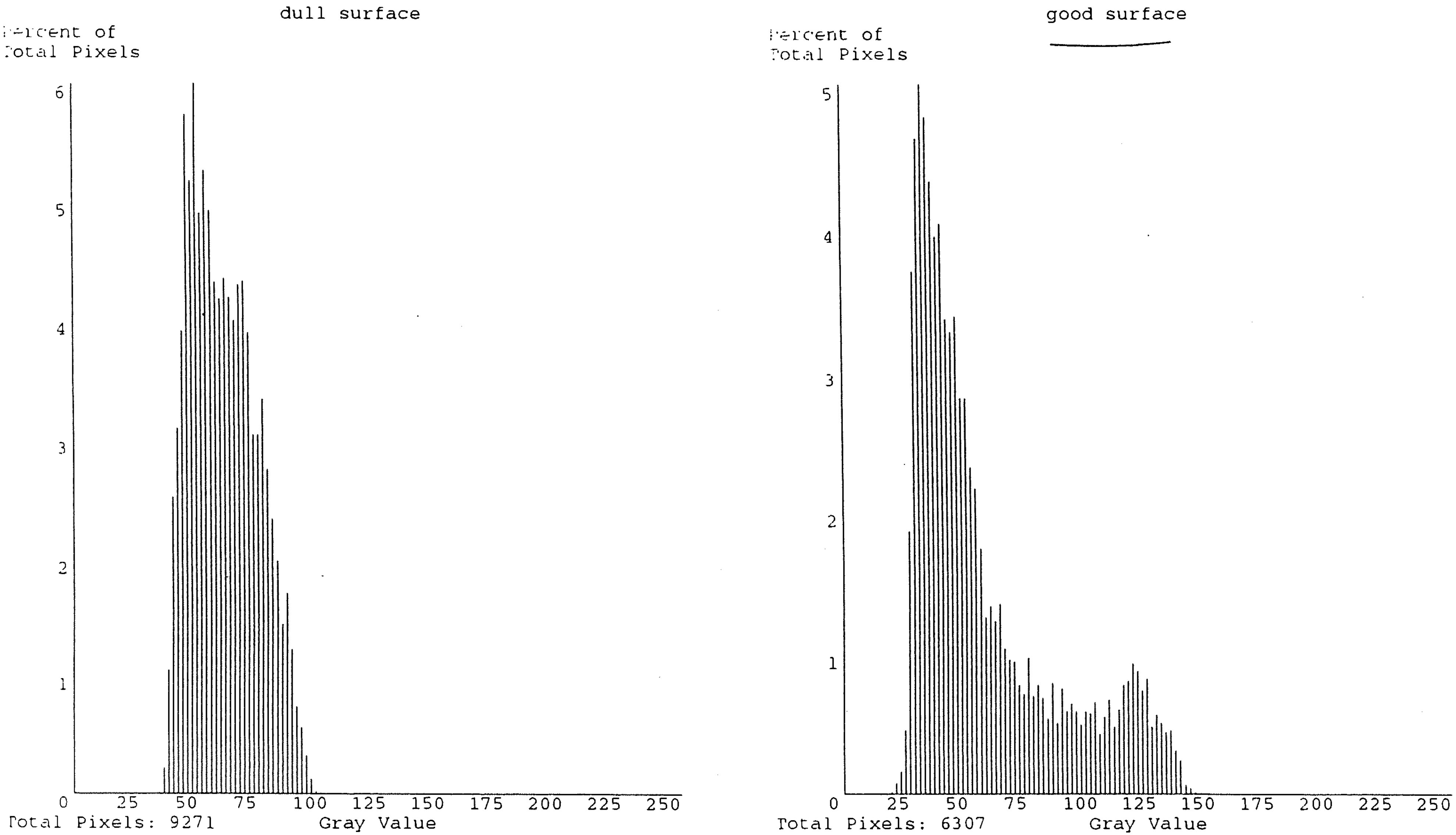


Fig. 15

Lustre Histograms

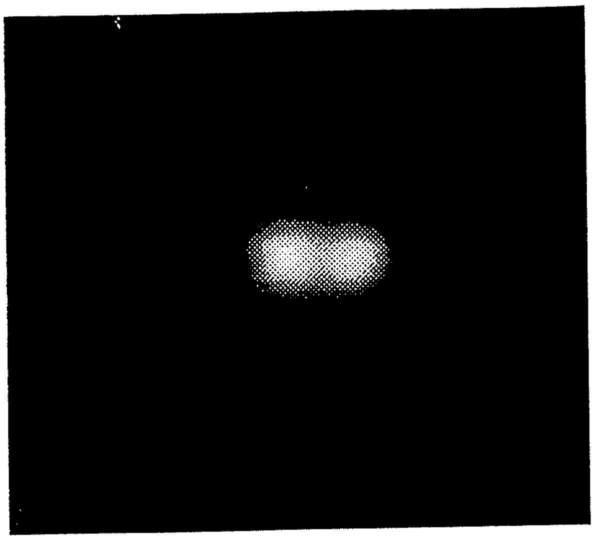

AS1 Round Grade 1

AS4 Round Grade 4

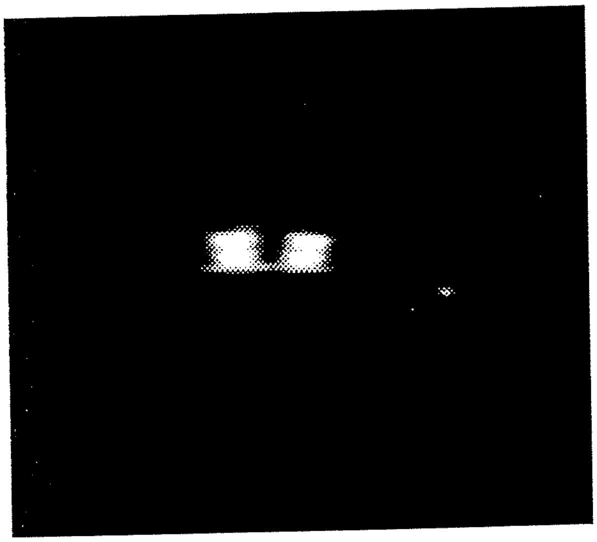

Ball Bearing

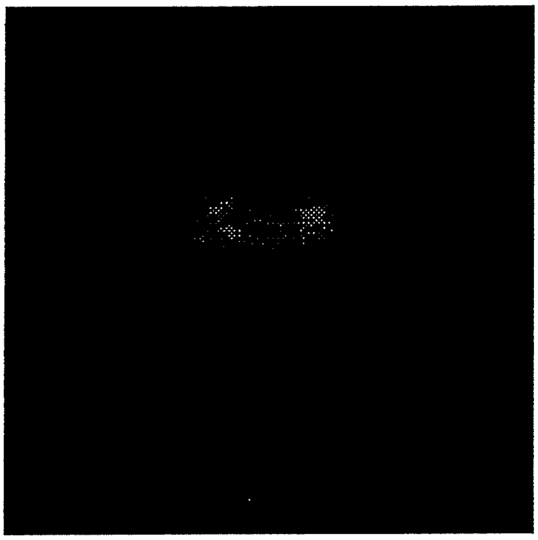

Roebuck Bay
Recoverable Reject

Fig. 16

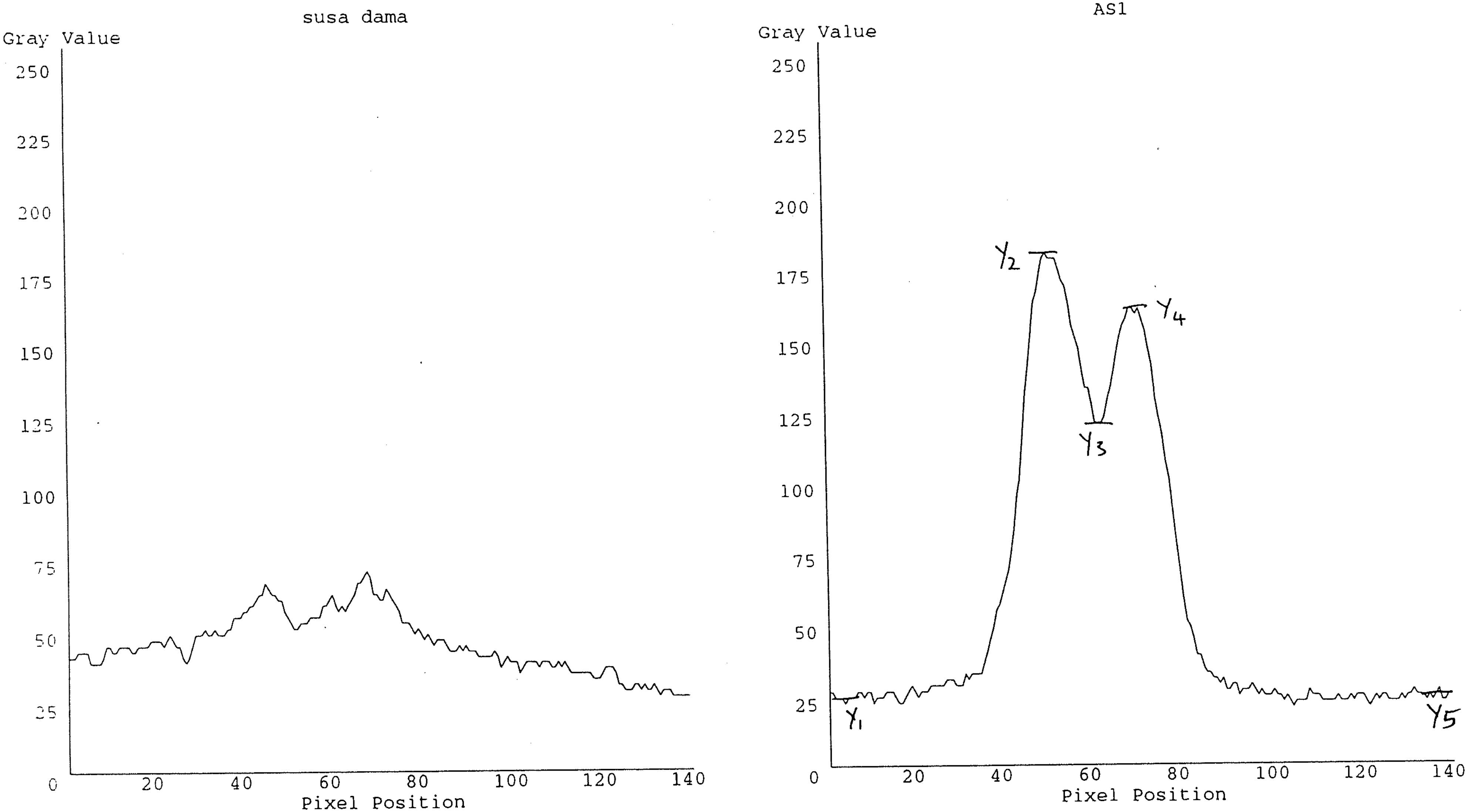


Fig. 17

Line Profiles for Lustre Measurement

| | | | | | | | | | | | |
|---|---|---|---|---|---|---|---|---|---|---|---|
| Lustre Measurement | | | | | | | | | | | |
| | | | | | | | | | | | |
| Pearl | Description | y1 (min1) | y2 (max1) | y3(min2) | y4(max2) | y5(min2) | Lustre Function, LF | | | | |
| | | | | | | | { \|y1-y2\| + \|y2-y3\| + \|y3-y4\| + \|y4-y5\| } | | | | LF |
| | | | | | | | | | | | |
| AS 1 | Round Grade 1 | 22 | 180 | 120 | 160 | 20 | 158 | 60 | 40 | 140 | 398 |
| | | | | | | | | | | | |
| AS 4 | Round Grade 4 | 25 | 181 | 130 | 176 | 23 | 156 | 51 | 46 | 153 | 406 |
| | | | | | | | | | | | |
| RBRR | Roebuck Bay | 40 | 66 | 52 | 70 | 26 | 26 | 14 | 18 | 44 | 102 |
| | Recoverable | | | | | | | | | | |
| | Reject | | | | | | | | | | |
| | | | | | | | | | | | |
| BB | Ball Bearing | 24 | 254 | 40 | 254 | 30 | 230 | 214 | 214 | 224 | 882 |

Fig. 18

# 8. Colour Measurement

A significant precursor to pearl classification attempts has been the development of high speed colour diamond classifiers for Argyle Diamond Mines. The machines use light integrating spheres for optical inspection stations, extracting colour spectral measurements in the visible spectrum at rates around 10 per second. The computer system receiving the spectral information allowed for the teaching of sample colour spectra to the machine memory. This information was then able to be used to best match the unknown diamonds in production to the taught categories. Twelve physical outlet categories were available to place production categories.

In practice, this probably turned out to be one of the most difficult of the set of 5 measurements, due to the spherical mirror-like action of the continually curved surface similar to a spherical mirror. Special care had to be taken to avoid measuring the direct (specular) reflection from the pearl of the light surface.

## 8.1 Imaging Measurement of Colour

The initial measurement system for pearls incorporated an integrating sphere diffusing the light illuminating the pearl, in an attempt to reduce effects of the spherical nature of the pearl surface. With the intention of using a common measurement station for colour and for the other four parameter measurements, the Data Translation HSI Colour Frame Grabber DT 2851 was used to process colour image information from the high quality Pulnix CCD video camera.

The measurement of colour on a shiny spherical surface requires special care. Direct light from the light source should not reflect to the detector, so care was taken to light the pearl as diffusely as possible. Colour readings were then taken by selecting the region of the pearl image in an annulus toward the outer edge of the pearl. By this means the worst of the mirror-like top surface (ie nearest the camera) was avoided.

The HSI (hue saturation and intensity) approach had the advantage that it returned "intensity-like" information on the three colour parameters, each parameter being able to be treated like a grey scale with the GLI imaging software. In this way, hue for example can be isolated and represented as a 256 level variable in the same way as grey scale in a monochrome image. In colour science, hue expresses the concept of rainbow colours, eg bluishness. Saturation is linked to the vividness of hue colours. Intensity corresponds to shades of grey.

Histograms of hue over the surface of the pearl can then be computed by GLI (or tas in this case by the supplied application software with the HSI frame grabber), and patterns matched by a classification routine.

Limited results were obtained due to the presence of only a few colour samples in the batch sent for testing. Numbers for HS&I were between 0 and 255. The summary results were

| | White | Blue/grey | Yellow |
|---|---|---|---|
| Hue | 180 | 178 | 200 |
| Saturation | 45 | 49 | 32 |
| Intensity | 110 | 110 | 95 |

A more detailed table of these results is shown in fig 19. The suggestion from this is that yellow is the only colour safely able to be separated by this method.

### 8.2 Fibre Optic Probe

Because of the difficulty of controlling the specular pattern of light reflecting from the spherical surface of the pearl, the above technique had only moderate success in classifying pearls by colour. It certainly didn't show encouragement toward the subtler shades mentioned by one expert grader. The specular reflection results in transferring essentially the colour of the light source to the light receiver (human eye or TV camera), whereas the diffuse reflection is the one with the colour information about the surface under inspection. During the last phase of measurement taking for the project, an alternative colour analysis system was briefly set up, and evaluated on the same 2 colour-identified samples as above. The apparatus is shown in fig. 22.

A bifurcated optical fibre probe station was set up, with combined (single) end positioned a few mm from the pearl surface (diameter of this end was approx 5mm). One of the separate ends was used as the illumination source (taking light from a stabilised quartz iodine lamp to the pearl surface. The other took reflected light from the pearl surface back to the input of an Oriel monochromator. A photomultiplier was coupled to the output of the monochromator and its response levels read for 10nm wavelength increments from 430 to 730nm.

The spectrum of a plain white card was used as a reference. The monochromator was a manual type, so each pearl took a considerable time to measure, having to read each 10 nm wavelength, and then compute normalised response. In fact a double normalising was applied, once with the white card to get a uniform system response, the again to make each spectrum refer to a 100 level at 430nm.

From graphs of figs 20 and 21, (one with one degree of normalisation, but showing level shifts, the other with those level shifts flattened out), although no formal quantification procedure was adopted, the resulting spectra for yellow, blue, blue/grey and white describe pearls showed some promise of displaying useful classification characteristics. However further quantitative work is needed to see whether the blue from white difference can be reliably picked up. Nevertheless uniformity of response appears to be better than for the imaging method, and as such the fibre optic station could be well integrated into a practical equipment sorting on colour, size and shape at least as a preliminary tool to assist grading.

| Colour Measurements | | | | | |
|---|---|---|---|---|---|
| | | | | | |
| Colour | Pearl | Description | Hue | Saturation | Intensity |
| | | | Mean | Mean | Mean |
| | | | (Std Dev'n) | (Std Dev'n) | (Std Dev'n) |
| | | | | | |
| White | AS 1 | Round Grade 1 | 179.00 | 47.40 | 113.30 |
| | | | (8.0) | (16.0) | (10.0) |
| | | | | | |
| | AS 2 | Round Grade 2 | 180.40 | 44.60 | 115.90 |
| | | | (8.5) | (15.0) | (10.0) |
| | | | | | |
| | AS 3 | Round Grade 3 | 178.60 | 39.30 | 120.60 |
| | | | (10.6) | (14.7) | (12.4) |
| | | | | | |
| | AS 4 | Round Grde 4 | 178.80 | 39.60 | 116.40 |
| | | | (9.0) | (13.0) | (10.2) |
| | | | | | |
| | | | | | |
| Blue/grey | AS 5 | Round Blue/grey | 177.96 | 48.69 | 112.32 |
| | | | (7.70) | (16.0) | (12.0) |
| | | | | | |
| | AS 11 | Button Blue/grey | 178.30 | 49.20 | 107.10 |
| | | | (8.4) | (16.8) | (13.6) |
| | | | | | |
| | | | | | |
| Blue | AS 19 | Circle Blue | 178.00 | 53.70 | 108.00 |
| | | | (7.9) | (18.8) | (14.7) |
| | | | | | |
| | | | | | |
| Yellow | AS 6 | Round Yellow | 198.50 | 32.66 | 100.14 |
| | | | (22.9) | (16.6) | (11.8) |
| | | | | | |
| | AS 20 | Circle Yellow | 203.60 | 34.50 | 88.00 |
| | | | (47.0) | (18.0) | (10.0) |



Fig. 19

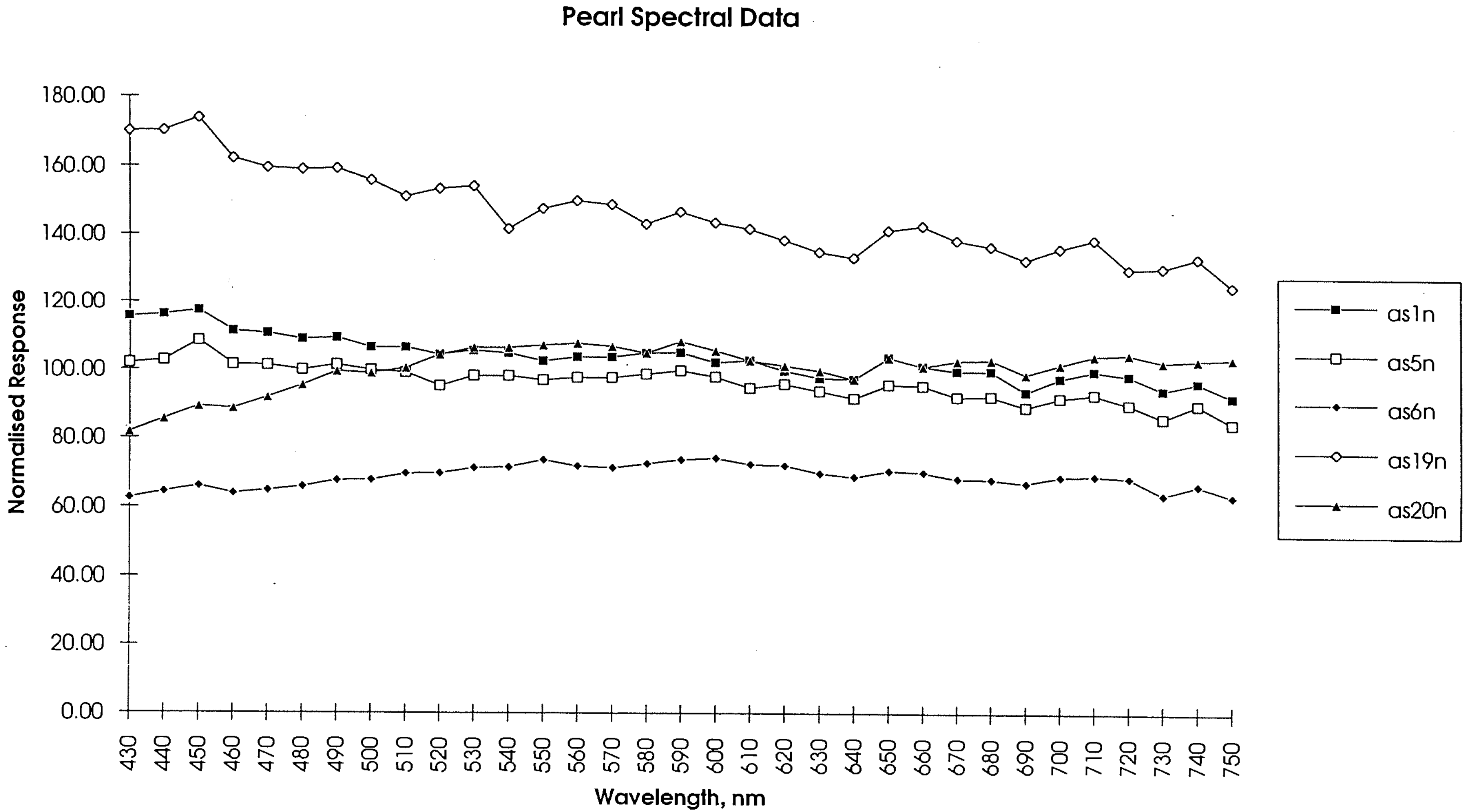
Pearl Spectral Data
180.00
160.00
140.00
120.00
100.00
80.00
60.00
40.00
20.00
0.00
Normalised Response
430 440 450 460 470 480 490 500 510 520 530 540 550 560 570 580 590 600 610 620 630 640 650 660 670 680 690 700 710 720 730 740 750
Wavelength, nm
as1n
as5n
as6n
as19n
as20n

Fig. 20

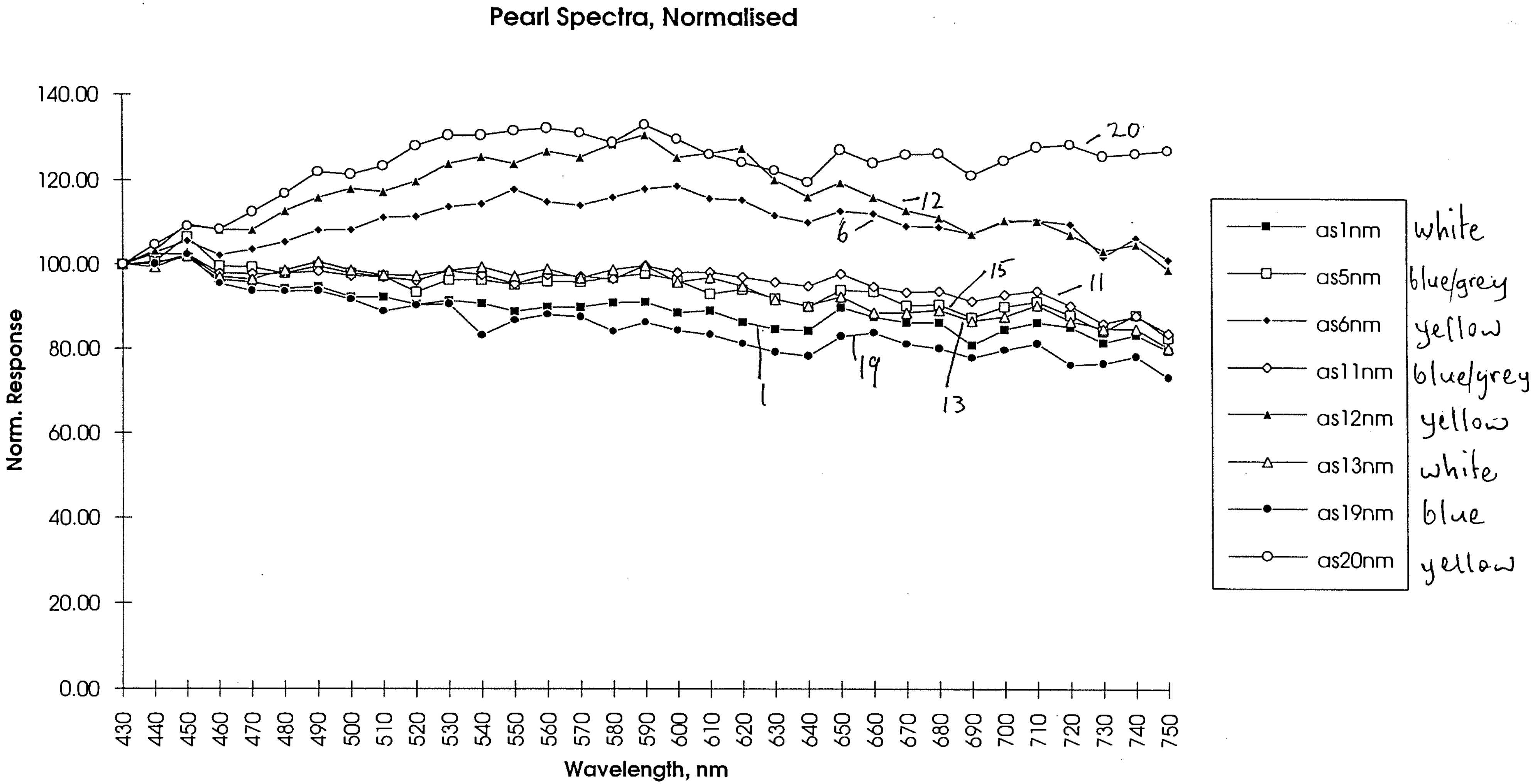
Pearl Spectra, Normalised
140.00
120.00
100.00
80.00
60.00
40.00
20.00
0.00
Norm. Response
430 440 450 460 470 480 490 500 510 520 530 540 550 560 570 580 590 600 610 620 630 640 650 660 670 680 690 700 710 720 730 740 750
Wavelength, nm
20
12
6
15
11
1
19
13
as1nm white
as5nm blue/grey
as6nm yellow
as11nm blue/grey
as12nm yellow
as13nm white
as19nm blue
as20nm yellow

Fig. 21

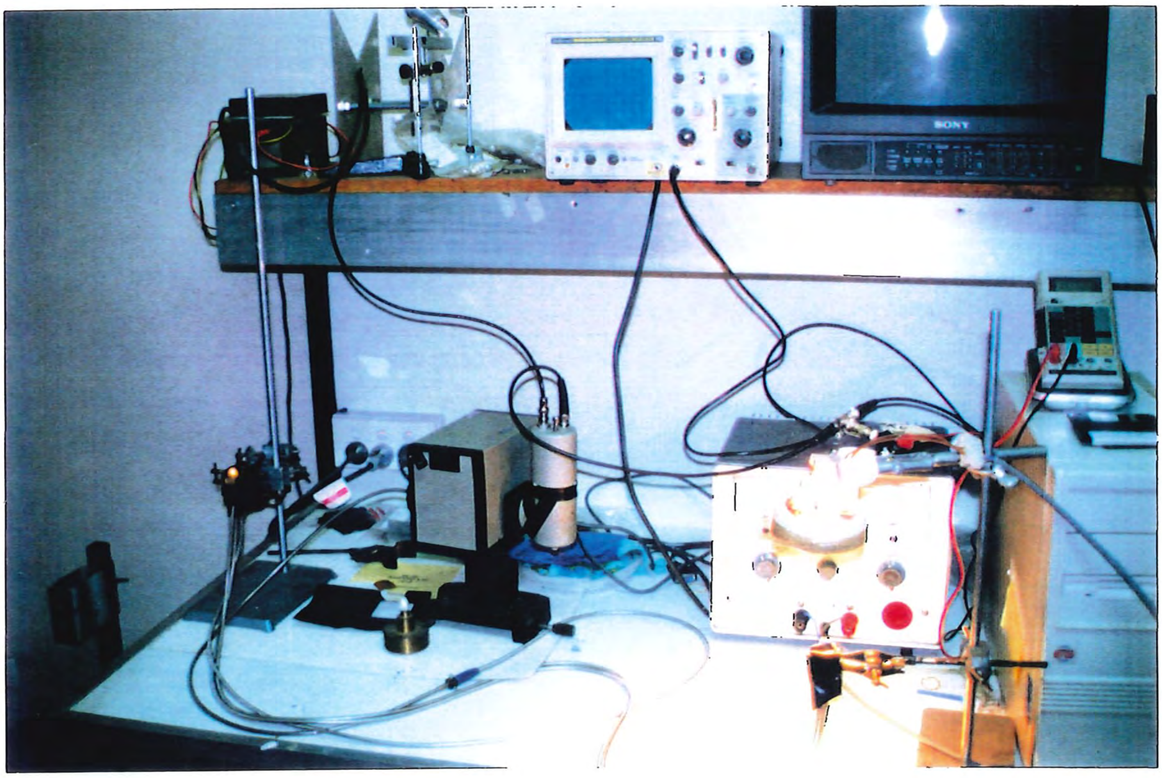


**Fibre Optic Probe Equipment for Colour Measurement**

**(showing on bench from left, pearl seated on brass spacer, bifurcated optical fibre, monochromator with photomultiplier attached, and QI light source with high current DC power supply, with oscilloscope above for output voltage measurement)**

Fig. 22

The colour measurement with a simultaneous spectrometer is rapid, with potential measurement rates of about 100 per second possible. A classification routine would need to be produced - this could be similar to the above described shape classifier system with the spherical harmonic values of the shape routine being replaced by wavelength series. Alternatively the spectra could be mathematically converted into x,y chromaticity coordinates which, as in the diamond classifier system development, could be used to describe like regions of pearl colour response.

The fibre probe system could be realised in a way the pearl is being rotated whilst the spectrum is being measured, thus averaging the colour over more of the pearl's surface.

Peter Hawkins
15th May, 1995

Appendix 1

# An algorithm for object shape classification.

*An interim report for Applied Sorting Pty Ltd*

K.A.Nugent
K.A.Nugent Consulting Pty Ltd
&
Professor of Physics, The University of Melbourne

**Aim.**
The aim of this report is to propose and describe a simple and computationally efficient approach to determining the shape of opaque objects, such as pearls.

**General approach.**
In discussion with Peter Hawkins of Applied Sorting, the intent of this part of the pearl classification project is to find some way of rapidly acquiring shape data and matching it to accepted shape classifications.

The approach proposed here is to observe the shadow of the object as it is rotated on a turntable, or equivalent, and to use some form of processing related to tomographic imaging to deduce its shape. Conventional tomograpic imaging is far too computationally intensive to perform on this problem. On the other hand, full volumetric information is neither desired nor available. Thus, I propose here an algorithm that is loosely based on tomographic ideas and which is able to determine the surface shape of the object.

**Surface algorithm.**
*1. The principle:* Consider first the two-dimensional problem. A projection in a direction specified by θ is shown below.

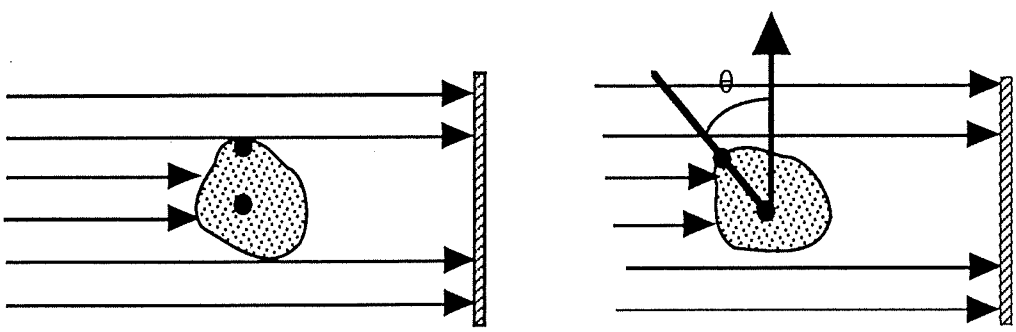


Figure 1: The object is illuminated and the shadow is recorded for a number of object orientations

The object casts a shadow describing the projection of the surface of the object onto the detector. The detector sees areas that are either illuminated or they are not. Further, given the object is a contiguous solid, there will be a well defined boundary separating illuminated regions from those which are not. That is, for the 2D problem, the projection may be fully described by the shadow boundary which is only two numbers in this case. These we denote as $X_1$ and $X_2$ in the figure below.

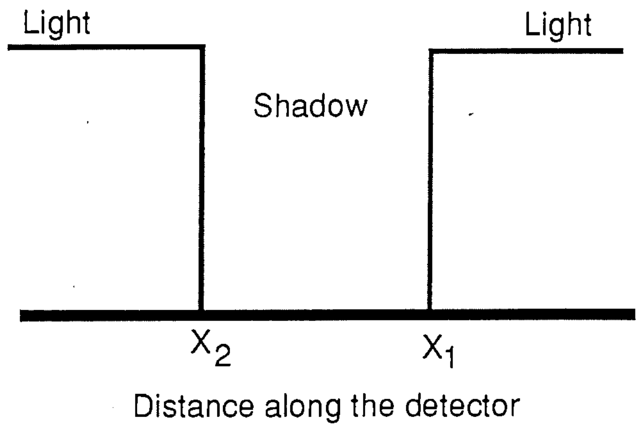


Figure 2: A 1D shadow recorded by the detector. The information in this shadow is fully specified through its boundaries $X_1$ and $X_2$.

We acquire these numbers $X_1$ and $X_2$ for each projection obtained and we denote the projection as 1 in the illuminated region and 0 in the shadow region. To reconstruct the boundary, we set up a 2D array (the "image") containing '0's. Each projection is "backprojected", that is the observed data is smeared back along its direction of projection, as shown below, such that if the image points are converted to '1' if the backprojection is '1' and is left alone if the backprojection is a '0'.

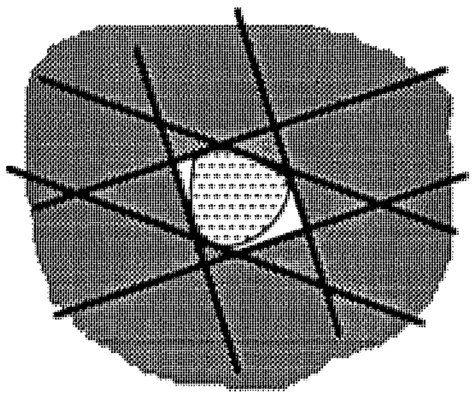

Figure 3: We describe a shadow such as in figure 1 as a 1 if illuminated and 0 if not. Backprojection consists of smearing this back over the object volume. In this figure we show the result of three backprojections for a 2D object. It can be seen that a reasonable representation of the object boundary is obtained.

For a sufficiently large number of backprojections, the area in the image containing '0's will be an excellent representation of the original opaque object. It will then be possible to use this data set to obtain the object boundary. It should be noted that the shadowing used by this approach will not allow the observation of hollows in the object: The algorithm will act to fill them in. I understand that this will not be an important drawback for the pearl classification project.

The principle outlined in preceding paragraphs applies equally well to the surface shape of three-dimensional opaque objects.

2. *Implementation:* For three-dimensional data sets, the approach described above will work but will acquire the retention of a three-dimensional data set in order to determine the surface shape. This imposed rather stringent requirements on data storage in the processing computer. With modern personal computers this will probably not be too much of a problem but it is nevertheless desirable to obtain a more efficient use of computational resources.

Without going into details, it is possible to write out the above principle as a geometric process in which, be choosing an appropriate co-ordinate system, all the above processing can be performed by determining shadow boundaries in the 2D projections and using geometry to determine the 3D object boundary. The geometry to do this is straightforward but messy and will allow the concept described here to be done via a very simple algorithm without requiring three-dimensional data sets.

**Summary**

This report has described a simple and efficient approach that will allow the rapid determination of the surface of the three-dimensional opaque object. The surface information so obtained may then be subsequently used to determine which shape classification that it best meets. The discussion here indicates that it should be possible to directly determine the shape information required for classification to occur. It remains to be seen how many backprojections will be required in order to obtain an adequate boundary description .

Appendix 2

# Shape Determination Using Spherical Harmonics

In the case of an object with aproximately spherical symmetry, such as a pearl, one may describe the shape of the object using the function $R(\theta,\phi)$ which gives the radius of the pearl as a function of two angles.

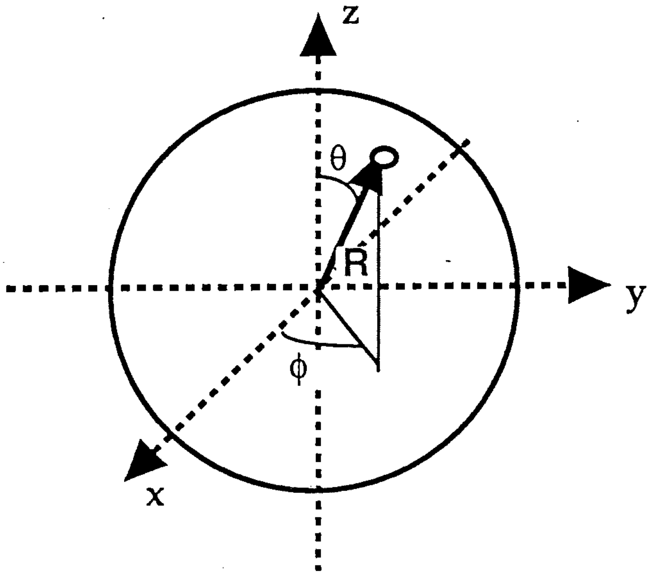


*Co-ordinates used to specify 'radius' as a function of the angles θ and ϕ.*

This description does not characterize the pearl shape very clearly and there are advantages to writing the pearl shape as a series of spherical harmonics,

$$R(\theta,\phi) = \sum_{\ell=0}^{p} \sum_{m=-\ell}^{+\ell} A_\ell^m Y_\ell^m(\theta,\phi)$$

where the pearl shape is now fully determined by the numbers $A_\ell^m$ where $\ell$ runs from 1 up to highest number chosen (eight in the work so far) and m runs from $-\ell$ to $+\ell$. $Y_\ell^m(\theta,\phi)$ are the functions known as spherical harmonics. The numbers $A_\ell^m$ are entirely analogous to the frequency distribution obtained by Fourier analysis for one and two dimensional signals.

In this case, for example, a perfect sphere has $A_0^0 = R$, where R is the radius of the sphere, and all the other terms are zero. As the pearl deviates from purely spherical, other A's become significant and the pattern of co-efficients excited is characteristic of the pearl shape. In this project, the aim is to determine the coefficients corresponding to different pearl shapes so as to allow their shape to be determined.

The output of the fitting program, then, is a set of numbers of the folowing form, where we show numbers only up to $\ell$=6.

| | | | | | | |
|---|---|---|---|---|---|---|
| | | | | | | $A_6^{+6}$ |
| | | | | | $A_5^{+5}$ | $A_6^{+5}$ |
| | | | | $A_4^{+4}$ | $A_5^{+4}$ | $A_6^{+4}$ |
| | | | $A_3^{+3}$ | $A_4^{+3}$ | $A_5^{+3}$ | $A_6^{+3}$ |
| | | $A_2^{+2}$ | $A_3^{+2}$ | $A_4^{+2}$ | $A_5^{+2}$ | $A_6^{+2}$ |
| | $A_1^{+1}$ | $A_2^{+1}$ | $A_3^{+1}$ | $A_4^{+1}$ | $A_5^{+1}$ | $A_6^{+1}$ |
| $A_0^0$ | $A_1^0$ | $A_2^0$ | $A_3^0$ | $A_4^0$ | $A_5^0$ | $A_5^0$ |
| | $A_1^{-1}$ | $A_2^{-1}$ | $A_3^{-1}$ | $A_4^{-1}$ | $A_5^{-1}$ | $A_6^{-1}$ |
| | | $A_2^{-2}$ | $A_3^{-2}$ | $A_4^{-2}$ | $A_5^{-2}$ | $A_6^{-2}$ |
| | | | $A_3^{-3}$ | $A_4^{-3}$ | $A_5^{-3}$ | $A_6^{-3}$ |
| | | | | $A_4^{-4}$ | $A_5^{-4}$ | $A_6^{-4}$ |
| | | | | | $A_5^{-5}$ | $A_6^{-5}$ |
| | | | | | | $A_6^{-6}$ |
| CL(1) | CL(2) | CL(3) | CL(4) | CL(5) | CL(6) | CL(7) |

This set of numbers acts as a unique fingerprint for the shape of the pearl.

For most purposes, there is more detail than is required in these numbers and so, in practice, they are compressed into two sets of seven (in the above example but nine are used in practice) numbers by adding along the rows and the columns, so that CL(1), CL(2) etc shown above are the sum of the squares of all the numbers above it. The data CJ(m) etc are the sums of squares for the rows for both plus and minus m.

| | | | | | | | |
|---|---|---|---|---|---|---|---|
| Shape tests on Second Series | | | | | | | |
| Minimum Distance Classifier | | | | | | | |
| | | | | | | | |
| Pearl | | Round | Drop | Button | Semi-<br>Baroque | Circle | Decision |
| Round | | | | | | | |
| Group | | | | | | | |
| | | | | | | | |
| 1 | | 0.979 | 9.123 | 4.178 | 4.530 | 14.007 | Round |
| 2 | | 1.358 | 9.181 | 4.262 | 4.200 | 13.963 | Round |
| 3 | | 1.860 | 8.430 | 5.376 | 5.105 | 12.913 | Round |
| 4 | | 1.005 | 9.150 | 4.608 | 4.931 | 14.162 | Round |
| 5 | | 1.099 | 9.085 | 4.929 | 5.597 | 14.385 | Round |
| 6 | | 1.414 | 7.982 | 3.878 | 3.795 | 13.041 | Round |
| 7 | | 1.346 | 9.027 | 4.356 | 5.152 | 13.972 | Round |
| 8 | | 1.642 | 7.556 | 4.276 | 4.163 | 12.601 | Round |
| 9 | | 2.482 | 7.351 | 4.062 | 4.080 | 12.628 | Round |
| 10 | | 1.327 | 7.405 | 4.620 | 4.508 | 12.527 | Round |
| | | | | | | | |
| 11 | | 0.922 | 8.930 | 4.383 | 4.812 | 13.806 | Round |
| 12 | | 1.156 | 8.441 | 5.075 | 4.896 | 13.462 | Round |
| 13 | | 1.017 | 9.063 | 4.849 | 5.073 | 13.939 | Round |
| 14 | | 0.980 | 9.242 | 4.663 | 4.952 | 14.117 | Round |
| 15 | | 1.385 | 8.435 | 4.727 | 5.077 | 12.915 | Round |
| 16 | | 0.740 | 9.168 | 4.659 | 4.964 | 14.156 | Round |
| 17 | | 1.008 | 9.125 | 4.440 | 4.839 | 14.029 | Round |
| 18 | | 2.367 | 6.858 | 4.302 | 2.981 | 11.969 | Round |
| 19 | | 2.040 | 7.635 | 4.343 | 3.624 | 12.703 | Round |
| 20 | | 1.388 | 8.300 | 4.925 | 4.908 | 13.158 | Round |
| | | | | | | | |
| 21 | | 1.397 | 8.640 | 4.056 | 3.988 | 13.544 | Round |
| 22 | | 1.802 | 9.603 | 5.067 | 5.765 | 14.491 | Round |
| 23 | | 0.679 | 8.860 | 4.821 | 5.071 | 13.736 | Round |
| 24 | | 1.020 | 9.164 | 4.488 | 5.243 | 14.133 | Round |
| 25 | | 1.585 | 8.105 | 3.629 | 3.781 | 13.079 | Round |
| 26 | | 1.403 | 9.333 | 4.059 | 4.418 | 14.097 | Round |
| 27 | | 0.933 | 8.698 | 4.747 | 4.776 | 13.524 | Round |
| 28 | | 1.830 | 7.688 | 4.223 | 3.363 | 12.597 | Round |
| 29 | | 1.303 | 8.271 | 4.793 | 4.666 | 13.146 | Round |
| 30 | | 1.405 | 9.549 | 4.466 | 4.799 | 14.322 | Round |
| 31 | | 2.316 | 7.573 | 4.672 | 4.826 | 12.166 | Round |

| Shape tests on Second Series | | | | | | | |
|---|---|---|---|---|---|---|---|
| Minimum Distance Classifier | | | | | | | |
| | | | | | | | |
| Pearl | | Round | Drop | Button | Semi-Baroque | Circle | Decision |
| Drop | | | | | | | |
| Group | | | | | | | |
| | | | | | | | |
| 1 | | 3.561 | 6.447 | 5.465 | 2.959 | 11.648 | S-Baroque |
| 2 | | 16.269 | 9.216 | 17.961 | 15.589 | 6.121 | Circle |
| 3 | | | | | | | |
| 4 | | 8.33 | 1.484 | 9.733 | 7.448 | 6.539 | Drop |
| 5 | | 12.119 | 4.706 | 12.913 | 11.218 | 7.488 | Drop |
| 6 | | 6.07 | 4.586 | 8.167 | 5.958 | 10.95 | Drop |
| 7 | | 9.809 | 3.442 | 11.889 | 9.565 | 6.128 | Drop |
| 8 | | 5.925 | 4.68 | 6.805 | 4.742 | 8.876 | Drop |
| 9 | | 4.164 | 5.252 | 5.44 | 3.75 | 11.352 | S-Baroque |
| 10 | | 6.441 | 4.611 | 7.264 | 4.547 | 10.253 | S-Baroque |
| | | | | | | | |
| 11 | | 14.379 | 8.716 | 16.209 | 13.886 | 14.42 | Drop |
| 12 | | 5.401 | 5.395 | 5.456 | 2.654 | 11.648 | S-Baroque |
| 13 | | 9.593 | 7.16 | 11.362 | 9.038 | 13.365 | Drop |
| 14 | | 16.223 | 9.788 | 18.234 | 15.91 | 15.297 | Drop |
| 15 | | 12.38 | 6.433 | 13.517 | 10.993 | 5.269 | Circle |
| 16 | | 14.103 | 6.347 | 13.37 | 11.675 | 6.576 | Drop |
| 17 | | 7.108 | 3.689 | 6.732 | 4.941 | 8.792 | Drop |
| 18 | | 14.78 | 6.159 | 15.089 | 13.394 | 2.588 | Circle |
| 19 | | 6.568 | 6.474 | 5.499 | 8.069 | 11.177 | Button |
| 20 | | 8.022 | 6.728 | 7.701 | 9.636 | 12.287 | Drop |
| | | | | | | | |
| 21 | | 9.785 | 2.319 | 10.579 | 8.884 | 5.07 | Drop |
| 22 | | 6.752 | 4.817 | 6.715 | 3.089 | 9.765 | S-Baroque |
| 23 | | 9.955 | 2.962 | 10.471 | 7.736 | 5.268 | Drop |
| 24 | | 11.332 | 4.093 | 9.632 | 6.586 | 6.817 | Drop |
| 25 | | 6.799 | 5.715 | 6.637 | 2.349 | 10.636 | S-Baroque |
| 26 | | 10.926 | 4.154 | 11.026 | 9.013 | 5.478 | Drop |
| 27 | | 9.108 | 3.481 | 7.787 | 4.89 | 8.307 | Drop |
| 28 | | 7.648 | 4.242 | 7.05 | 3.479 | 9.045 | S-Baroque |
| 29 | | 7.033 | 6.319 | 6.326 | 2.138 | 11.084 | S-Baroque |
| 30 | | 5.495 | 3.891 | 6.388 | 3.785 | 9.031 | S-Baroque |
| | | | | | | | |
| 31 | | 9.383 | 1.303 | 9.684 | 7.989 | 5.889 | Drop |
| 32 | | 7.892 | 2.316 | 7.629 | 5.613 | 8.183 | Drop |
| 33 | | 5.593 | 4.452 | 5.806 | 3.483 | 10.141 | S-Baroque |
| 34 | | 8.213 | 3.271 | 7.752 | 5.696 | 7.321 | Drop |
| 35 | | 5.837 | 4.408 | 5.913 | 4.138 | 10.045 | S-Baroque |
| 36 | | 7.668 | 3.773 | 7.45 | 5.516 | 9.3 | Drop |
| 37 | | 4.397 | 4.845 | 4.913 | 3.162 | 10.122 | S-Baroque |
| 38 | | 6.826 | 3.75 | 7.53 | 4.567 | 8.276 | Drop |
| 39 | | 4.467 | 6.422 | 3.822 | 3.35 | 12.422 | S-Baroque |
| 40 | | 4.102 | 5.566 | 5.087 | 3.728 | 11.676 | S-Baroque |

| | | | | | | | |
|---|---|---|---|---|---|---|---|
| 41 | | 3.556 | 6.172 | 4.456 | 2.769 | 11.3 | S-Baroque |
| 42 | | 4.408 | 5.674 | 4.318 | 2.137 | 11.185 | S-Baroque |
| 43 | | 3.578 | 6.046 | 3.807 | 3.376 | 12.146 | S-Baroque |
| 44 | | 5.794 | 5.674 | 5.934 | 2.26 | 11.438 | S-Baroque |
| 45 | | 5.407 | 5.321 | 5.108 | 3.413 | 10.62 | S-Baroque |
| 46 | | 5.33 | 5.347 | 4.526 | 2.376 | 10.55 | S-Baroque |
| 47 | | 4.409 | 5.952 | 4.294 | 1.707 | 11.092 | S-Baroque |
| 48 | | 7.592 | 5.242 | 8.006 | 4.462 | 10.26 | S-Baroque |
| 49 | | 4.951 | 5.919 | 5.055 | 2.024 | 10.684 | S-Baroque |
| 50 | | 6.309 | 2.971 | 8.765 | 5.18 | 7.936 | Drop |

| | | | | | | | |
|---|---|---|---|---|---|---|---|
| Shape tests on Second Series | | | | | | | |
| Minimum Distance Classifier | | | | | | | |
| | | | | | | | |
| Pearl | | Round | Drop | Button | Semi-Baroque | Circle | Decision |
| | | | | | | | |
| Button | | | | | | | |
| Group | | | | | | | |
| | | | | | | | |
| 1 | | 6.083 | 6.298 | 4.293 | 7.154 | 11.778 | Button |
| 2 | | 1.771 | 8.838 | 5.486 | 6.107 | 14.080 | Round |
| 3 | | 2.878 | 10.389 | 7.221 | 7.347 | 14.546 | Round |
| 4 | | 3.552 | 9.495 | 3.919 | 6.439 | 15.495 | Round |
| 5 | | 1.892 | 9.033 | 2.824 | 5.239 | 14.050 | Round |
| 6 | | 2.354 | 8.867 | 5.560 | 6.953 | 14.462 | Round |
| 7 | | 7.400 | 5.521 | 6.809 | 8.923 | 11.184 | Drop |
| 8 | | 6.941 | 7.888 | 9.037 | 7.179 | 14.252 | Round |
| 9 | | 2.488 | 8.914 | 3.372 | 6.653 | 13.667 | Round |
| 10 | | | | | | | |
| | | | | | | | |
| 11 | | 4.691 | 7.567 | 2.857 | 5.916 | 12.916 | Button |
| 12 | | 7.591 | 8.512 | 5.898 | 5.714 | 13.321 | ~~Button~~ SB. |
| 13 | | 4.804 | 9.710 | 2.624 | 4.067 | 14.611 | Button |
| 14 | | 6.619 | 8.544 | 2.923 | 5.650 | 13.685 | Button |
| 15 | | 4.476 | 8.214 | 3.365 | 5.320 | 13.307 | Button |
| 16 | | 2.231 | 8.838 | 2.826 | 6.209 | 14.250 | Round |
| 17 | | 10.122 | 9.294 | 6.463 | 8.815 | 14.978 | Button |
| 18 | | 5.521 | 9.703 | 3.710 | 5.332 | 14.604 | Button |
| 19 | | 4.213 | 9.760 | 3.144 | 7.042 | 13.580 | Button |
| 20 | | 5.232 | 9.663 | 3.346 | 4.535 | 14.615 | Button |
| | | | | | | | |
| 21 | | 2.377 | 10.281 | 4.538 | 5.352 | 15.242 | Round |
| 22 | | 4.405 | 11.514 | 5.570 | 9.216 | 14.727 | Round |
| 23 | | 2.615 | 10.692 | 3.311 | 5.039 | 15.457 | Round |
| 24 | | 3.423 | 9.963 | 4.292 | 4.278 | 14.712 | Round |
| 25 | | 3.873 | 9.863 | 3.533 | 5.421 | 15.942 | Button |
| 26 | | 2.900 | 9.375 | 3.664 | 6.086 | 15.190 | Round |
| 27 | | 2.427 | 10.057 | 4.138 | 4.905 | 14.828 | Round |
| 28 | | 5.283 | 10.999 | 2.732 | 5.048 | 16.237 | Button |
| 29 | | 2.526 | 9.815 | 3.738 | 5.576 | 15.152 | Round |
| 30 | | 3.266 | 9.078 | 4.367 | 3.870 | 13.441 | Round |

| | | | | | | | |
|---|---|---|---|---|---|---|---|
| Shape tests on Second Series | | | | | | | |
| Minimum Distance Classifier | | | | | | | |
| | | | | | | | |
| Pearl | | Round | Drop | Button | Semi-Baroque | Circle | Decision |
| | | | | | | | |
| Semi-Baroque | | | | | | | |
| Group | | | | | | | |
| | | | | | | | |
| 1 | | 8.361 | 9.723 | 9.684 | 8.150 | 16.035 | S-Baroque |
| 2 | | 6.939 | 4.181 | 8.663 | 6.183 | 9.852 | Drop |
| 3 | | 1.803 | 8.905 | 5.548 | 5.482 | 13.818 | Round |
| 4 | | 3.695 | 6.457 | 5.257 | 3.830 | 12.588 | Round |
| 5 | | 2.522 | 9.726 | 6.750 | 6.489 | 14.909 | Round |
| 6 | | 2.233 | 7.748 | 5.367 | 5.155 | 12.525 | Round |
| 7 | | 5.978 | 7.692 | 7.792 | 6.009 | 12.064 | Round |
| 8 | | 7.262 | 4.300 | 9.125 | 6.703 | 9.298 | Drop |
| 9 | | 2.266 | 9.237 | 6.133 | 6.358 | 14.476 | Round |
| 10 | | 6.217 | 10.512 | 8.330 | 8.989 | 14.859 | Round |
| | | | | | | | |
| 11 | | 6.694 | 4.115 | 7.624 | 4.662 | 8.580 | Drop |
| 12 | | 13.964 | 7.522 | 14.312 | 11.795 | 6.100 | Circle |
| 13 | | 4.603 | 7.790 | 5.225 | 1.508 | 12.755 | S-Baroque |
| 14 | | 4.970 | 5.178 | 6.720 | 4.708 | 10.527 | S-Baroque |
| 15 | | 8.930 | 4.520 | 10.263 | 7.868 | 6.306 | Drop |
| 16 | | 3.886 | 9.468 | 5.294 | 6.143 | 13.155 | Round |
| 17 | | 3.020 | 6.160 | 5.096 | 3.583 | 10.810 | Round |
| 18 | | 4.164 | 8.259 | 5.311 | 2.729 | 12.910 | S-Baroque |
| 19 | | 3.722 | 11.868 | 6.720 | 5.683 | 16.853 | Round |
| 20 | | 8.163 | 4.444 | 8.918 | 7.215 | 9.492 | Drop |
| | | | | | | | |
| 21 | | 4.186 | 5.161 | 4.949 | 2.857 | 10.870 | S-Baroque |
| 22 | | 5.974 | 6.156 | 4.298 | 6.979 | 11.087 | Button |
| 23 | | 6.222 | 5.524 | 7.596 | 5.748 | 8.194 | Drop |
| 24 | | 3.207 | 7.107 | 3.533 | 3.169 | 13.075 | S-Baroque |
| 25 | | 4.649 | 10.984 | 6.961 | 5.942 | 17.091 | Round |
| 26 | | 8.850 | 4.878 | 8.197 | 6.436 | 10.384 | Drop |
| 27 | | 10.205 | 4.091 | 9.564 | 5.963 | 6.813 | Drop |
| 28 | | 13.298 | 5.692 | 14.274 | 12.359 | 2.339 | Circle |
| 29 | | 17.205 | 8.905 | 17.990 | 16.295 | 6.458 | Circle |
| 30 | | 16.939 | 11.029 | 19.143 | 16.259 | 9.786 | Circle |
| | | | | | | | |
| 31 | | 22.027 | 16.199 | 24.078 | 21.030 | 10.605 | Circle |
| 32 | | 4.229 | 5.319 | 4.790 | 3.370 | 11.392 | S-Baroque |
| 33 | | 3.397 | 7.383 | 5.039 | 3.374 | 12.148 | S-Baroque |
| 34 | | 2.596 | 7.887 | 3.454 | 2.927 | 12.683 | Round |
| 35 | | 2.204 | 9.165 | 4.030 | 3.634 | 14.525 | Round |
| 36 | | 2.073 | 8.661 | 4.542 | 4.360 | 13.574 | Round |
| 37 | | 1.750 | 7.956 | 4.035 | 5.002 | 12.860 | Round |
| 38 | | 2.781 | 7.805 | 4.840 | 4.225 | 12.577 | Round |
| 39 | | 1.252 | 8.849 | 4.057 | 4.453 | 13.810 | Round |
| 40 | | 3.007 | 9.424 | 4.828 | 4.566 | 14.800 | Round |

| | | | | | | | |
|---|---|---|---|---|---|---|---|
| | | | | | | | |
| 41 | | 1.583 | 8.302 | 4.064 | 3.610 | 13.252 | Round |
| 42 | | 3.012 | 10.311 | 5.871 | 3.865 | 15.186 | Round |
| 43 | | 3.468 | 5.715 | 4.548 | 2.740 | 10.635 | S-Baroque |
| 44 | | 2.200 | 9.522 | 4.515 | 5.645 | 14.435 | Round |
| 45 | | 2.699 | 9.070 | 4.534 | 4.397 | 15.091 | Round |
| 46 | | 2.908 | 10.879 | 5.331 | 4.143 | 15.867 | Round |
| 47 | | 2.516 | 8.987 | 4.753 | 6.568 | 15.246 | Round |
| 48 | | 2.422 | 7.220 | 3.514 | 3.460 | 12.961 | Round |
| 49 | | 2.496 | 7.878 | 3.707 | 2.878 | 12.989 | Round |
| 50 | | 2.355 | 8.433 | 3.540 | 4.533 | 14.286 | Round |

| | | | | | | | |
|---|---|---|---|---|---|---|---|
| Shape tests on Second Series | | | | | | | |
| Minimum Distance Classifier | | | | | | | |
| | | | | | | | |
| Pearl | | Round | Drop | Button | Semi-Baroque | Circle | Decision |
| | | | | | | | |
| Circle | | | | | | | |
| Group | | | | | | | |
| | | | | | | | |
| 1 | | 9.095 | 2.850 | 10.274 | 8.228 | 5.448 | Drop |
| 2 | | 5.446 | 5.573 | 7.482 | 5.104 | 11.089 | S-Baroque |
| 3 | | 11.250 | 5.634 | 13.735 | 10.478 | 5.549 | Circle |
| 4 | | 8.226 | 4.412 | 10.410 | 7.011 | 6.994 | Drop |
| 5 | | 2.837 | 6.339 | 4.323 | 2.866 | 11.385 | Round |
| 6 | | 15.978 | 9.855 | 18.124 | 15.370 | 6.218 | Circle |
| 7 | | 6.357 | 7.585 | 7.514 | 5.463 | 13.662 | S-Baroque |
| 8 | | 8.220 | 2.032 | 8.813 | 6.895 | 6.107 | Drop |
| 9 | | 14.770 | 6.625 | 15.930 | 14.232 | 4.350 | Circle |
| 10 | | 6.707 | 5.988 | 7.477 | 7.501 | 9.319 | Drop |
| | | | | | | | |
| 11 | | 18.581 | 12.066 | 18.442 | 14.922 | 10.200 | Circle |
| 12 | | 10.243 | 4.190 | 10.861 | 8.537 | 9.761 | Drop |
| 13 | | 2.706 | 10.822 | 3.081 | 5.143 | 15.873 | Round |
| 14 | | 9.541 | 5.362 | 11.887 | 8.925 | 8.490 | Drop |
| 15 | | 20.393 | 13.575 | 19.683 | 16.897 | 10.254 | Circle |
| 16 | | 25.210 | 32.368 | 27.976 | 29.905 | 38.732 | Round |
| 17 | | 19.576 | 11.910 | 18.214 | 15.669 | 9.764 | Circle |
| 18 | | 11.005 | 7.184 | 12.243 | 10.651 | 10.645 | Drop |
| 19 | | 15.617 | 8.285 | 17.159 | 14.835 | 4.759 | Circle |
| 20 | | 17.080 | 8.844 | 17.850 | 16.155 | 4.252 | Circle |
| | | | | | | | |
| 21 | | 21.626 | 13.363 | 22.637 | 20.942 | 8.568 | Circle |
| 22 | | 16.280 | 8.086 | 17.171 | 15.476 | 5.056 | Circle |
| 23 | | 13.611 | 7.430 | 15.496 | 13.162 | 2.987 | Circle |
| 24 | | 16.495 | 8.232 | 17.364 | 15.669 | 3.933 | Circle |
| 25 | | 11.418 | 3.250 | 11.915 | 10.135 | 4.833 | Circle |
| 26 | | 13.847 | 6.364 | 14.270 | 12.281 | 2.531 | Circle |
| 27 | | 30.609 | 24.166 | 30.883 | 28.491 | 22.212 | Circle |
| 28 | | 8.845 | 2.187 | 9.853 | 7.422 | 5.185 | Drop |
| 29 | | 9.285 | 4.663 | 10.040 | 8.340 | 7.415 | Drop |
| 30 | | 11.474 | 5.309 | 12.457 | 9.971 | 5.181 | Circle |
| | | | | | | | |
| 31 | | 13.732 | 5.227 | 14.043 | 12.348 | 2.998 | Circle |
| 32 | | 11.425 | 4.456 | 12.666 | 10.507 | 2.593 | Circle |
| 33 | | 10.834 | 2.487 | 11.729 | 10.034 | 4.088 | Drop |
| 34 | | 9.030 | 2.586 | 10.073 | 7.328 | 5.494 | Drop |
| 35 | | 9.485 | 6.800 | 10.728 | 9.249 | 8.612 | Drop |
| 36 | | 11.660 | 4.859 | 11.377 | 8.594 | 8.324 | Drop |
| 37 | | 5.103 | 4.306 | 6.443 | 4.417 | 10.053 | Drop |
| 38 | | 6.613 | 3.712 | 6.343 | 4.525 | 9.061 | Drop |
| 39 | | 5.040 | 11.488 | 6.014 | 8.160 | 13.745 | Round |
| 40 | | 7.786 | 6.325 | 9.148 | 9.172 | 9.828 | Drop |

| | | | | | | | |
|---|---|---|---|---|---|---|---|
| | | | | | | | |
| 41 | | 6.681 | 7.714 | 3.493 | 5.416 | 12.292 | Button |
| 42 | | 4.799 | 5.154 | 7.045 | 4.979 | 10.564 | Round |
| 43 | | 3.812 | 11.340 | 5.614 | 8.131 | 15.312 | Round |
| 44 | | 4.602 | 8.784 | 3.074 | 7.403 | 14.805 | Button |
| 45 | | 4.460 | 10.824 | 5.577 | 9.156 | 15.386 | Round |
| 46 | | 2.397 | 6.998 | 4.167 | 5.164 | 12.791 | Round |
| 47 | | 6.574 | 2.800 | 6.689 | 4.952 | 8.491 | Drop |
| 48 | | 5.226 | 5.982 | 6.810 | 5.112 | 8.777 | S-Baroque |
| 49 | | 4.922 | 10.317 | 3.813 | 6.369 | 14.805 | Button |
| 50 | | | | | | | |

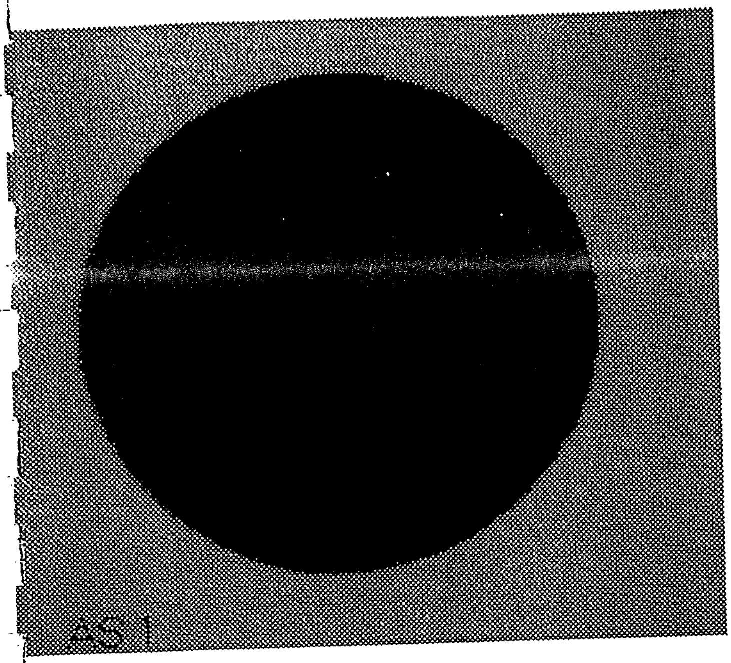

AS 1

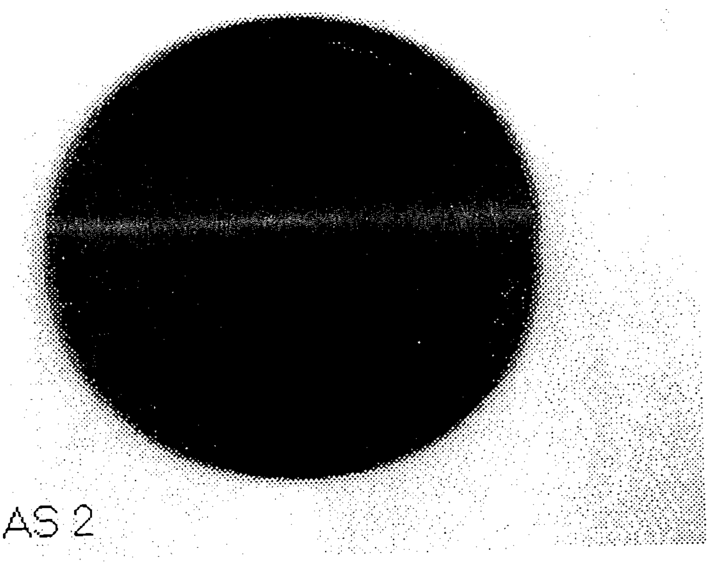

AS 2

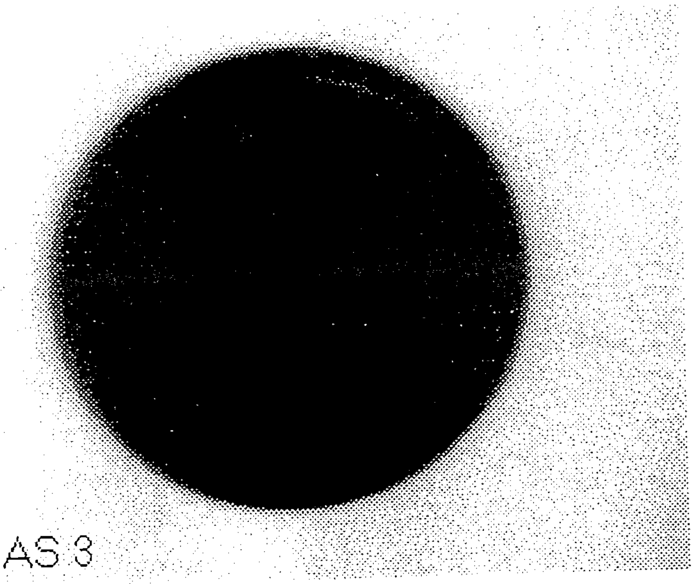

AS 3

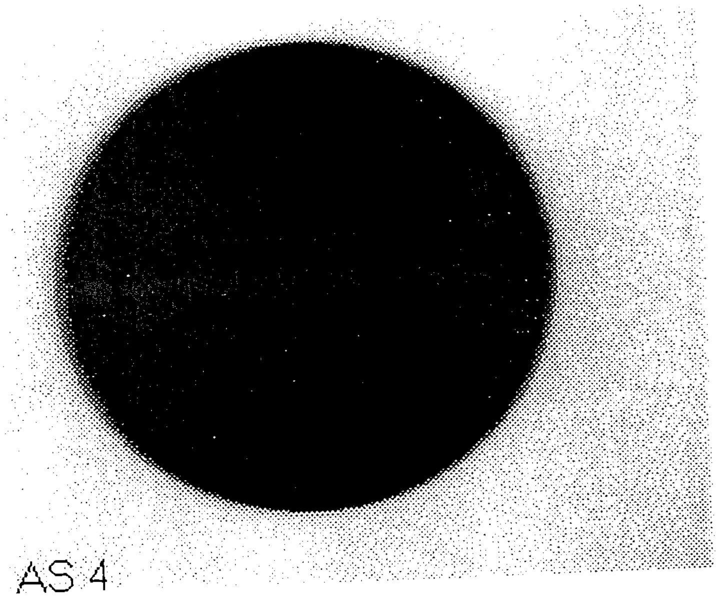

AS 4

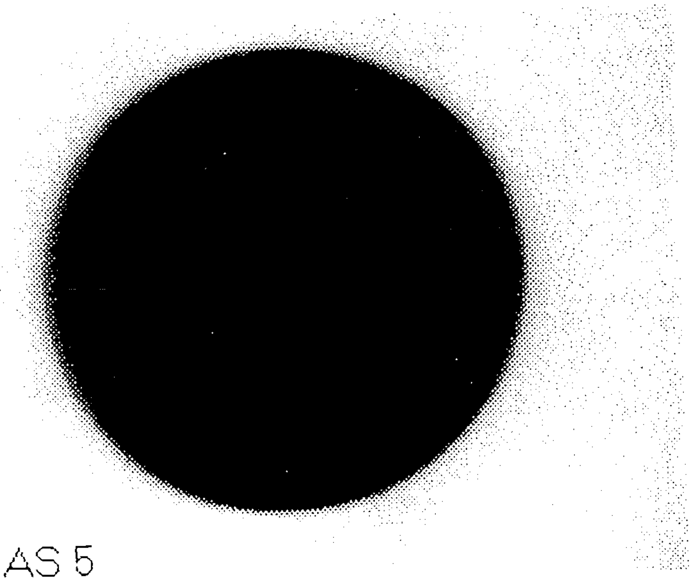

AS 5

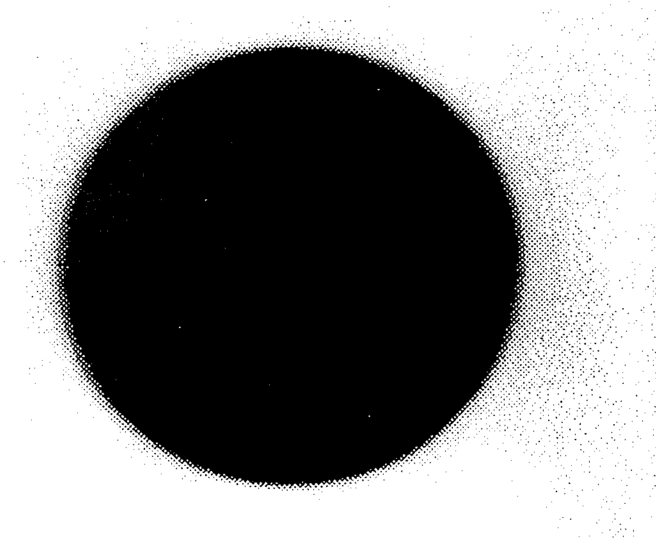

AS 6

Appendix 4

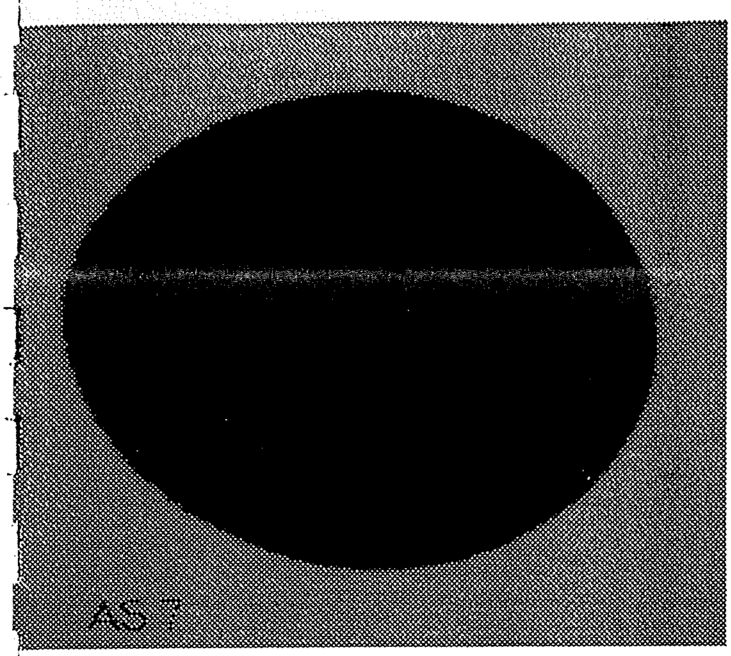
AS 7

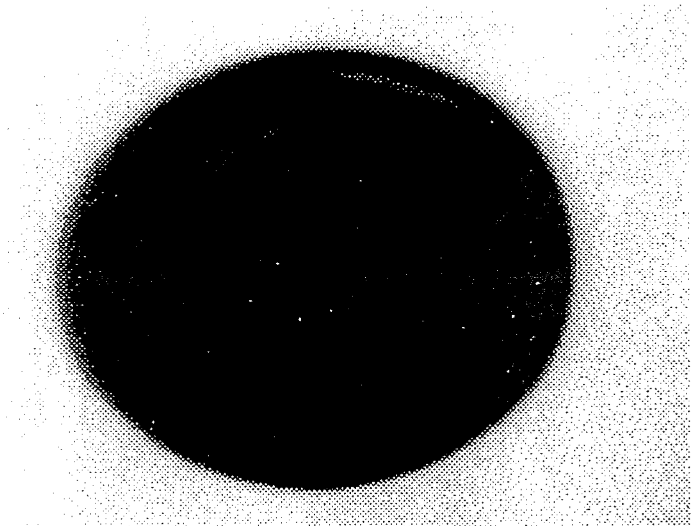
AS 8

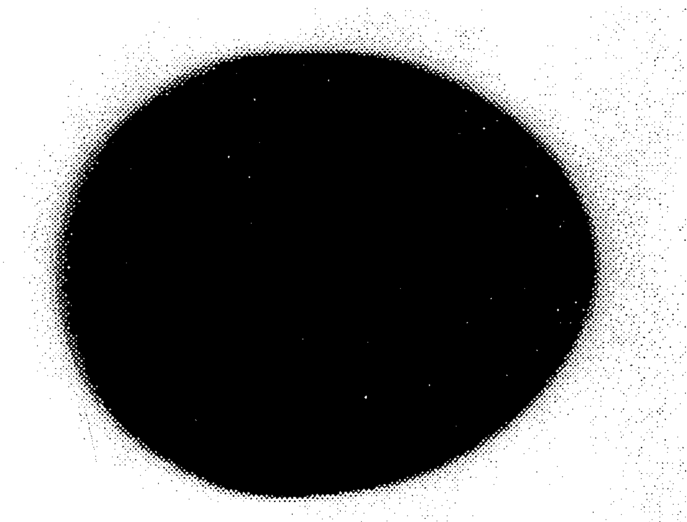
AS 9

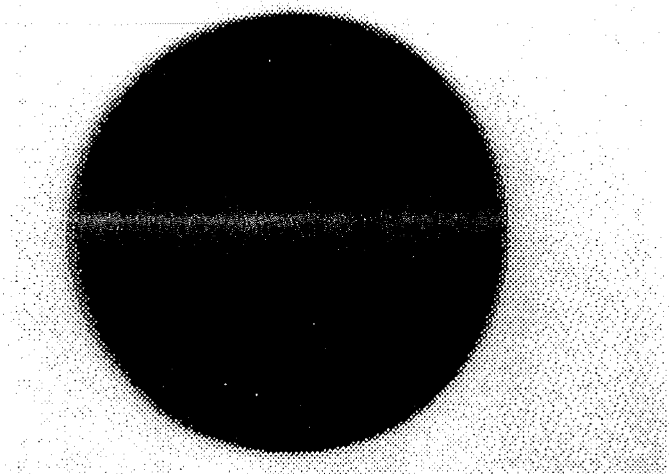
AS 10

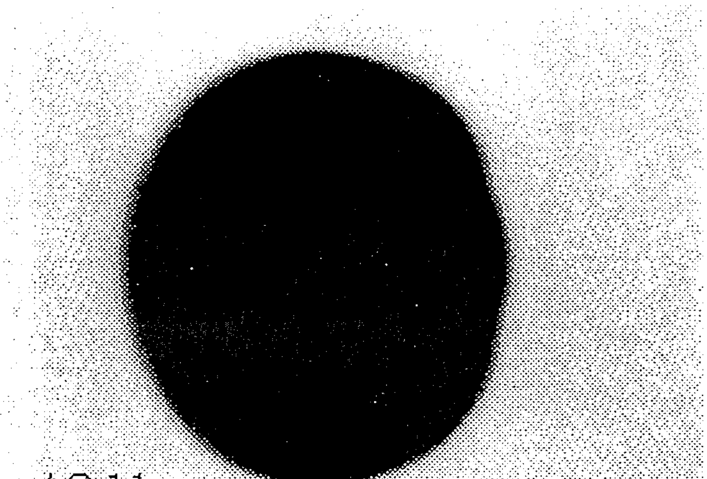
AS 11

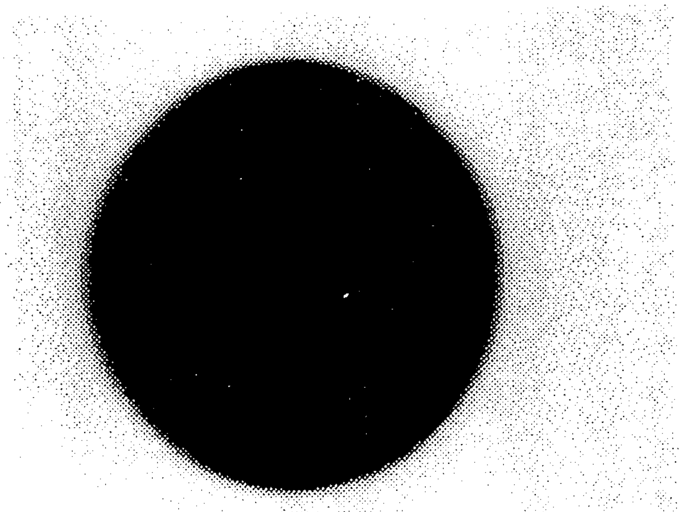
AS 12

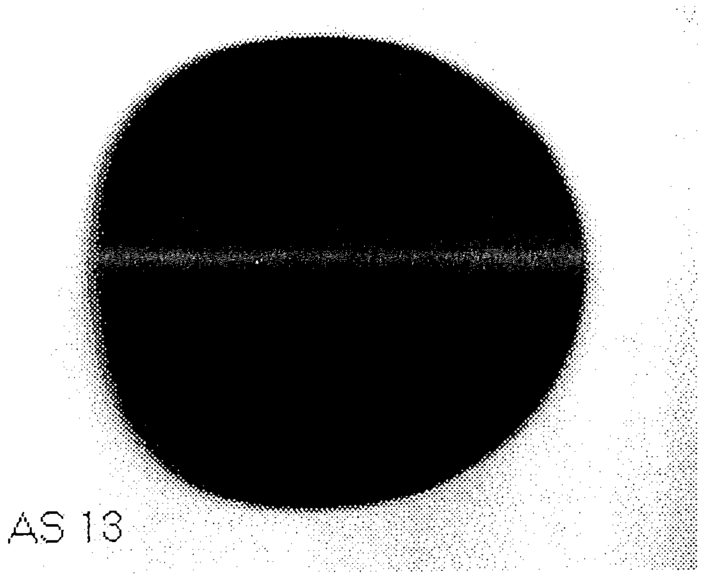
AS 13
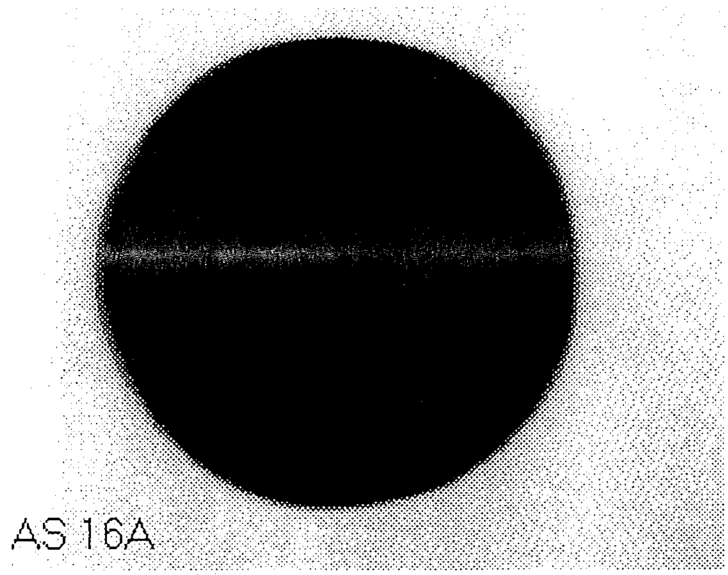
AS 16A
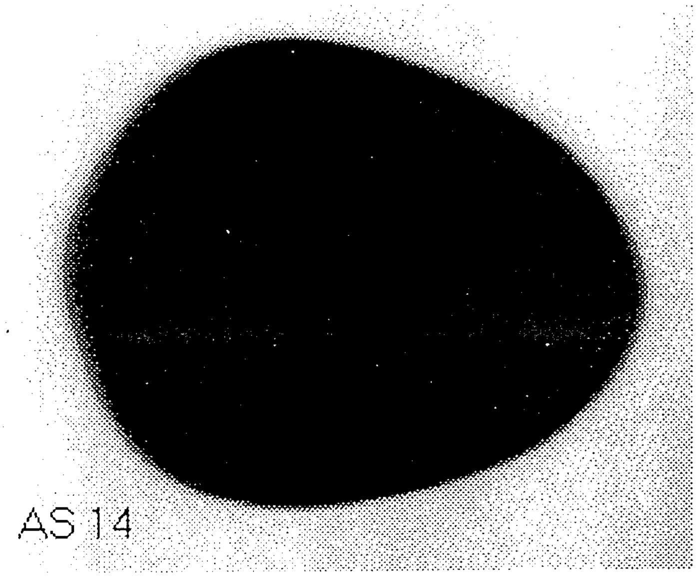
AS 14
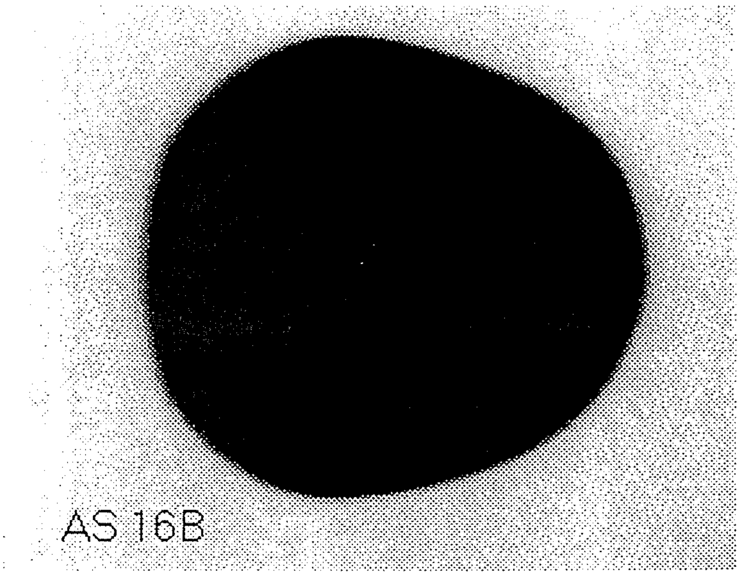
AS 16B
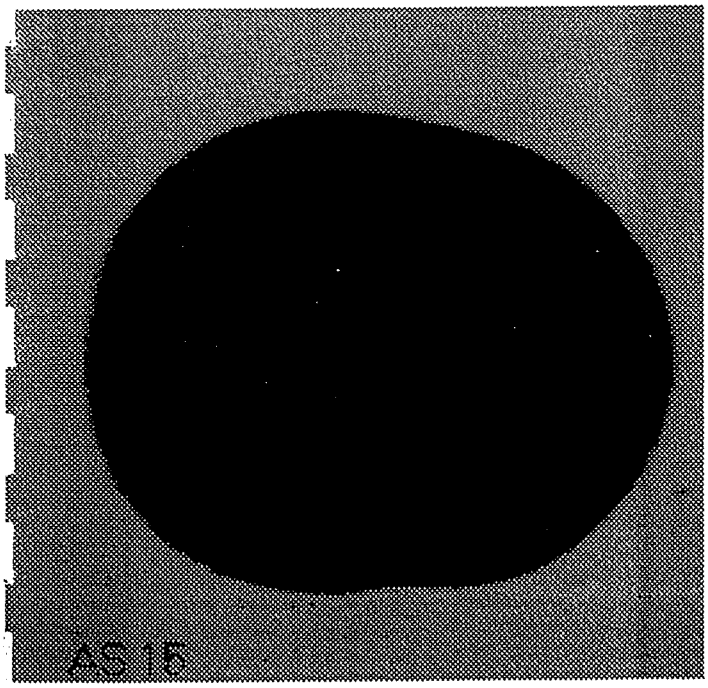
AS 15

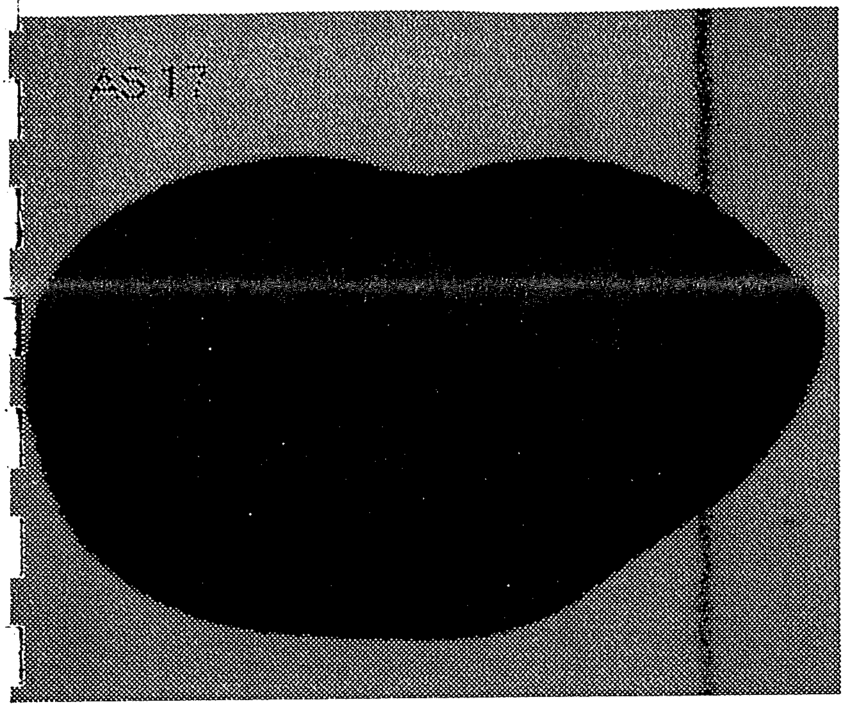
AS 17

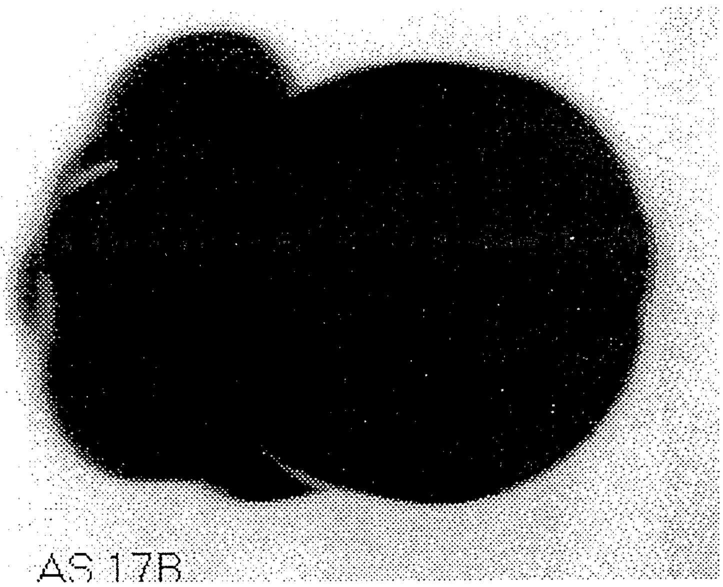
AS 17B

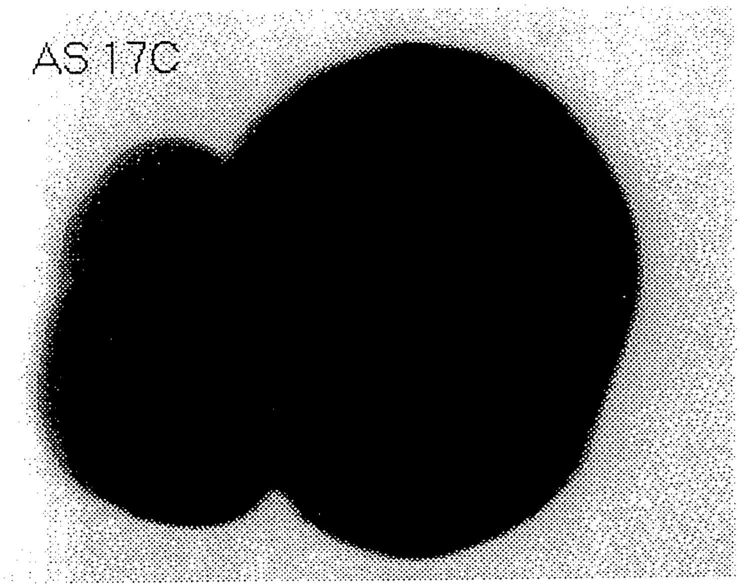
AS 17C

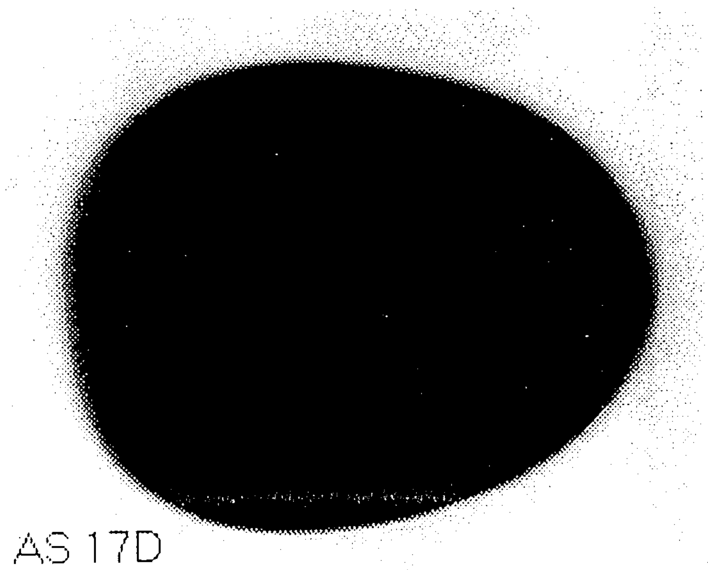
AS 17D

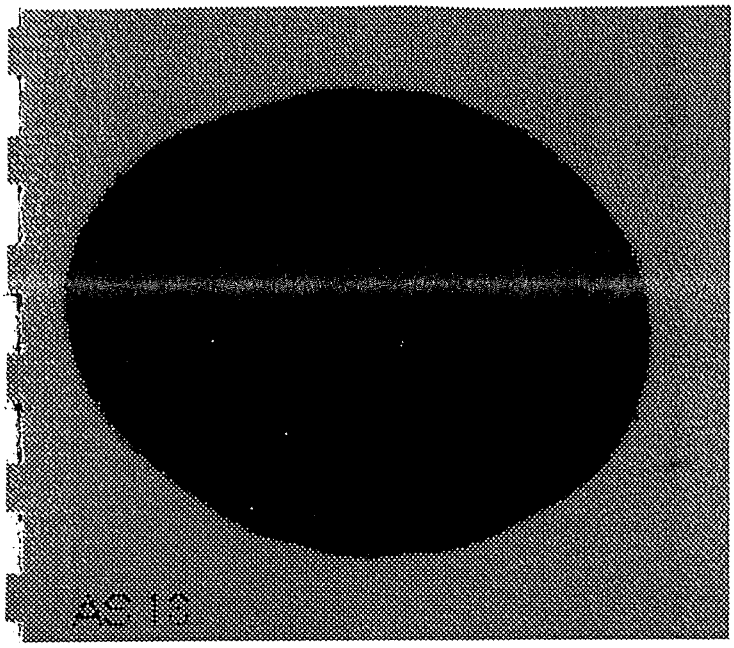

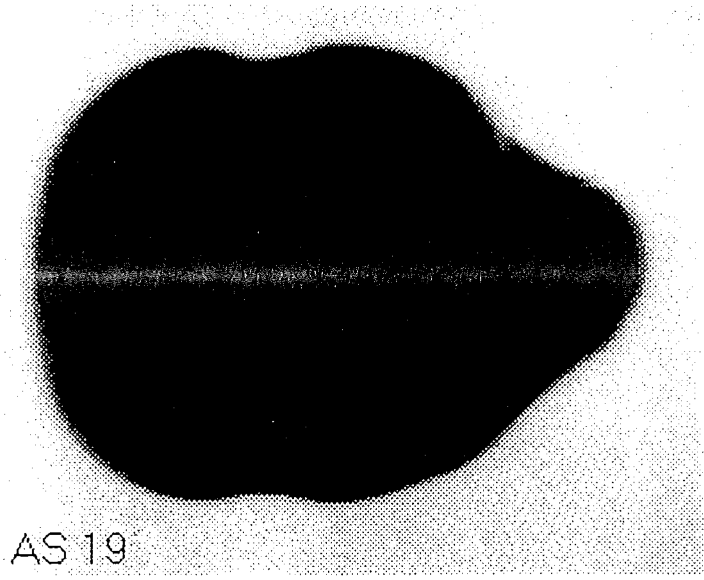
AS 19

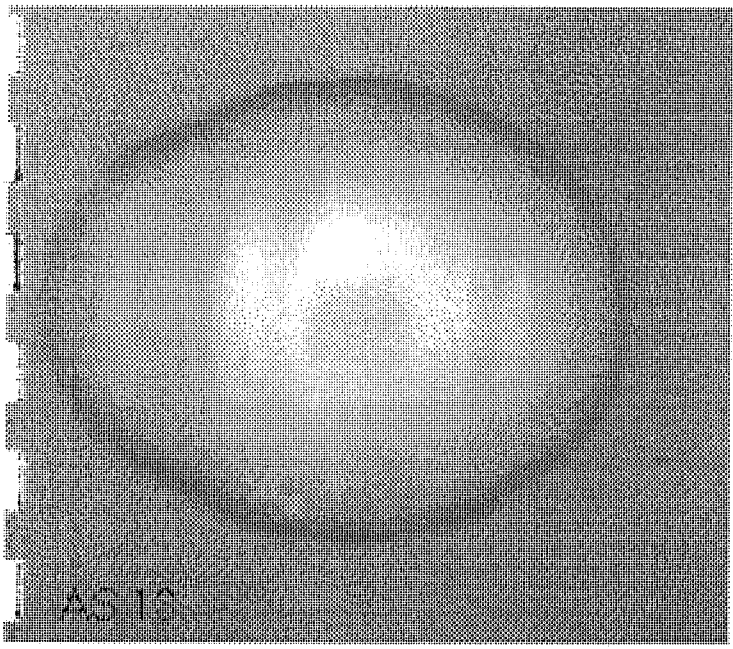

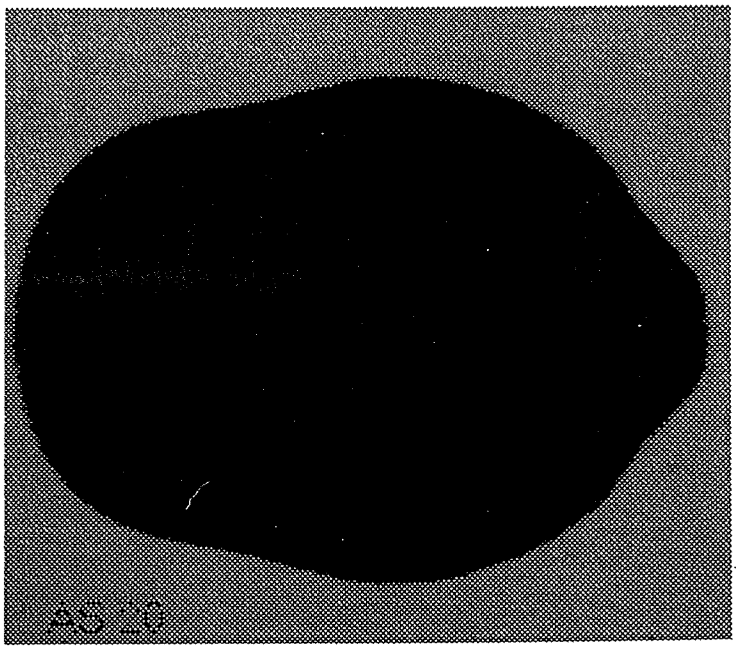

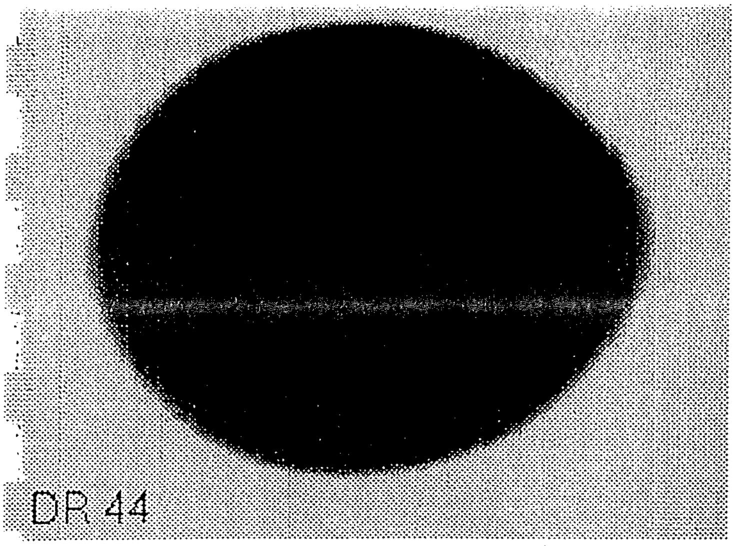


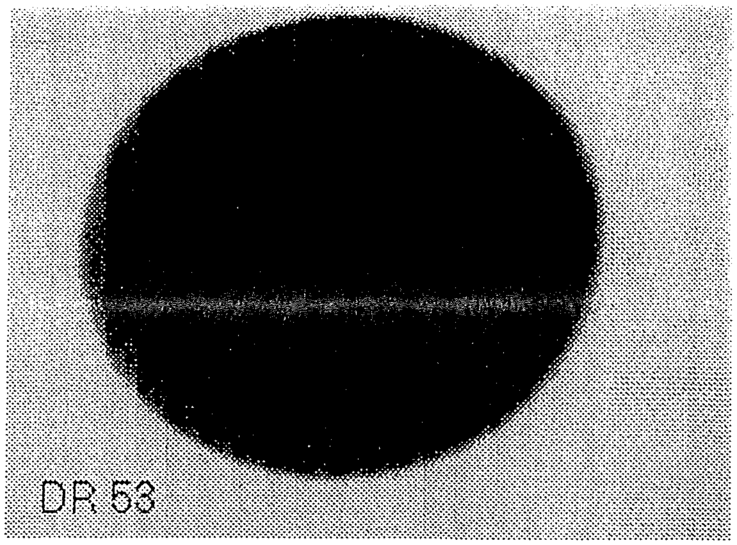


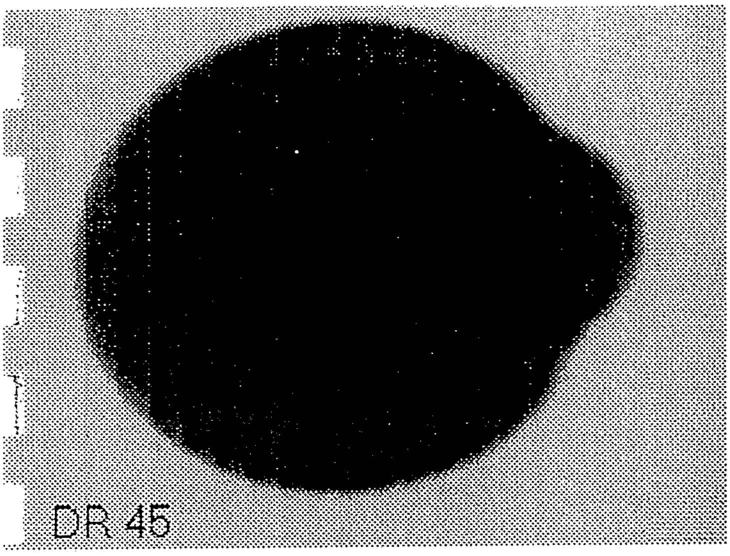


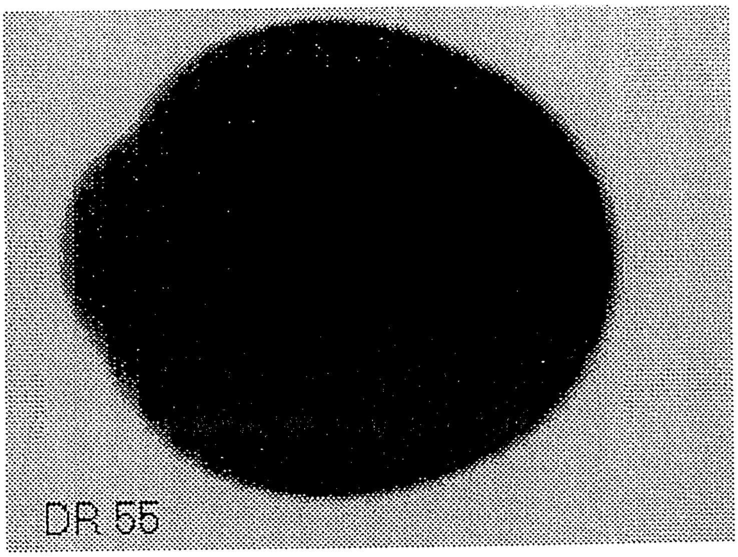


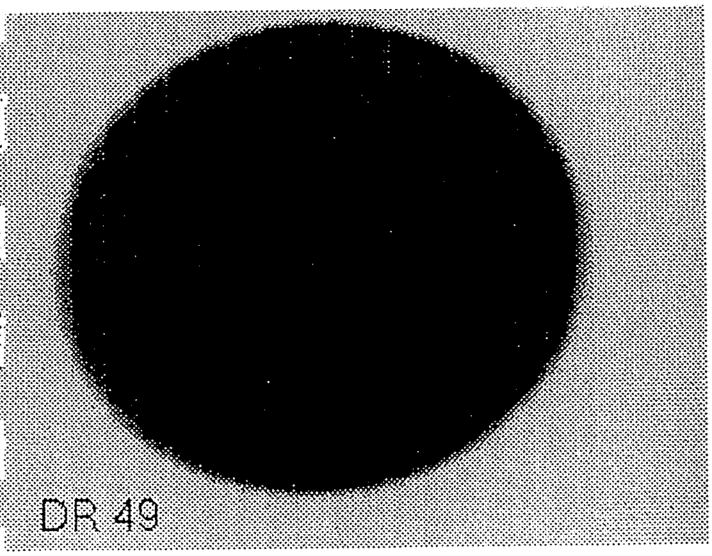


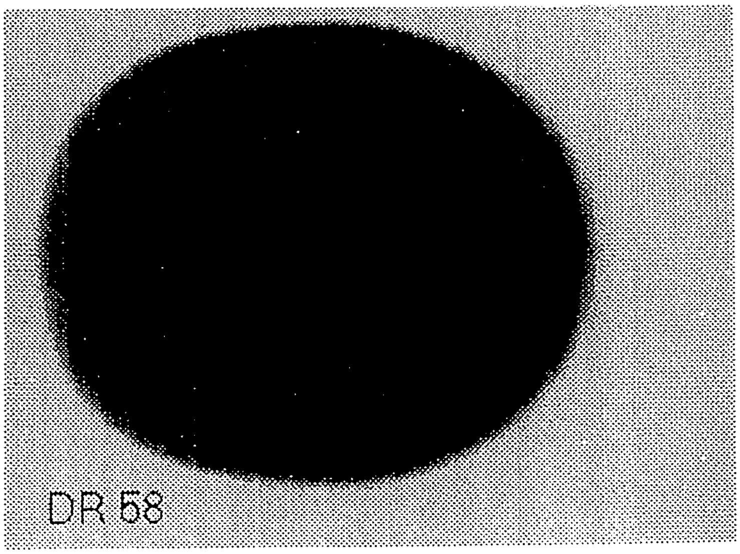


Appendix 5

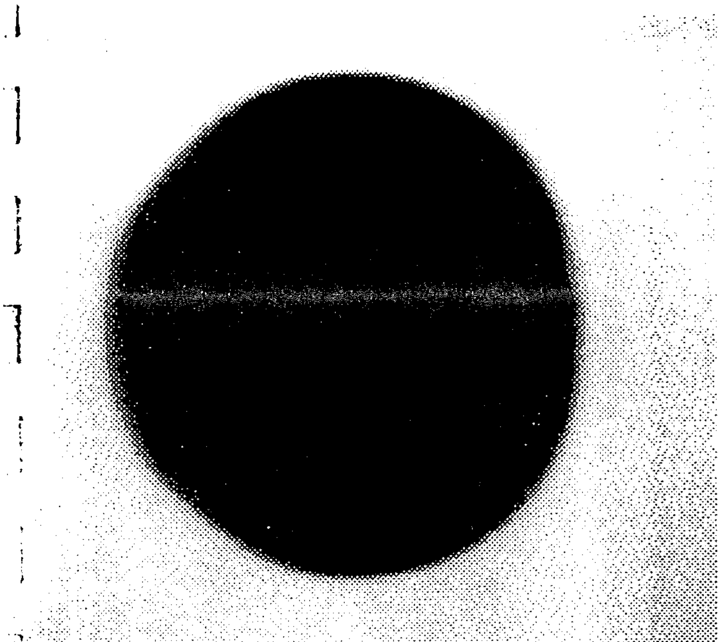

BU 11

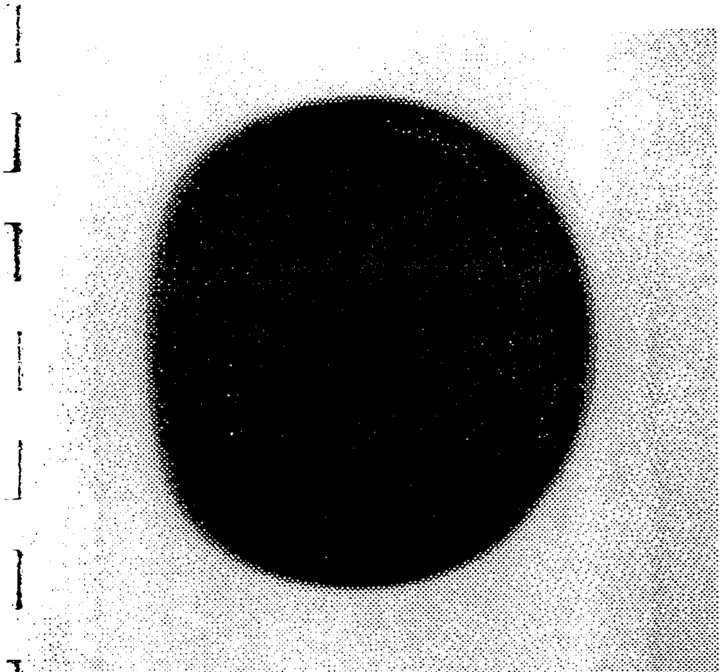

BU 12

BU 21

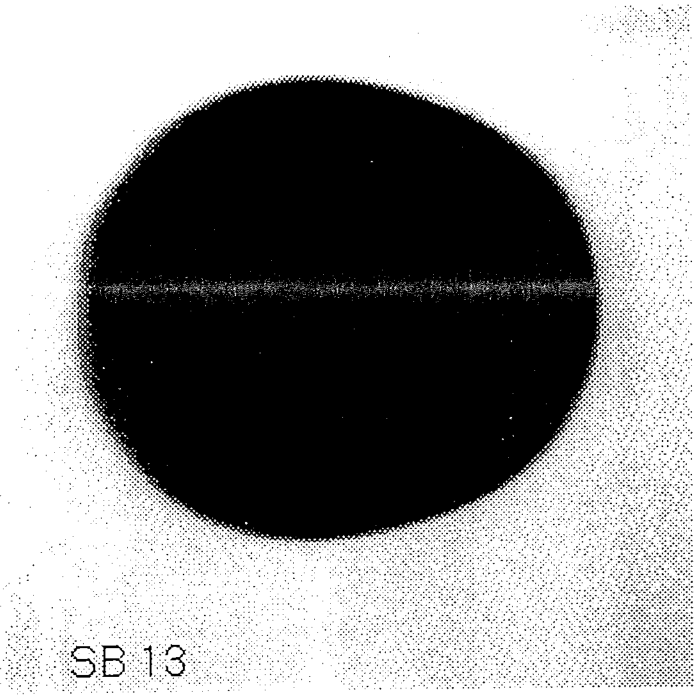
SB 13

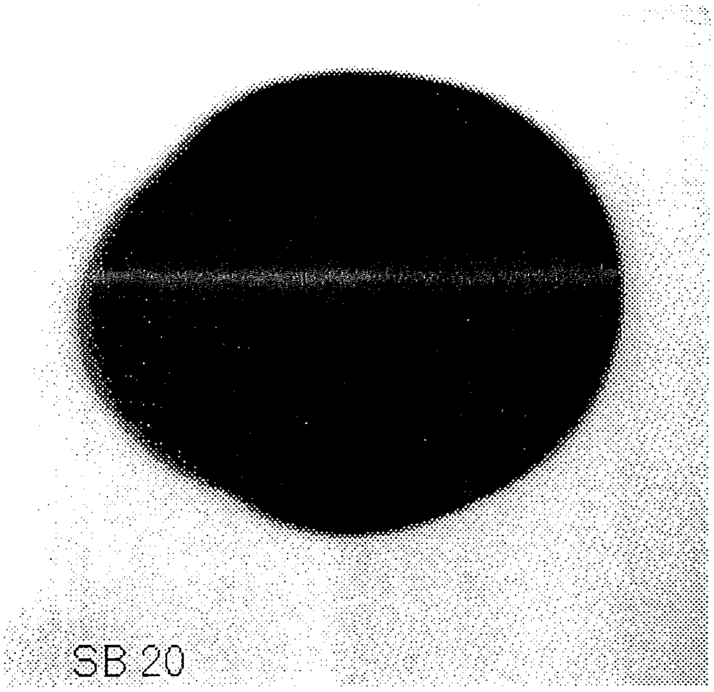
SB 20

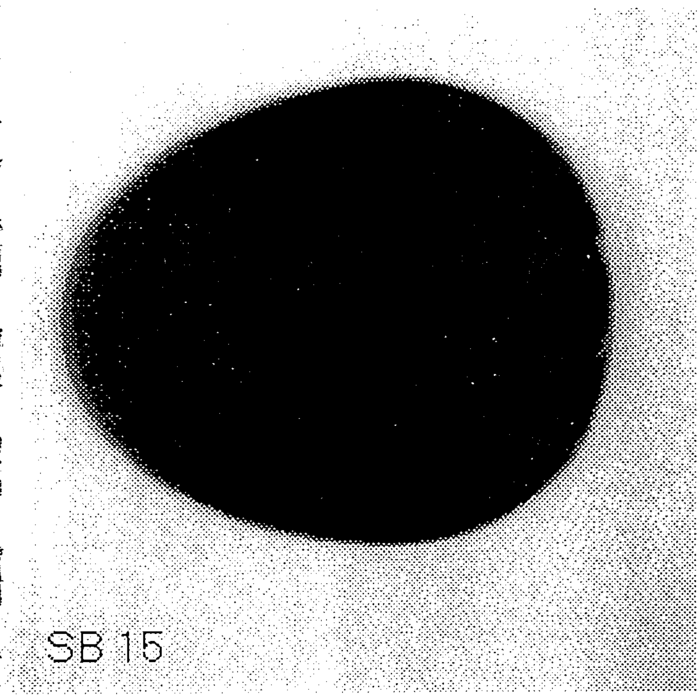
SB 15

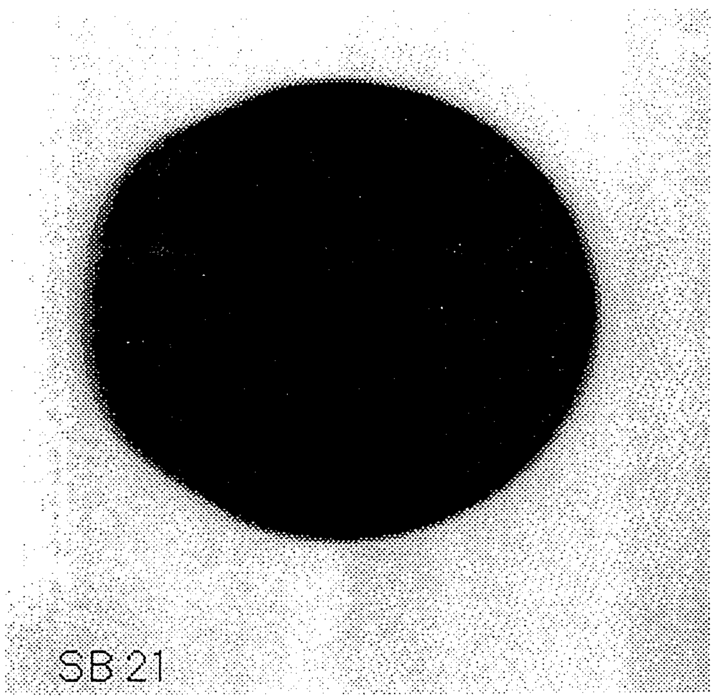
SB 21

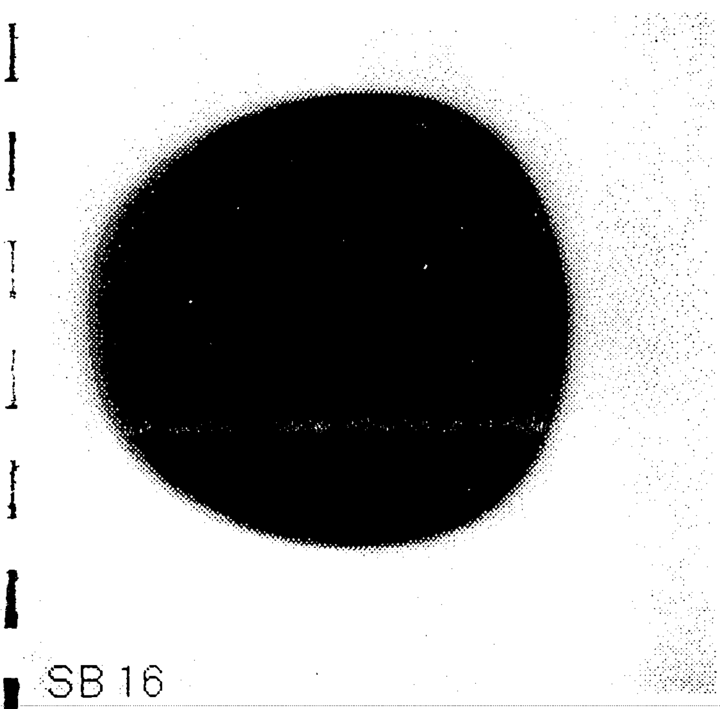
SB 16


SB 22

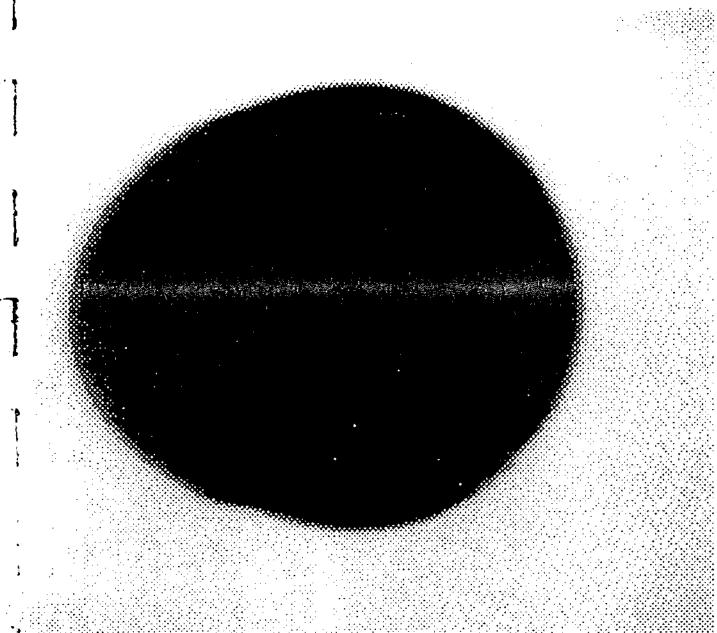

SB 23

SB 27

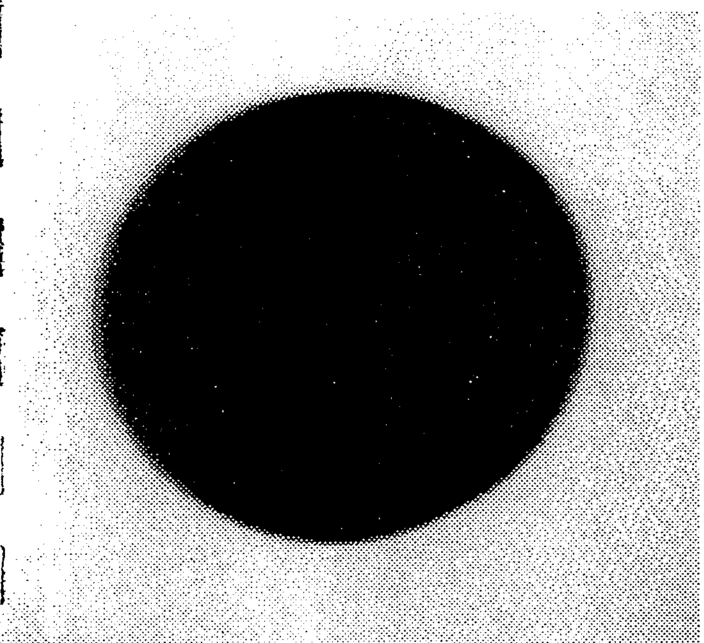

SB 24

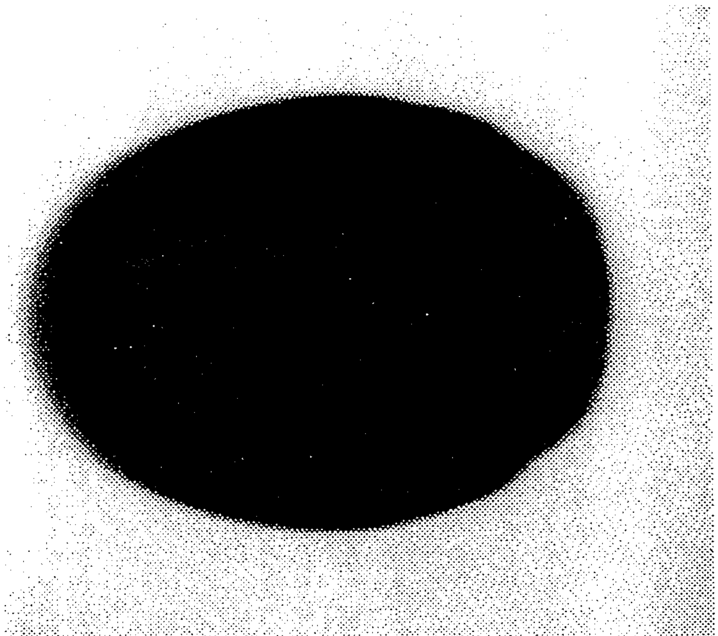

SB 28

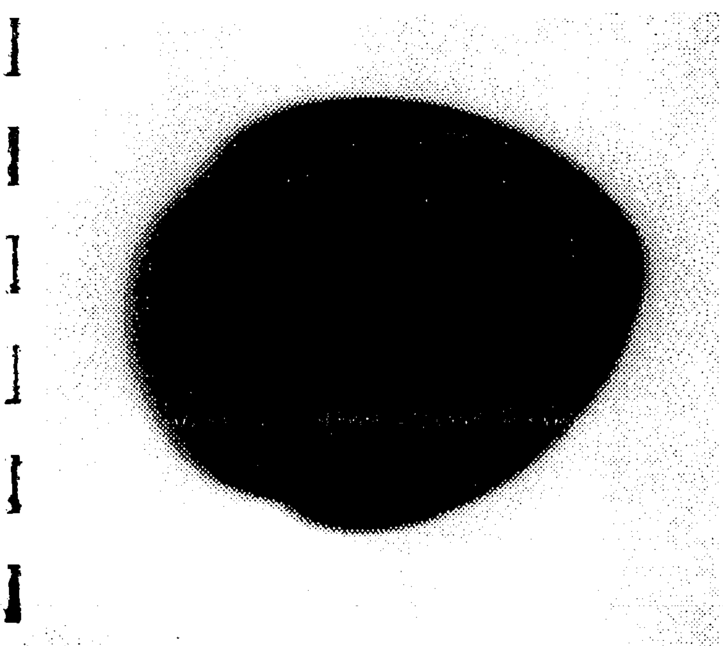

SB 26

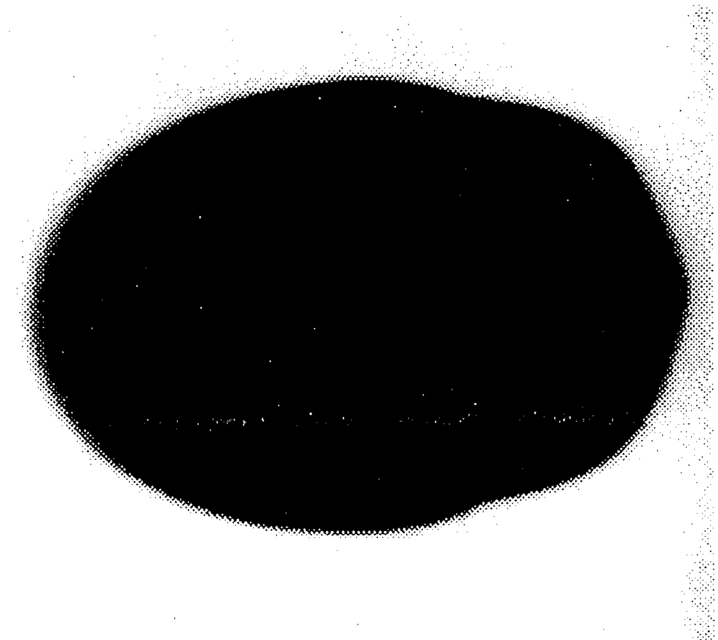

SB 29

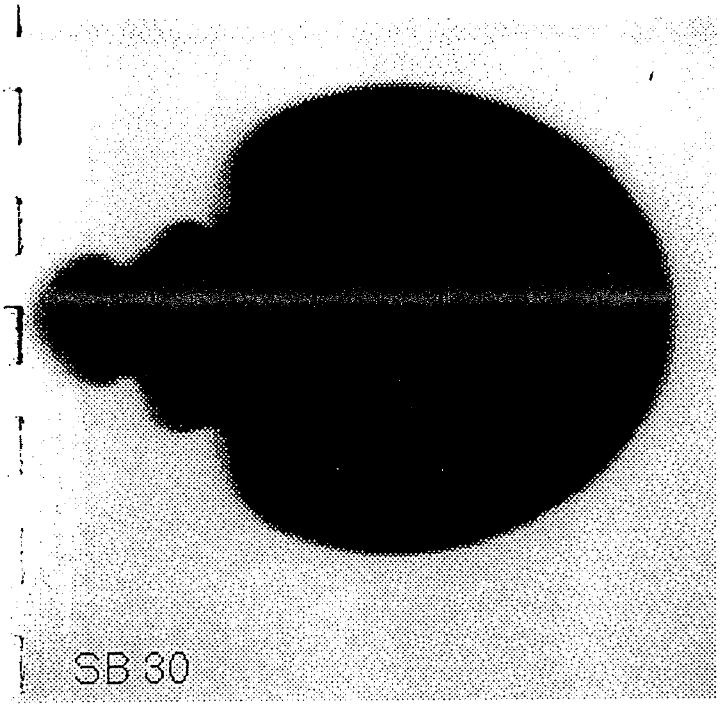
SB 30

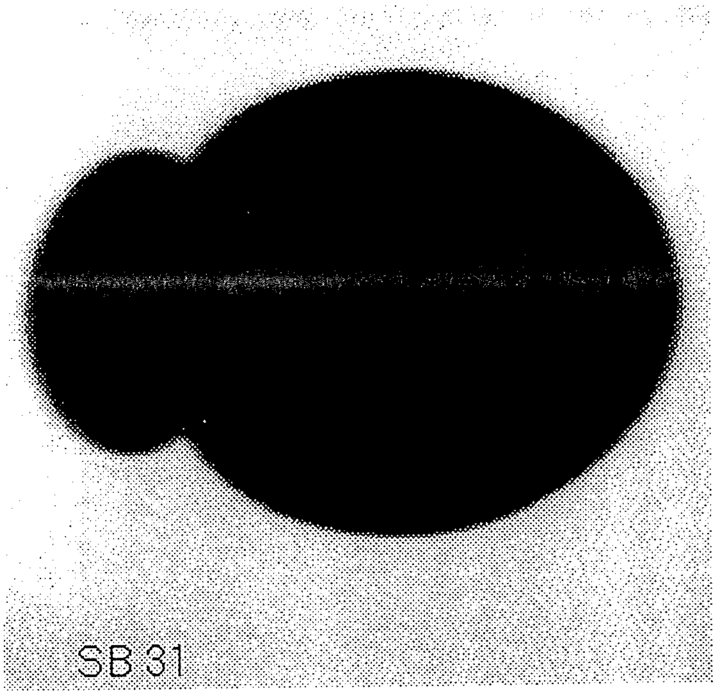
SB 31

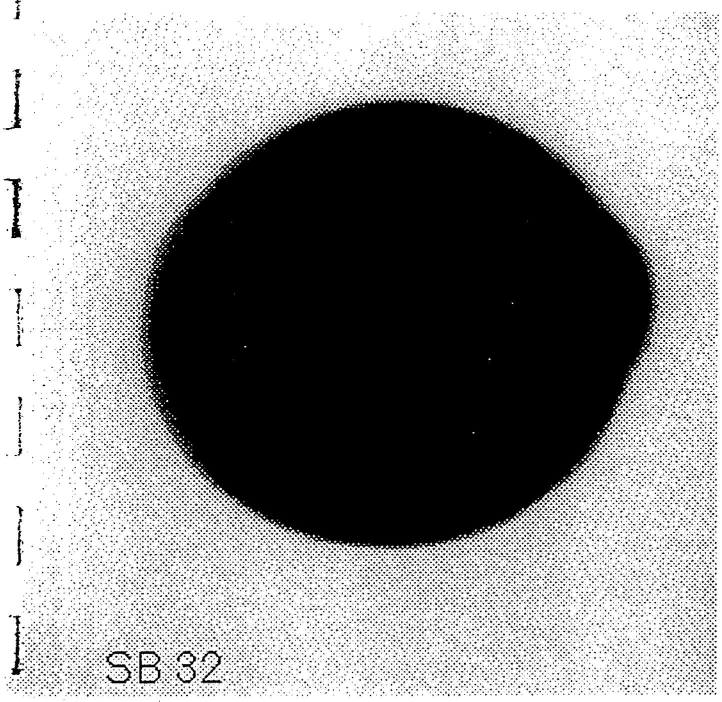
SB 32

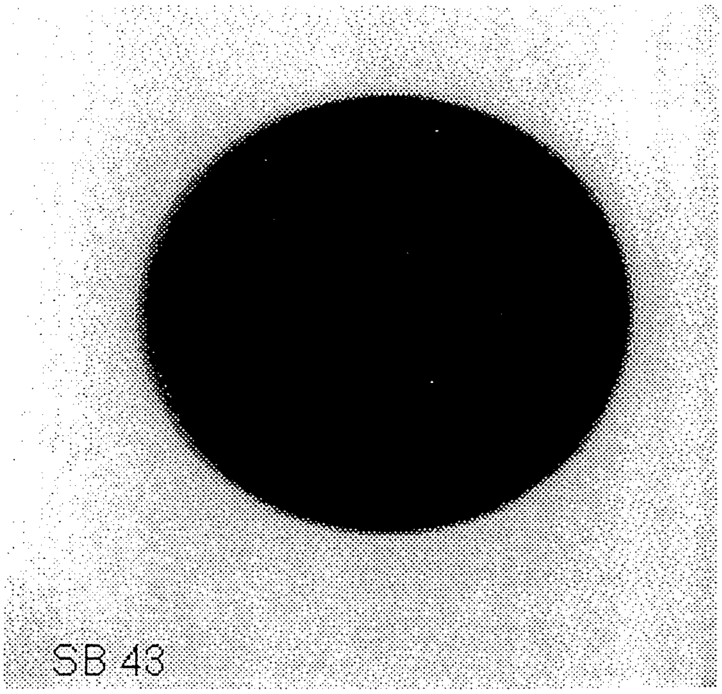
SB 43

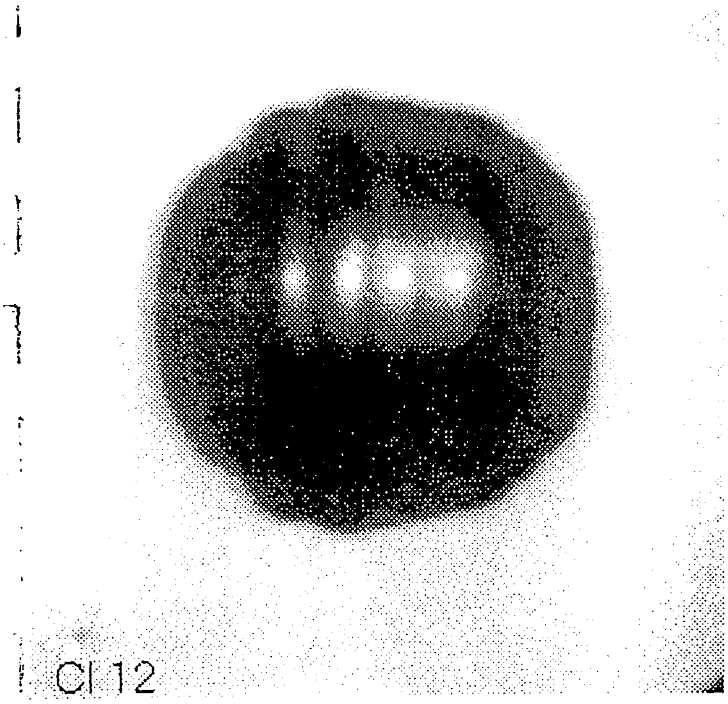
Cl 12

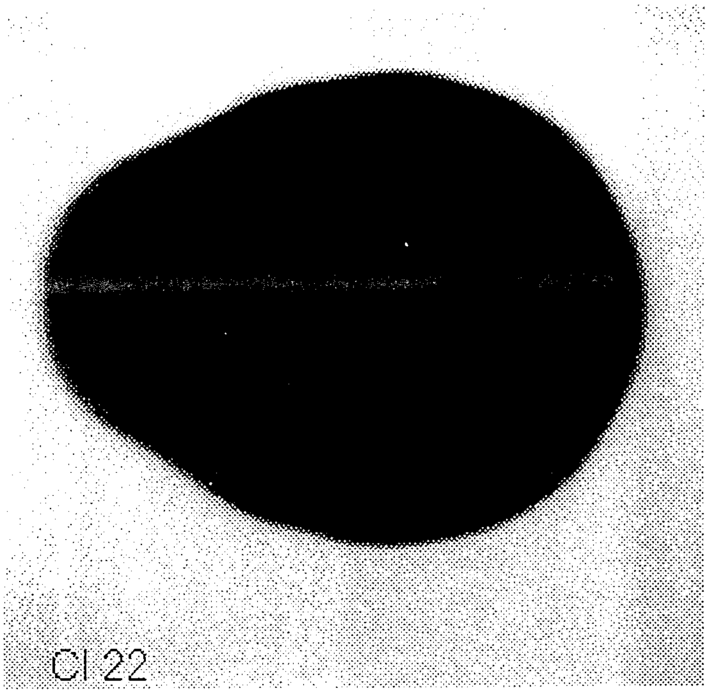
Cl 22

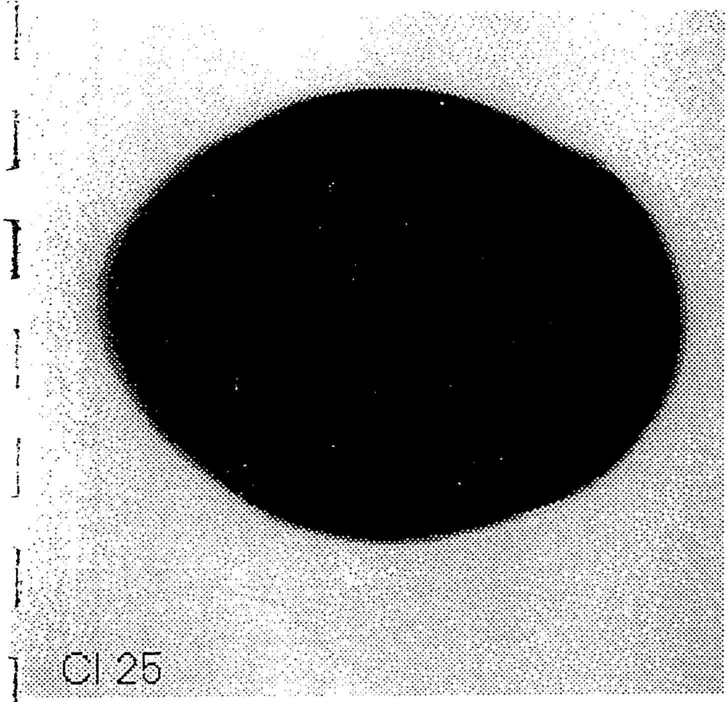
Cl 25

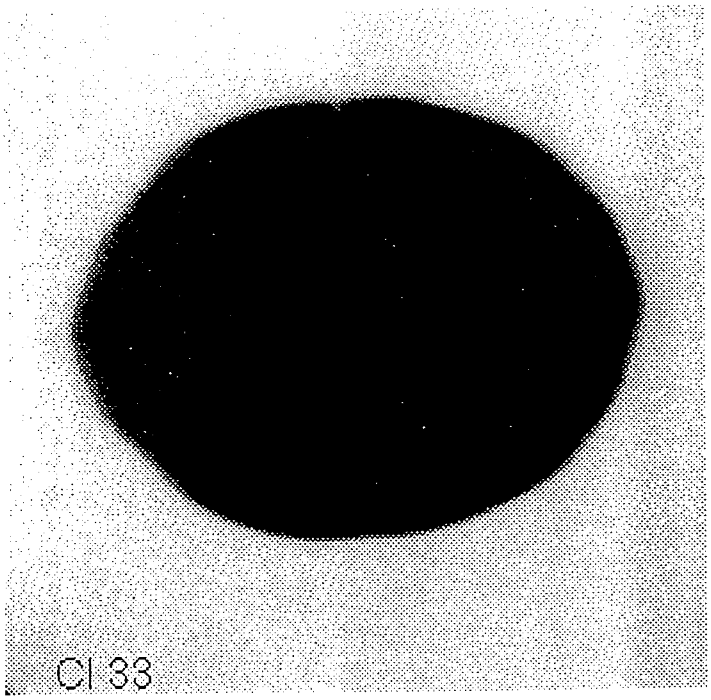
Cl 33

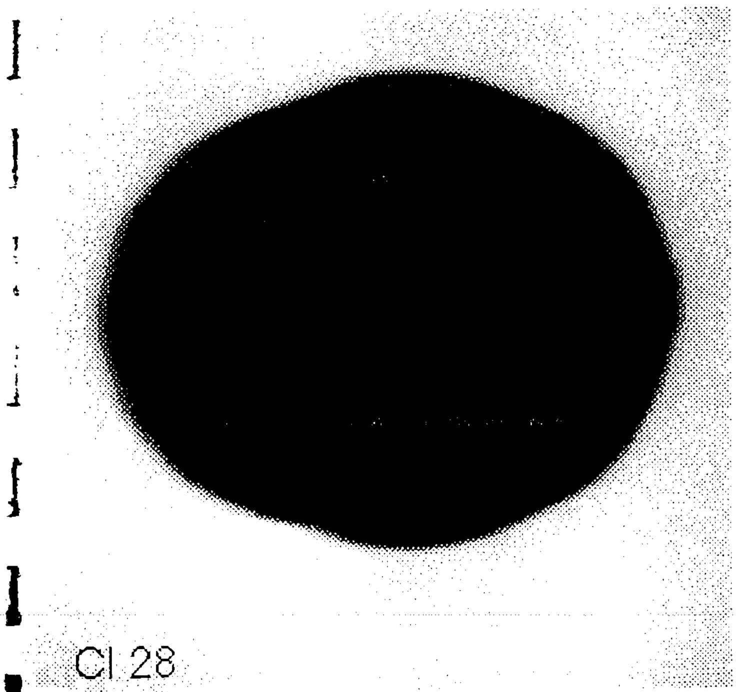
Cl 28

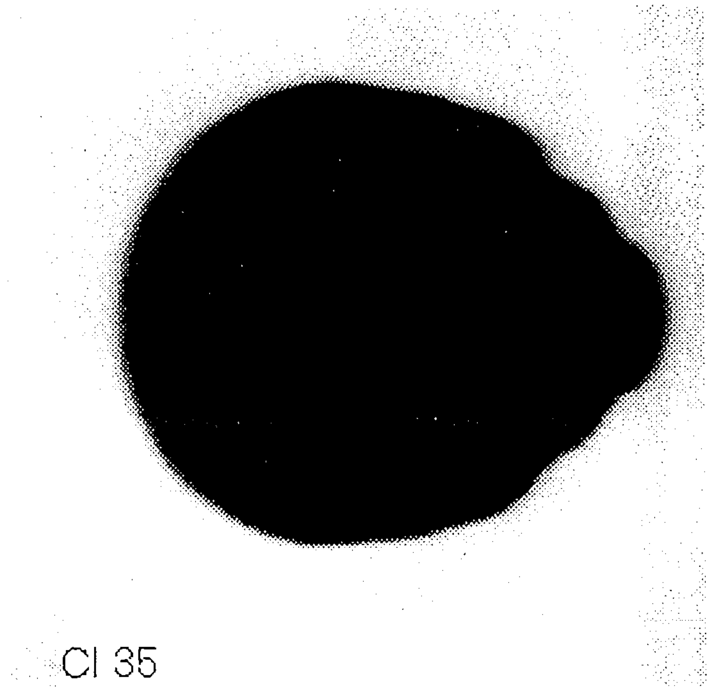
Cl 35

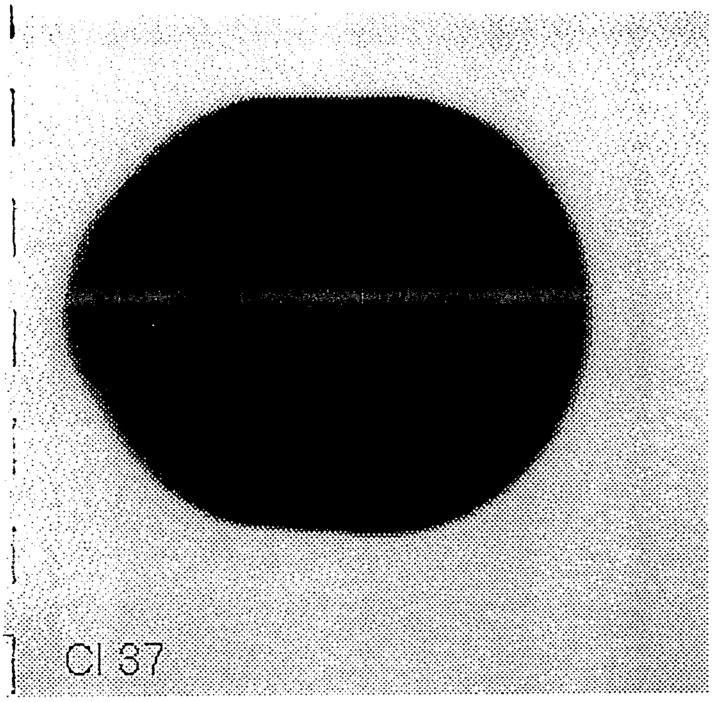
Cl 37

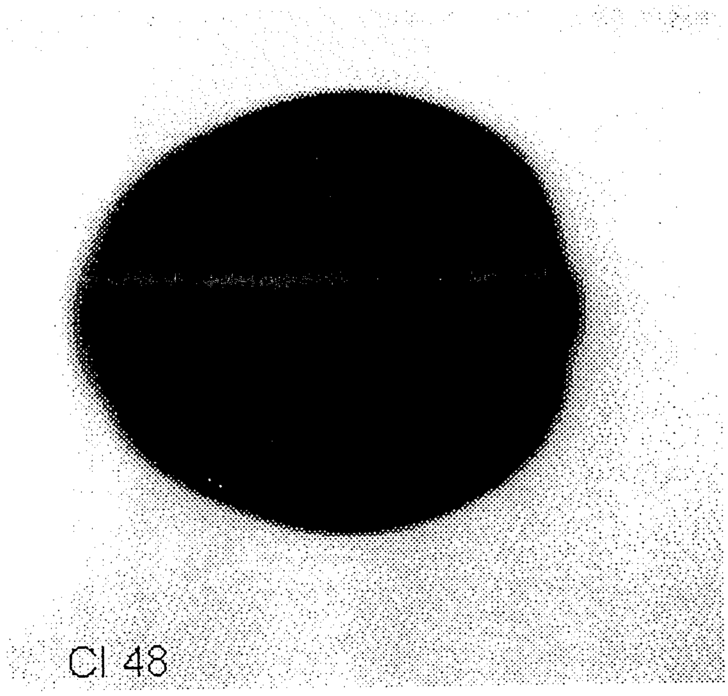
Cl 48

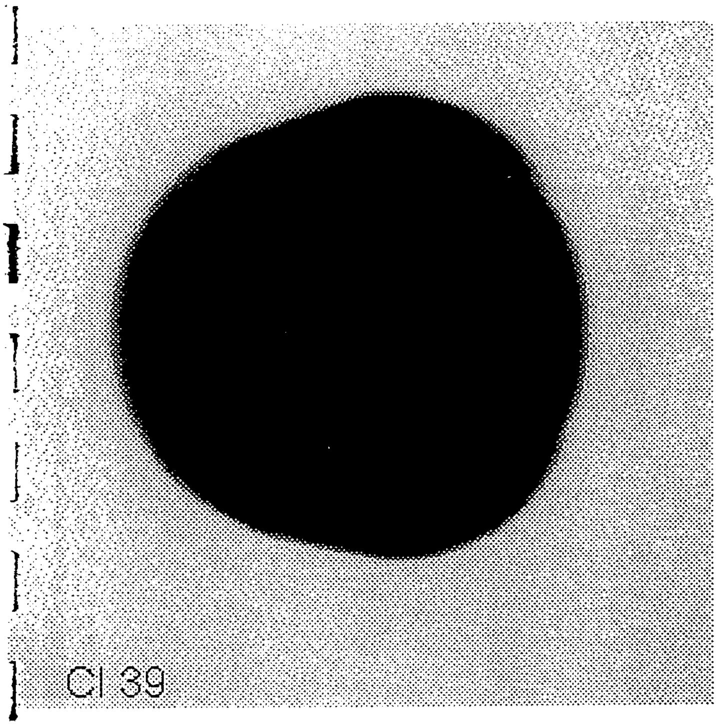
Cl 39

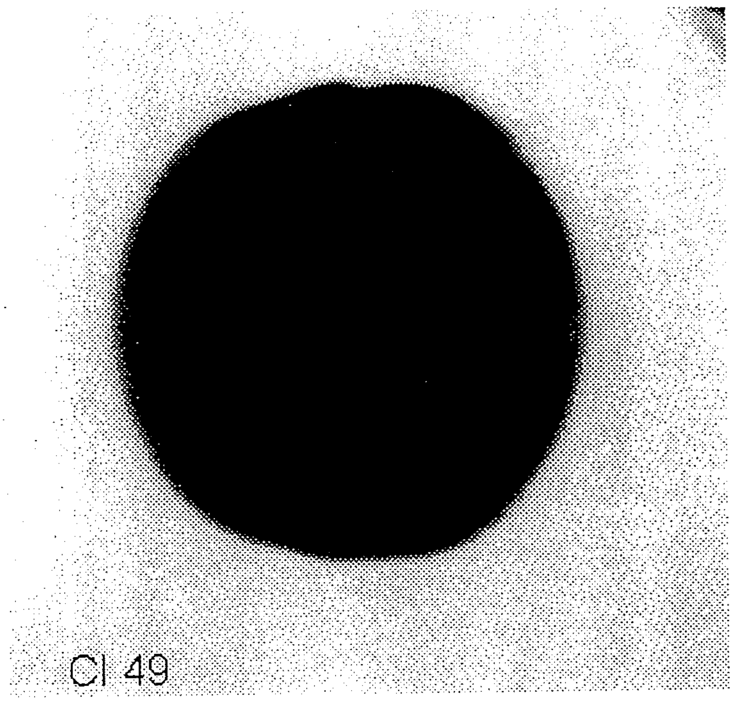
Cl 49

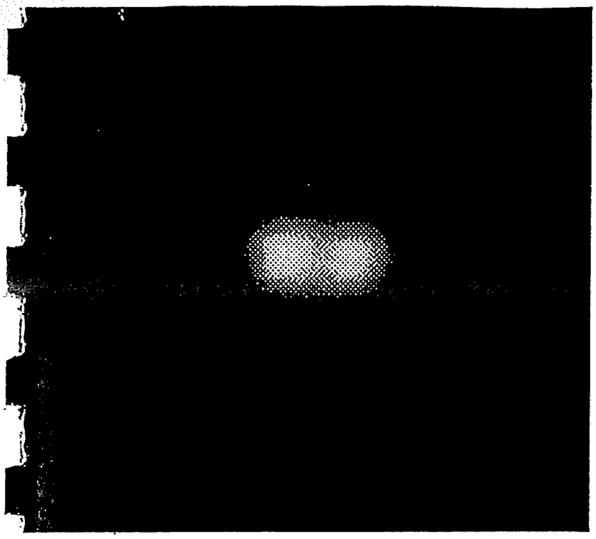

AS1 Round Grade 1

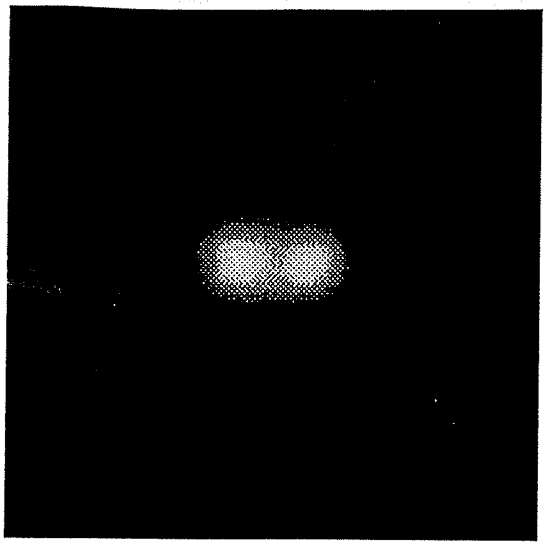

AS4 Round Grade 4

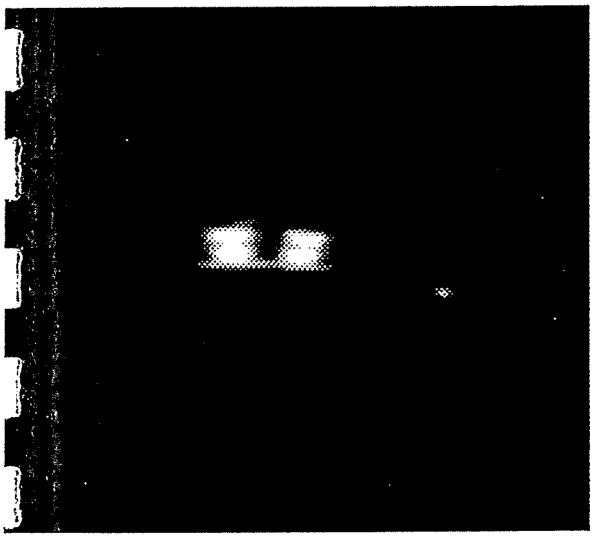

Ball Bearing

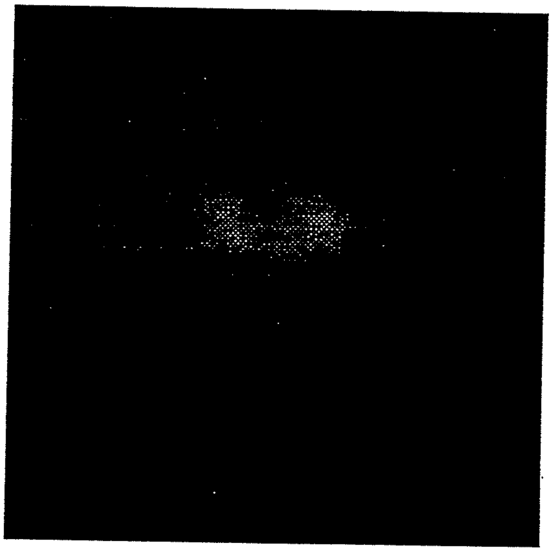

Roebuck Bay
Recoverable Reject

fig. 16